Investigations into the role of inflammation in tumorigenesis

Sheryl Coutermarsh-Ott

Dissertation submitted to the faculty of the Virginia Polytechnic Institute and State University in partial fulfillment of the requirements for the degree of

Doctor of Philosophy
In
Biomedical and Veterinary Sciences

Irving C. Allen
Nikolaos G. Dervisis
William R. Huckle
Tanya LeRoith
X.J. Meng

November 17, 2017
Blacksburg, VA

Keywords: inflammation, tumorigenesis, histiocytic sarcoma, signaling pathways, breast cancer

Investigations into the role of inflammation in tumorigenesis

Sheryl Coutermarsh-Ott

ABSTRACT

Inflammation has been found to play a role in the development of many different tumors. However, a tumor's ability to evade immune cell recognition can be integral to its progression as well. The following works explore this complicated role with a focus on histiocytic sarcoma (HS) and breast cancer. Chapter 1 opens with a broad overview of inflammation in tumorigenesis while Chapter 2 focuses on a review and discussion of current HS literature. Our investigations into the role of inflammation specifically in HS are initiated in Chapter 3 where we explore the role of the regulatory NLR, NLRX1, in the development of HS in mice. NLRX1 is an intracellular patter recognition receptor that functions to regulate pro-inflammatory cell pathways. Our studies reveal that in carcinogen-induced HS in mice, NLRX1 acts as a tumor suppressor. Moreover, when NLRX1 is lost, tumors that develop are associated with increases in expression of genes in NF-κB and AKT pathways. Though uncommon, HS is a clinically relevant tumor in dogs. In Chapter 4, we further investigate the role of the pathways identified in Chapter 3 in canine patients. Not only were these pathways increased, but our results also revealed previously unreported differences in tumors diagnosed as HS versus those diagnosed as hemophagocytic HS. To improve the use of canine HS both as an experimental and translational model, we sought to create a murine xenograft model. In Chapter 5, we discuss the development of our model and the results of pilot studies using targeted drug therapy. The focus of Chapters 3-5 is to further explore the role of inflammation in the development of HS. However, as aforementioned, the role of inflammation in tumorigenesis is quite complicated. In Chapter 6, we aim to address the concept that the lack of inflammation through immune evasion, can also be important in tumors. Breast cancer in humans is traditionally recognized as being highly immunosuppressive. In this final chapter, we investigate the use of an attenuated strain of bacteria to treat these tumors by way of shifting the immunosuppressive tumor microenvironment to a more pro-inflammatory state.

Investigations into the role of inflammation in tumorigenesis

Sheryl Coutermarsh-Ott

GENERAL AUDIENCE ABSTRACT

The role of inflammation in the development and progression of cancer has been studied for many years. It is well-accepted that chronic inflammation can lead to an environment that is favorable for tumor development. However, more recently it has been shown that being able to escape the immune system and avoid inflammation can also be important in tumor development. The aim of this work was to further investigate these dichotomous roles. In Chapters 1-5 we review and further explore the role of inflammation in a poorly studied tumor called histiocytic sarcoma (HS). Through our studies we have found that a receptor protein present in many cells, NLRX1, is important in the development of chemically-induced HS in mice. Moreover, the development of these tumors is associated with increases in pro-inflammatory and cell growth pathways. Further studies reveal that these pathways are also important to the development of the tumor in dogs. Because HS is rare and poorly studied in humans, we describe the development of an additional mouse model to study HS. This model will help reveal important information about the disease in dogs that can help us study it in humans. Finally, in Chapter 6, we sought to investigate the other potential role of inflammation in decreasing tumorigenesis. In these studies, we used a mouse model of breast cancer to investigate whether or not we could decrease tumorigenesis by increasing the immune system's ability to recognize the tumor.

Acknowledgements

I would like to acknowledge the many people who contributed to the following works and to my graduate career as a whole including my graduate committee Dr. Allen, Dr. LeRoith, Dr. Huckle, Dr. Meng, and Dr. Dervisis. Thank you especially to my mentor, Dr. Coy Allen who has facilitated my growth as a student and researcher. I also would like to acknowledge and thank Dr. Vilma Yuzbasiyan-Gurkan. Dr. Yuzbasiyan-Gurkan has agreed to travel the long distance to VA from Michigan in order to serve as an external examiner. The many pathologists who have either directly contributed to the following works or indirectly through support and mentorship include Dr. Tanya LeRoith, Dr. Tom Cecere, Dr. Kevin Lahmers, Dr. Phil Sponenberg, Dr. Geoff Saunders, and Dr. Sarah Hammond. Additionally, I would like to acknowledge my lab mates, Daniel Rothschild, Dr. Kristen Eden, Dylan McDaniel, and Veronica Ringel. Without their input and continued support, none of this would have been possible. Bettina Heid was incredibly important in assisting with techniques and managing laboratory projects. The TRACSS staff was integral to helping maintain the animal colony and health. Finally, I would certainly like to thank my husband and family for all the personal support throughout this decade of academic journey.

Table of Contents

Attribution

Chapter 4 is a manuscript that was co-first authored by Katherine Broadway. In this manuscript, I performed and contributed all data for the mouse studies included in Figures 1-4 and 6. I also contributed heavily to the writing of the majority of the manuscript.

Chapter 1

Introduction

Inflammation and tumorigenesis have a well-recognized relationship, first suggested by Rudolf Virchow in 1863. His initial observation of lymphocytes within tumor tissue led him to suggest that it was chronic inflammation at these sites that led to the development of cancer [1]. Concurrent with these observations, large bodies of research currently exist to support the fact that sites of chronic inflammation are often at a much higher risk for the development of tumors of the bladder, stomach, liver, colon, mesothelium, lung, and others [2-7]. However, we also now know that, depending on a host of genetic and environmental factors, inflammatory cells and cytokines can play a dichotomous role in the initiation and progression of tumors. This is no better summarized than in Hanahan and Weinberg's, "Hallmarks of Cancer: The Next Generation" [8]. In this review, the authors include avoiding immune destruction as an emerging hallmark of cancer, or, a characteristic acquired by cells allowing them to become neoplastic. This view is supported by studies that show experimental animals lacking an immune system are at a much higher risk of developing tumors compared to those with intact immune systems [8]. Thus, it is clear that the role of inflammation in tumorigenesis is much more complicated than originally thought.

Tumor-promoting inflammation as set forth by Hanahan and Weinberg is consistent with Virchow's initial observations and, since then, numerous examples in multiple organs and types of tumors have been shown to support this role. One very well-described example of this is the link between chronic hepatic viral infection and the development of liver cancer. This is best described in humans. In human patients, chronic, persistent infection with hepatitis C virus leads to a persistent but ineffective immune response against infected hepatocytes [9]. This leads to

repeated cycles of hepatocyte destruction with subsequent attempts at regeneration in a microenvironment dominated by DNA-damaging reactive oxygen species production [9]. In this environment, patients with hepatitis C virus are 17 times more likely to develop liver cancer than patients without hepatitis C infection [10]. A similar link has been made in woodchucks infected with Woodchuck hepatitis virus. This is a virus related to hepatitis B virus that was found to cause hepatocellular carcinomas in woodchucks in a potentially similar manner as hepatitis C in humans [11]. Another good example of the link between inflammation and tumorigenesis is the predisposition of human chronic obstructive pulmonary disease (COPD) patients to the development of lung cancer [12]. COPD is characterized by chronic damage of the lung parenchyma by cigarette smoke and/or air pollution caused by the burning of fuels. This damage leads to infiltration and damage of airways by neutrophils, macrophages, T cells, and B cells that secrete a variety of pro-inflammatory and pro-fibrotic cytokines such as TGF-β, IL-1, IL-8, and G-CSF [12]. As in the liver, these repeated cycles of epithelial cell damage and regeneration provide a microenvironment favorable for the development of non-small cell lung cancer [12]. In fact, smokers with COPD are 5 times more likely to develop lung cancer than those with normal lung function and non-smokers with COPD are still twice as likely to develop lung cancer as those without COPD [13].

Whether the liver, the lung, or any other organ where chronic inflammation has been shown to drive tumorigenesis, the mechanisms by which inflammation can lead to neoplastic change are two-fold. First, the presence of persistent inflammation typically leads to an environment where cells are constantly undergoing damage. In the case of viral hepatitis, it is in an attempt to destroy virally infected cells while in smokers' lungs, it is due to persistent exposure of cells to damaging chemicals from cigarette smoke. This cellular damage leads to an

increase in repair signals within the tissue [12]. Repair means increasing proliferation and/or growth of progenitor cells or remaining cells, which can be an important facilitator of neoplastic change. Secondly, the presence of inflammation leads to an increase in release of free radicals from immune cells and cells undergoing destruction. Free radicals are directly damaging to DNA and can lead to changes allowing for neoplastic transformation.

Histiocytic sarcoma (HS) is an uncommon, poorly studied neoplasm compared to liver and lung tumors. Currently, it is unclear if dysregulated inflammation or inflammatory signaling pathways contribute to its pathobiology. It is a tumor derived from histiocytic cells of the immune system and can arise in a variety of different organs. Chapter 2 provides a detailed literature review, summarizing what is currently known about HS. Because HS arises from an immune cell, we hypothesized that pro-inflammatory cell signaling pathways would be important in the pathogenesis if this disease. The majority of the following chapters are spent exploring this relationship and highlighting the need for additional research on the topic. Studies described in Chapters 3-5 focus on our investigations in HS. The results of experiments described in Chapter 3 reveal that the unique tumor suppressor NLRX1 plays an important role in the development of carcinogen-induced HS in mice. Moreover, the development of these tumors is associated with increases in signaling pathways involved in inflammation and cell proliferation. Because HS does occur in both human and veterinary medicine, and the dog has been shown to be a good clinical model of the disease in humans, we next sought to investigate whether the signaling pathways we identified in mice were relevant to the disease in canines [14]. As described in Chapter 4, we were able to show that not only are these pathways important, but also that mechanistic differences of diagnostic relevance exist between HS and the even less characterized hemophagocytic HS sub-type. Though the disease in canines can be a useful tool

to continue to study, the need for more refined experimental manipulation and controls led us to develop a xenograft model. Chapter 5 describes the development of our model using a canine HS cell line in an immunocompromised strain of mouse. Here, we also discuss the results of pilot studies using our xenograft model to investigate novel therapeutics.

Though tumor-promoting inflammation has been shown to be an enabling characteristic in the development of tumors of the liver and lung, as well as, tumors of histiocytic origin, an emerging hallmark is the ability to evade recognition by the immune system and subsequent destruction by inflammatory cells [8]. The purpose of the immune system is to maintain homeostasis through the recognition and response to harmful entities such as pathogens, infected cells, and tumors. Once something that should not be there is recognized, cells of the immune system can initiate several different responses including inflammation, cell death, autophagy, and others. There are many examples of ways in which tumors have adapted to avoid recognition by the immune system and one of them is through the recruitment of immunosuppressive immune cells. Examples of such cells are myeloid derived suppressor cells and (MDSC) and macrophages polarized to an M2 phenotype. MDSCs are a group of myeloid precursor cells that have been found to be expanded in numerous disease states including sepsis, trauma, and cancer [15, 16]. These cells are immunosuppressive and contribute to tumorigenesis through the direct protection of tumor cells from immune cell destruction, modulation of the local microenvironment, and ability to facilitate metastasis [17, 18]. Another mechanism by which tumor cells evade the immune system is through the recruitment of M2 macrophages (also known as tumor-associated macrophages or TAMs). M2 macrophages secrete a variety of immunosuppressive substances, such as IL-10 and TGF-β that prevent immune cells (such as tumor infiltrating lymphocytes) from recognizing and responding to the tumor [19]. One

example of a tumor known to be immunosuppressive through these mechanisms and others is breast cancer [20, 21]. In Chapter 6 we use a mouse model of breast cancer to investigate this opposite role of inflammation in potentially decreasing tumorigenesis through the use of an attenuated strain of *Salmonella typhimurium.* The supposition of these studies is that the inoculation of bacteria will facilitate a shift in the immunosuppressive tumor microenvironment and drive localized immune cell infiltration and inflammation. In a tumor that uses immune evasion as a mechanism for growth and dissemination, this could lead to recognition and destruction of tumor cells.

Collectively, the following work contributes to our knowledge pertaining to the complicated role of inflammation in tumorigenesis. Though a great deal of research has been done, more is certainly needed. The purpose of our studies and this body of work is to summarize our investigations into these dynamic relationships using mouse models of clinically relevant tumors in human and veterinary patients.

References

1. Balkwill F, Mantovani A. Inflammation and cancer: back to Virchow? Lancet. 2001; 357: 539-45. doi: 10.1016/s0140-6736(00)04046-0.

2. Gakis G. The role of inflammation in bladder cancer. Adv Exp Med Biol. 2014; 816: 183-96. doi: 10.1007/978-3-0348-0837-8_8.

3. Qadri Q, Rasool R, Gulzar GM, Naqash S, Shah ZA. H. pylori infection, inflammation and gastric cancer. J Gastrointest Cancer. 2014; 45: 126-32. doi: 10.1007/s12029-014-9583-1.

4. Bishayee A. The role of inflammation and liver cancer. Adv Exp Med Biol. 2014; 816: 401-35. doi: 10.1007/978-3-0348-0837-8_16.

5. Grivennikov SI. Inflammation and colorectal cancer: colitis-associated neoplasia. Semin Immunopathol. 2013; 35: 229-44. doi: 10.1007/s00281-012-0352-6.

6. Westbom CM, Shukla A, MacPherson MB, Yasewicz EC, Miller JM, Beuschel SL, Steele C, Pass HI, Vacek PM, Shukla A. CREB-induced inflammation is important for malignant mesothelioma growth. Am J Pathol. 2014; 184: 2816-27. doi: 10.1016/j.ajpath.2014.06.008.

7. Gomes M, Teixeira AL, Coelho A, Araujo A, Medeiros R. The role of inflammation in lung cancer. Adv Exp Med Biol. 2014; 816: 1-23. doi: 10.1007/978-3-0348-0837-8_1.

8. Hanahan D, Weinberg RA. Hallmarks of cancer: the next generation. Cell. 2011; 144: 646-74. doi: 10.1016/j.cell.2011.02.013.

9. Mitchell JK, Lemon SM, McGivern DR. How do persistent infections with hepatitis C virus cause liver cancer? Curr Opin Virol. 2015; 14: 101-8. doi: 10.1016/j.coviro.2015.09.003.

10. de Oliveria Andrade LJ, D'Oliveira A, Melo RC, De Souza EC, Costa Silva CA, Parana R. Association between hepatitis C and hepatocellular carcinoma. J Glob Infect Dis. 2009; 1: 33-7. doi: 10.4103/0974-777x.52979.

11. Tennant BC, Toshkov IA, Peek SF, Jacob JR, Menne S, Hornbuckle WE, Schinazi RD, Korba BE, Cote PJ, Gerin JL. Hepatocellular carcinoma in the woodchuck model of hepatitis B virus infection. Gastroenterology. 2004; 127: S283-93. doi:

12. Adcock IM, Caramori G, Barnes PJ. Chronic obstructive pulmonary disease and lung cancer: new molecular insights. Respiration. 2011; 81: 265-84. doi: 10.1159/000324601.

13. Durham AL, Adcock IM. The relationship between COPD and lung cancer. Lung Cancer. 2015; 90: 121-7. doi: 10.1016/j.lungcan.2015.08.017.

14. Rowell JL, McCarthy DO, Alvarez CE. Dog models of naturally occurring cancer. Trends Mol Med. 2011; 17: 380-8. doi: 10.1016/j.molmed.2011.02.004.

15. Gabrilovich DI, Nagaraj S. Myeloid-derived suppressor cells as regulators of the immune system. Nat Rev Immunol. 2009; 9: 162-74. doi: 10.1038/nri2506.

16. Cuenca AG, Delano MJ, Kelly-Scumpia KM, Moreno C, Scumpia PO, Laface DM, Heyworth PG, Efron PA, Moldawer LL. A paradoxical role for myeloid-derived suppressor cells in sepsis and trauma. Mol Med. 2011; 17: 281-92. doi: 10.2119/molmed.2010.00178.

17. Marvel D, Gabrilovich DI. Myeloid-derived suppressor cells in the tumor microenvironment: expect the unexpected. J Clin Invest. 2015; 125: 3356-64. doi: 10.1172/jci80005.

18. Blidner AG, Salatino M, Mascanfroni ID, Diament MJ, Bal de Kier Joffe E, Jasnis MA, Klein SM, Rabinovich GA. Differential response of myeloid-derived suppressor cells to the

nonsteroidal anti-inflammatory agent indomethacin in tumor-associated and tumor-free microenvironments. J Immunol. 2015; 194: 3452-62. doi: 10.4049/jimmunol.1401144.

19. Mantovani A, Sozzani S, Locati M, Allavena P, Sica A. Macrophage polarization: tumor-associated macrophages as a paradigm for polarized M2 mononuclear phagocytes. Trends Immunol. 2002; 23: 549-55. doi:

20. Yu J, Du W, Yan F, Wang Y, Li H, Cao S, Yu W, Shen C, Liu J, Ren X. Myeloid-derived suppressor cells suppress antitumor immune responses through IDO expression and correlate with lymph node metastasis in patients with breast cancer. J Immunol. 2013; 190: 3783-97. doi: 10.4049/jimmunol.1201449.

21. Sousa S, Brion R, Lintunen M, Kronqvist P, Sandholm J, Monkkonen J, Kellokumpu-Lehtinen PL, Lauttia S, Tynninen O, Joensuu H, Heymann D, Maatta JA. Human breast cancer cells educate macrophages toward the M2 activation status. Breast Cancer Res. 2015; 17: 101. doi: 10.1186/s13058-015-0621-0.

Chapter 2

Literature review: A Review of Histiocytic Sarcoma in Veterinary and Human Medicine

Coutermarsh-Ott, SL

Abstract

Histiocytic sarcoma (HS) is an uncommon and poorly studied disease in both human and veterinary medicine. It is well-characterized to arise from a dendritic cell or macrophage origin in dogs, whereas in humans, the cell of origin is somewhat inconsistent and most often simply termed histiocytic. In the following work, the literature exploring HS in dogs and humans is reviewed with additional consideration for current studies investigating mechanisms of disease. In addition to highlighting the need for additional research on HS in general, the review also speculates on new and emerging therapeutic technologies.

Introduction

Histiocytic sarcoma (HS) is an uncommonly diagnosed tumor in veterinary medicine and an exceptionally rare tumor in humans. Because of this, a paucity of information is currently available investigating this disease. The majority of information in human medicine comes from scattered case reports with limited literature reviews. In veterinary medicine the situation is slightly improved, however, similar to human medicine, few studies have evaluated the epidemiology, incidence, and clinical characteristics of the disease. While in veterinary medicine, primarily in dogs, the tumor is known to arise from a dendritic cell or macrophage, the cell of origin in human tumors is not well-defined. In the following pages, we attempt to review the current literature available for HS in human and veterinary medicine.

HS in veterinary medicine

In veterinary medicine, HS is a disease primarily of dogs. However, individual case reports of the disease in cats, ferrets, rabbits, horses, hippopotamuses, cows, and hedgehogs have been described [1-8]. In the dog, it can present in 2 forms, either localized or disseminated. In the localized form, solitary tumors are identified in the subcutis, spleen, liver, periarticular tissues, lung, CNS or other tissues [1, 9]. In the disseminated form, multiple, poorly discernible tumors are readily identified in multiple organs. Clinically, HS can have a variable presentation depending on the organ systems affected. However, non-specific symptoms such as lethargy and inappetence are common [1]. The disease can occur in any age, breed, or sex of dog but is most commonly diagnosed in older, large breed animals. There are well-documented breed predispositions in the Bernese mountain dog and Flat-coated retriever; however, other predispositions are potentially emerging such as recently described in a population of Miniature schnauzers [10-12]. Histologically these patients are diagnosed with an infiltrative neoplasm

composed of histiocytic cells that efface normal tissue architecture. Cells often exhibit multiple criteria of malignancy such as cyto- and karyomegaly, frequent and often bizarre mitoses, and marked pleomorphism (**Figure 1**). The initial diagnosis is made by the identification of these cells histologically, but confirmatory testing is often necessary. This typically is done through immunohistochemistry utilizing a host of different markers discussed later. In most cases, the prognosis for HS is generally poor as it is associated with high rates of metastasis and limited treatment options. However, some studies have shown that periarticular tumors may be associated with a better prognosis while those diagnosed with a sub-type termed hemophagocytic HS are associated with a grave prognosis [13, 14].

The Bernese mountain dog and Flat-coated retriever are well-described as having breed predispositions to the development of HS [1]. In fact, two studies documenting the causes of death in populations of Dutch and Swiss Bernese mountain dogs found the cause of death to be HS in 15.3% and 6% of all Bernese mountain dog deaths respectively [11, 15]. The Dutch study also evaluated causes of death in Flat-coated retrievers and found that 14.3% succumbed to the disease [11]. Though common in both breeds, there are documented differences in both clinical presentation and genetic anomalies. In Bernese mountain dogs, the most common manifestation of the disease is the disseminated form, previously termed malignant histiocytosis [16]. One study found that out of a population of 89 Bernese mountain dogs diagnosed with HS, more than 55% of the dogs had involvement of multiple internal organs at the time of diagnosis and the spleen and lung/mediastinum were the most common sites involved [17]. This is different than in the Flat-coated retriever where the most common clinical manifestation is a localized mass within the muscle of the limb or adjacent to a joint [10, 16]. In one study evaluating 180 Flat-coated retrievers diagnosed with HS, 56.7% of the lesions occurred on the limb while only

26.4% of the lesions occurred within visceral organs [18]. However, of those visceral tumors, the spleen and lung were the most common organs involved, which is similar to what is seen in Bernese mountain dogs [18]. Initial studies looking for predisposing causes of HS in Bernese mountain dogs found that, in cases of periarticular HS, pre-existing joint inflammation was found to be highly correlated with the development of a tumor in that same joint [19, 20]. This was shown to be true not just in Bernese mountain dogs but in the canine population as a whole [21]. Studies evaluating copy number aberrations (CNAs) have identified similar genetic alterations in HS of both breeds [16]. These include a loss of heterozygosity mutation in the region of the *CDKN2A/B* locus, deletions of regions of *RB1*, and deletions of regions of *PTEN [16]*. All three are important tumor suppressors. CDKN2A and RB1 act by regulating cell cycle progression while PTEN acts through the negative regulation of AKT signaling. Interestingly, these authors also describe a gain in the *TP53* locus. TP53 is also a tumor suppressor that acts through multiple different pathways and the relevance this gain of function mutation is unknown [16]. Recent studies have identified an additional gain-of-function mutation in the gene *PTPN11* in non-hemophagocytic histiocytic sarcomas from Bernese mountain dogs [22]. *PTPN11* encodes for the non-receptor protein tyrosine phosphatase, SHP2, which has been shown to be involved in a wide array of biological functions including growth factor signaling [23].

In all animals, the diagnosis of HS can be somewhat challenging. The morphology of the tumor can be highly suggestive of HS but is certainly not pathognomonic. Further complicating this is the fact that, at least in dogs, HS can derive from two different types of histiocytic cells. HS, or non-hemophagocytic HS, arises from tissue specific interstitial dendritic cells [1]. These are histiocytic cells of myeloid origin that reside in many different tissue types and are responsible for sampling antigens, migrating to local lymph nodes and presenting that antigen to

cells of the adaptive immune system. Hemophagocytic HS (HHS) arises from splenic macrophages responsible for sampling circulating antigens and phagocytosing senescent cells [24]. Owing to the nature of the cell type, non-hemophagocytic HS can be diagnosed in many different tissue types including lung, lymph node, skin and subcutis, spleen, and periarticular tissues [1]. HHS is diagnosed in the spleen and is often associated with significant hematologic abnormalities including thrombocytopenia and anemia due to the phagocytosis of patient blood cells by tumor cells [24]. A variety of immunohistochemical markers have been investigated to aid in the diagnosis of these tumors and have included CD18, Iba-1, CD204, CD163, and others [1, 25, 26]. CD18 is the β subunit of a family of integrins found on leukocytes. Thus, it is a pan-leukocyte marker that will positively stain most leukocytes [27]. It is useful in distinguishing HS from a carcinoma or a non-hematologic sarcoma but otherwise cannot differentiate it from other hematologic malignancies such as lymphoma. Iba-1 is a calcium-binding protein that has been shown in previous studies to be a marker of microglia as well as cells of the monocyte/macrophage system in mice [28]. Investigations in canine round cell tumors showed that it was a good marker of canine HS with no cross-reactivity in other canine round cell tumors and/or hematologic malignancies [25]. It is, however, unable to differentiate between neoplasms of dendritic cell versus macrophage origin [25]. CD204 is a macrophage scavenger receptor that has also been evaluated as a diagnostic marker. Studies investigating this marker have shown that all HS samples evaluated stained strongly positively while only one sample out of 81 other round cell tumors and sarcomas was positive [26, 29]. However, tumors that were determined to be hemophagocytic and thus of macrophage origin were also positive [29]. Thus, improvements in IHC markers for differentiating HS from other mesenchymal tumors have been made, but the only marker currently able to differentiate HS of dendritic cell versus macrophage origin is

CD11d. CD11d is the alpha subunit of the β2 integrin protein and is upregulated in inflammatory macrophages [30]. It is found in macrophages from the spleen and bone marrow and, when positive, is diagnostic for HHS. Unfortunately, CD11d IHC has not been widely validated. Also the canine CD11d antibody performs best on frozen tissue samples which are not as commonly available as formalin-fixed, paraffin-embedded tissues (FFPE). Studies investigating more rapid, widely available diagnostic tests that work equally well on FFPE tissues could improve management of patients diagnosed with this disease.

Treatment for the disease in canines is limited and can have variable effects on prognosis. Chemotherapy is almost always indicated whether or not surgical excision is possible. Often, disease that remains localized, such as within the spleen, subcutis, or periarticular region, may be amenable to surgical excision. However, removal of the primary tumor does not negate the possibility of microscopic disease or presence of metastasis. The most common chemotherapeutic currently in use is lomustine (CCNU); however, doxorubicin, combination protocols, liposomal clodronate, and bisphosphonates, have been used with variable success [31-35]. In general, chemotherapy response rates range from 29% to 56% and overall survival times average from 55 to 391 days [13, 32, 36]. Beyond surgery and chemotherapy, other experimental approaches have yielded optimistic results. For example, one case report briefly describes the successful treatment and palliation of a large, periarticular HS in a canine with the novel therapeutic irreversible electroporation (IRE) [37]. In this case, surgical excision was not possible due to tumor size and pre-existing osteoarthritis. IRE treatment in combination with CCNU chemotherapy was ultimately curative for this patient (personal communication).

Despite the published variation in treatment success rates, studies have identified certain parameters that can be associated with prognosis. One study evaluating dogs diagnosed with

periarticular HS or non-periarticular HS (all other forms) found that periarticular HS is associated with a better prognosis, improved response to treatment, and longer survival times [13]. One potential explanation for this is that tumors of the limb producing limping or lameness may be noticed earlier and more easily by owners. Tumors located in the viscera often produce non-specific, waxing and waning signs and thus may not warrant veterinary visits until disease is more advanced. A second potential explanation for this finding is that, depending on the location and size of the tumor, leg amputation may produce much wider surgical margins than possible for visceral tumors. Others studies evaluating prognosis in canine HS have found that a diagnosis of disseminated HS, palliative treatment only, and/or concurrent treatment with corticosteroids were found to be negative prognostic indicators with decreased survival [14].

Histiocytic sarcoma in humans

The incidence of HS, formerly known as "true" histiocytic lymphoma, in humans is exceptionally low and has been reported to make up less than 1% of all hematopoietic tumors diagnosed in human patients [38]. As in dogs, it is defined to arise from cells of the macrophage/monocyte system, however, a lack of consensus regarding diagnostic criteria and terminology have made much of the data available for HS in humans questionable. In fact, many cases originally diagnosed as HS have been postulated to actually represent cases of non-Hodgkin like lymphomas [38]. However, recently, better immunohistochemical and genetic techniques have improved diagnostic accuracy and consistency. In general, HS in humans can be diagnosed in any age group but is more common in adult to geriatric individuals [38]. In one study evaluating 18 cases including both nodal and extra-nodal HS, the median patient age was 46 years-old with a range from 6 months to 74 years-old [39]. A second study evaluating 14 cases of only extranodal HS found similar results with a median patient age of 55 and a range

from 15 to 89 years-old [40]. HS most commonly involves the lymph nodes but can also occur in extra-nodal sites such as the spleen, gastrointestinal tract, uterus, lung, soft tissue, skin, and CNS [38, 41, 42]. Like in dogs, HS in humans can be a localized or disseminated disease. Unfortunately, discordance exists in the diagnostic terms used to describe the disseminated form. Depending on the literature source, it has been characterized as malignant histiocytosis, disseminated histiocytic sarcoma, and/or disseminated histiocytosis [43, 44]. Because of the wide variety of potential organs affected and/or the possibility of localized or disseminated disease, the clinical picture can vary widely depending on the primary organ affected. The most common presenting signs are often systemic signs such as fever, lethargy, weight loss and weakness [38].

Diagnosis of HS in humans can be difficult and is currently defined as "a malignant proliferation of cells showing morphologic and immunophenotypic features of mature tissue histiocytes" [38]. Unlike in dogs where the cell of origin of HS can be of dendritic cell or macrophage origin, the human literature describes only a histiocytic cell of origin. Morphologically these tumors look fairly similar to what is seen in dogs. Sheets of round to spindle histiocytic cells efface normal tissue architecture. Neoplastic cells are often pleomorphic with multinucleation and bizarre cells being fairly common [38]. These tumors can be infiltrated by a variable degree of reactive inflammatory cells including neutrophils, macrophages, and lymphocytes; however, this has been found to be most severe and consistent in tumors within the central nervous system [38, 42, 45, 46]. A multitude of histiocytic markers are available for human samples and include: CD163, CD68, CD11c, CD14, CD15, CD43, CD45, MAC387, and HLA-DR. Additionally, tumor samples should be tested to rule out other potentially, morphologically similar tumor types such as B and T cell markers for lymphoma, CD1a for

Langerhans cell origin, CD21 and CD23 for follicular dendritic cell origin, pancytokeratin for carcinomas, and Melan A for melanocytic tumors [38].

In humans, unlike in dogs, there have been no well-defined sub-types of HS such as HHS in dogs. However, it appears that there is a poorly defined continuum of histiocytic proliferations associated with host cell phagocytosis. These range from a benign proliferation of histiocytes in response to concurrent infectious/inflammatory diseases termed hemophagocytic syndrome (HPS) to effacement of host tissues by neoplastic histiocytes in the disseminated form of HS. Initial studies investigating the differences between malignant histiocytosis and HPS were able to show that individuals infected with active herpes virus exhibited a proliferation of histiocytes within lymph nodes, bone marrow, liver, spleen and, occasionally, the leptomeninges [47]. These proliferations were cytologically benign, expanded but did not efface tissue architecture, and were associated with marked erythrophagocytosis [47]. This is in contrast to malignant histiocytosis, or disseminated HS, where neoplastic cells are quite pleomorphic, efface tissue architecture and may or may not phagocytize host erythrocytes and leukocytes. A subsequent case report documenting a splenic HS in a 71 year-old woman described a concurrent proliferation of phagocytic histiocytes "morphologically indistinguishable from reactive macrophages" [48]. These cells exhibited marked erythro- and lymphophagocytosis and were found throughout the tumor and unaffected splenic parenchyma [48]. In a second report, the authors describe a case of a 24 year-old man diagnosed concurrently with a malignant histiocytosis of the spleen, a mediastinal germ cell tumor and concurrent HPS [49]. In this case report it is unclear if the authors consider the HPS a direct result of ingestion of erythrocytes by neoplastic cells or if they believe there is also a benign proliferation of reactive histiocytes in response to the presence of concurrent tumors. In dogs, hemophagocytic HS has been shown to

arise from a macrophage origin and that tumor cells will actively phagocytose the red and white blood cells of the host [24]. This leads to secondary cytopenias, most notable anemia and thrombocytopenia [24]. In humans, however, hemophagocytic syndrome is considered a primary or secondary, benign proliferation and activation of histiocytes ultimately leading to a large release of cytotoxic chemokines and cytokines [49]. In both previously mentioned reports, patients suffered from severe anemia and thrombocytopenia [48, 49]. These findings are similar to the hemophagocytic form of HS described in dogs. However, IHC for CD11d was not performed in either case. Many of the immunohistochemical markers used for diagnosis in these cases can cross-react among different histiocytic cells. Thus, additional case studies using CD11d are necessary to characterize whether or not HPS in concurrence with HS in humans may or may not represent a hemophagocytic form of HS as seen in dogs.

Another interesting characteristic of HS in humans that has not been well-investigated in dogs is a proposed relationship between HS and lymphoma. Initial classification of HS by the World Health Organization (WHO) in 2001 defined HS as those tumors morphologically and immunophenotypically consistent with histiocytic cells, but that also lacked clonal B and T cell rearrangements characteristically found in lymphomas [38]. However, a study published in 2008 suggested that histiocytic/dendritic cell neoplasms occurring concurrently or up to 12 years following the development of follicular lymphoma not only had clonal B cell rearrangements, but also that these rearrangements were identical to the concurrent or previously diagnosed lymphoma [50]. Furthering this, Chen et al performed a study in 2009 evaluating the presence of clonal immunoglobulin receptor gene rearrangements in HS patients with no concurrent or previous history of any type of lymphoma [51]. Indeed, these authors were able to show that in 11 out of 23 tumors, there were clonal rearrangements in the B cell receptor [51]. In these

experiments, they were also able to show that of the 7 tumors found to have clonal gene rearrangements, 4 of them showed nuclear positivity for Oct2 via immunohistochemistry [51]. Oct2 is a B cell transcription factor important in the proliferation and differentiation of B cells. Since then, numerous case reports of HS with gene rearrangements either in conjunction with or following mantle zone lymphoma, chronic lymphocytic/small lymphocytic lymphoma, and diffuse large B cell lymphoma have been reported [52-56]. Though the significance of these findings is largely unknown, these reports suggest that hematopoietic derived cells may in fact exhibit a certain degree of plasticity.

Few studies have evaluated the presence of gene mutations associated with the development of HS in humans. One study utilized immunohistochemistry to evaluate the expression of the tumor suppressors PTEN and $p16^{INK4A}$ in human HS samples and found that there was loss of these proteins in 40% and 50% of evaluated cases respectively [57]. They subsequently found, through nested PCR, deletions of exons 6 to 9 in *PTEN* and through methylation-specific PCR identified methylations of the promoters for $p16^{INK4a}$ and $p14^{ARF}$ [57]. Another author investigated somatic mutations in 5 cases of HS [58]. In these studies, several *BRAF* mutations were identified in 3 out of 5 cases [58]. *BRAF* is a proto-oncogene encoding for the protein B-raf. B-raf is a serine-threonine kinase involved in the regulation of cell growth through the regulation of MAPK/ERK signaling. This study also revealed mutations in *KRAS*, *PTPN1*, and *PIK3CA* each in a single patient sample [58]. Other studies have confirmed the presence of *BRAF* mutations in HS, however, these studies have collectively identified a specific amino acid substitution identified as $BRAF^{V600E}$ not identified in the aforementioned study [59-61].

In human medicine, like in veterinary medicine, there is no general consensus on treating HS. In the case of localized tumors, these can be surgically resected though recurrence is common [40]. In most cases, whether surgical excision is possible or not, treatment includes the use of radiation or chemotherapy. Case reports have described treatment with combination chemotherapies and autologous stem cell transplantation [62-64]. Despite treatment, most patients succumb to the disease within 2 years of diagnosis [38]. One retrospective study found that there were no significant differences in overall survival rates for patients diagnosed with localized or metastatic disease [65]. Moreover, of those with localized disease who underwent surgical excision with complete margins, there were no significant differences in overall survival with the use of adjuvant or neo-adjuvant chemotherapy [65].

Mechanisms of Disease

Because HS is an uncommon disease in veterinary medicine and extremely rare in humans, a paucity of research has been done evaluating molecular mechanisms of disease. Early studies using genetically modified mouse models found that the tumor suppressors PTEN and IN4A/ARF play a role in the spontaneous development of HS in mice [57]. In these studies, *Pten*$^{+/-}$ *Ink4a/Arf*$^{-/-}$ mice developed biphasic tumors composed of both lymphomatous and histiocytic cellular components [57]. PTEN is an important tumor suppressor in all species that is responsible for the de-phosphorylation of PIP3, an important substrate involved in AKT signaling. *Ink4a/Arf* is a locus that encodes for the tumor suppressors p16^{INK4A} and p14^{ARF} which are responsible for regulating pRB and p53 respectively. Interestingly, when evaluated by Southern blot analysis, the histiocytic portions of these tumors had deletion of *Pten* in approximately 13/40 tumors evaluated [57]. This is opposed to the lymphomatous tumors where 31/32 maintained the wild type allele [57]. Moreover, the authors performed Western blotting to

evaluate levels of phosphorylated AKT and found that there were increases in HS tumors but no significant increases in the lymphomas when compared to normal wild-type animals [57]. Collectively, this suggests that PTEN plays an important role in the development of HS but not so much in the development of lymphoma. This finding is supported by previously mentioned studies identifying the presence of gene deletions in *PTEN* in HS of Bernese mountain dogs, Flat-coated retrievers, and humans [16, 57].

Recently, studies have implicated a novel tumor suppressor in the development and progression of carcinogen-induced HS in mice [66]. NLRX1 is a regulatory NLR that has been best characterized in its regulation of NF-κB signaling, autophagy, Type I interferon production, and ROS signaling in host viral infections [67-69]. Recently it has been suggested to play a role as a tumor suppressor by regulating cell death [70, 71]. Therefore, we hypothesized that NLRX1 would function as a tumor suppressor in a mouse model of HS. Genetically modified mice deficient in NLRX1 were exposed to the carcinogen urethane over a 14 week period [66]. These mice developed marked splenomegaly that was subsequently diagnosed as HS [66]. Using gene expression analysis, these studies also showed that the development of these tumors was associated with increases in NF-κB and AKT signaling [66].

Additional studies in mice evaluating novel chemotherapeutics have further revealed potential mechanisms of HS development and progression. Recent studies have evaluated the use of the novel therapeutic dasatinib for the treatment of HS [72]. Dasatinib is a Bcr-Abl and Src family tyrosine kinase inhibitor approved for humans diagnosed with chronic myelogenous leukemia or Philadelphia-chromosome positive acute lymphoblastic leukemia [73, 74]. Initial studies screened 171 compounds, including dasatinib, in an attempt to identify novel drugs that would inhibit growth of multiple canine HS cell lines [72]. These found that dasatinib

selectively reduced the growth of HS cells without affecting the growth of other tumor cell lines suggesting it as a potential targeted therapy for HS [72]. In an attempt to determine mechanism of action, the authors were able to successfully generate a mouse xenograft model by injecting a previously characterized canine HS cell line, CHS-1, into nude mice. Their results confirmed that indeed treatment with dasatinib did reduce overall tumor volume, which was associated with a decreased mitotic index, decreased Ki-67 expression, and increased apoptotic index [72]. However, the mechanism of action was not defined. Another study sought to investigate the drug YM155 as a potential novel chemotherapeutic. YM155, or Sepantronium bromide, is a small molecule inhibitor of the protein survivin. Survivin is a member of the inhibitors of apoptosis (IAP) family that act primarily to inhibit cellular apoptosis. Initial studies using canine HS cell lines showed that expression of the survivin gene was increased in HS cell lines when compared to normal canine fibroblasts [75]. When the survivin gene was knocked down using siRNA, HS cells exhibited a reduced viability, higher levels of apoptosis, and enhanced susceptibility to the chemotherapeutic drugs lomustine and doxorubicin [75]. Later studies showed that the survivin gene expression also correlated with clinical behavior in canine samples [76]. Using quantitative PCR, the authors showed that those dogs with high levels of survivin gene expression had shorter disease free intervals and overall survival times than those with decreased survivin gene expression [76]. In a separate study using a xenograft model of canine HS in which HS cell lines were transplanted into nude mice, they showed that the inhibition of survivin by the drug YM155 reduced overall tumor volume, enhanced the tumor cells sensitivity to the chemotherapeutic lomustine, and reduced the incidence of pulmonary metastasis [77]. Overall, the recent development of novel mouse models of HS have resulted in a significant expansion of potential therapeutic targets and molecules for further studies.

Concluding remarks

Histiocytic sarcoma is a poorly studied disease in both dogs and humans. However, the current literature in dogs seems to have better defined the disease in terms of cell origin and diagnostic criteria. This is imperative in order to be able to make collective conclusions about disease characteristics such as prevalence, prognosis, and treatment outcomes. In human medicine, improved genetic and immunohistochemical methods have recently been identified to better diagnose HS. However, there still exists a great deal of disagreement on a uniform terminology and set of diagnostic criteria for describing the disease. These discrepancies are scattered throughout the literature and make it difficult to study and fully characterize clinical characteristics of HS in humans. Thankfully, the importance of translational medicine and comparative oncology is increasingly well-recognized. Thus, HS in dogs may very well provide a framework for our abilities to study such a rare disease in human medicine.

References

1. Moore PF. A review of histiocytic diseases of dogs and cats. Vet Pathol. 2014; 51: 167-84. doi: 10.1177/0300985813510413.

2. Scurrell E, Trott A, Rozmanec M, Belford CJ. Ocular histiocytic sarcoma in a cat. Vet Ophthalmol. 2013; 16 Suppl 1: 173-6. doi: 10.1111/vop.12052.

3. Warschau M, Hoffmann M, Dziallas P, Hansmann F, Baumgartner W, Mischke R, Cichowski S, Fehr M. Invasive histiocytic sarcoma of the lumbar spine in a ferret (Mustela putorius furo). J Small Anim Pract. 2017; 58: 115-8. doi: 10.1111/jsap.12632.

4. Ishimori M, Michishita M, Yoshimura H, Azakami D, Ochiai K, Ishiwata T, Takahashi K. Disseminated histiocytic sarcoma with hemophagocytosis in a rabbit. J Vet Med Sci. 2017; 79: 1503-6. doi: 10.1292/jvms.17-0297.

5. Paciello O, Passantino G, Costagliola A, Papparella S, Perillo A. Histiocytic sarcoma of the nasal cavity in a horse. Res Vet Sci. 2013; 94: 648-50. doi: 10.1016/j.rvsc.2013.01.005.

6. Ogihara K, Itoh T, Mizuno Y, Tamukai K, Madarame H. Disseminated Histiocytic Sarcoma in an African Hedgehog (Atelerix albiventris). J Comp Pathol. 2016; 155: 361-4. doi: 10.1016/j.jcpa.2016.09.001.

7. Matsuda K, Nomoto H, Kawamura Y, Someya Y, Koiwa M, Taniyama H. Hemophagocytic histiocytic sarcoma in a Japanese black cow. Vet Pathol. 2010; 47: 339-42. doi: 10.1177/0300985809358428.

8. da Costa LF, Malta MC, Tinoco HP, de Medeiros LB, Bittar AL, Hoffmann AR, Pierezan F, da Paixao TA, Santos RL. SYSTEMIC HISTIOCYTIC SARCOMA IN A COMMON HIPPOPOTAMUS (HIPPOPOTAMUS AMPHIBIUS). J Zoo Wildl Med. 2016; 47: 650-3. doi: 10.1638/2015-0271.1.

9. Ide T, Uchida K, Kagawa Y, Suzuki K, Nakayama H. Pathological and immunohistochemical features of subdural histiocytic sarcomas in 15 dogs. J Vet Diagn Invest. 2011; 23: 127-32. doi: 10.1177/104063871102300123.

10. Fidel J, Schiller I, Hauser B, Jausi Y, Rohrer-Bley C, Roos M, Kaser-Hotz B. Histiocytic sarcomas in flat-coated retrievers: a summary of 37 cases (November 1998-March 2005). Vet Comp Oncol. 2006; 4: 63-74. doi: 10.1111/j.1476-5810.2006.00090.x.

11. Erich SA, Rutteman GR, Teske E. Causes of death and the impact of histiocytic sarcoma on the life expectancy of the Dutch population of Bernese mountain dogs and Flat-coated retrievers. Vet J. 2013; 198: 678-83. doi: 10.1016/j.tvjl.2013.09.062.

12. Lenz JA, Furrow E, Craig LE, Cannon CM. Histiocytic sarcoma in 14 miniature schnauzers - a new breed predisposition? J Small Anim Pract. 2017; 58: 461-7. doi: 10.1111/jsap.12688.

13. Klahn SL, Kitchell BE, Dervisis NG. Evaluation and comparison of outcomes in dogs with periarticular and nonperiarticular histiocytic sarcoma. J Am Vet Med Assoc. 2011; 239: 90-6. doi: 10.2460/javma.239.1.90.

14. Dervisis NG, Kiupel M, Qin Q, Cesario L. Clinical prognostic factors in canine histiocytic sarcoma. Vet Comp Oncol. 2016. doi: 10.1111/vco.12252.

15. Klopfenstein M, Howard J, Rossetti M, Geissbuhler U. Life expectancy and causes of death in Bernese mountain dogs in Switzerland. BMC Vet Res. 2016; 12: 153. doi: 10.1186/s12917-016-0782-9.

16. Hedan B, Thomas R, Motsinger-Reif A, Abadie J, Andre C, Cullen J, Breen M. Molecular cytogenetic characterization of canine histiocytic sarcoma: A spontaneous model for human histiocytic cancer identifies deletion of tumor suppressor genes and highlights influence

of genetic background on tumor behavior. BMC Cancer. 2011; 11: 201. doi: 10.1186/1471-2407-11-201.

17. Abadie J, Hedan B, Cadieu E, De Brito C, Devauchelle P, Bourgain C, Parker HG, Vaysse A, Margaritte-Jeannin P, Galibert F, Ostrander EA, Andre C. Epidemiology, pathology, and genetics of histiocytic sarcoma in the Bernese mountain dog breed. J Hered. 2009; 100 Suppl 1: S19-27. doi: 10.1093/jhered/esp039.

18. Constantino-Casas F, Mayhew D, Hoather TM, Dobson JM. The clinical presentation and histopathologic-immunohistochemical classification of histiocytic sarcomas in the Flat Coated Retriever. Vet Pathol. 2011; 48: 764-71. doi: 10.1177/0300985810385153.

19. Ruple A, Morley PS. Risk Factors Associated with Development of Histiocytic Sarcoma in Bernese Mountain Dogs. J Vet Intern Med. 2016; 30: 1197-203. doi: 10.1111/jvim.13964.

20. van Kuijk L, van Ginkel K, de Vos JP, Brearley MJ, Butinar J, Gielen I, van Garderen E, Chiers K, Verhoeven PS. Peri-articular histiocytic sarcoma and previous joint disease in Bernese Mountain Dogs. J Vet Intern Med. 2013; 27: 293-9. doi: 10.1111/jvim.12059.

21. Manor EK, Craig LE, Sun X, Cannon CM. Prior joint disease is associated with increased risk of periarticular histiocytic sarcoma in dogs. Vet Comp Oncol. 2017. doi: 10.1111/vco.12338.

22. Thaiwong T, Sirivisoot S, Takada M, Yuzbasiyan-Gurkan V, Kiupel M. Gain-of-function mutation in PTPN11 in histiocytic sarcomas of Bernese Mountain Dogs. Vet Comp Oncol. 2017. doi: 10.1111/vco.12357.

23. Neel BG, Gu H, Pao L. The 'Shp'ing news: SH2 domain-containing tyrosine phosphatases in cell signaling. Trends Biochem Sci. 2003; 28: 284-93. doi: 10.1016/s0968-0004(03)00091-4.

24. Moore PF, Affolter VK, Vernau W. Canine hemophagocytic histiocytic sarcoma: a proliferative disorder of CD11d+ macrophages. Vet Pathol. 2006; 43: 632-45. doi: 10.1354/vp.43-5-632.

25. Pierezan F, Mansell J, Ambrus A, Rodrigues Hoffmann A. Immunohistochemical expression of ionized calcium binding adapter molecule 1 in cutaneous histiocytic proliferative, neoplastic and inflammatory disorders of dogs and cats. J Comp Pathol. 2014; 151: 347-51. doi: 10.1016/j.jcpa.2014.07.003.

26. Kato Y, Murakami M, Hoshino Y, Mori T, Maruo K, Hirata A, Nakagawa TL, Yanai T, Sakai H. The class A macrophage scavenger receptor CD204 is a useful immunohistochemical marker of canine histiocytic sarcoma. J Comp Pathol. 2013; 148: 188-96. doi: 10.1016/j.jcpa.2012.06.009.

27. Danilenko DM, Moore PF, Rossitto PV. Canine leukocyte cell adhesion molecules (LeuCAMs): characterization of the CD11/CD18 family. Tissue Antigens. 1992; 40: 13-21. doi:

28. Kohler C. Allograft inflammatory factor-1/Ionized calcium-binding adapter molecule 1 is specifically expressed by most subpopulations of macrophages and spermatids in testis. Cell Tissue Res. 2007; 330: 291-302. doi: 10.1007/s00441-007-0474-7.

29. Kato Y, Funato R, Hirata A, Murakami M, Mori T, Maruo K, Yanai T, Sakai H. Immunocytochemical detection of the class A macrophage scavenger receptor CD204 using air-dried cytologic smears of canine histiocytic sarcoma. Vet Clin Pathol. 2014; 43: 589-93. doi: 10.1111/vcp.12190.

30. Yakubenko VP, Belevych N, Mishchuk D, Schurin A, Lam SC, Ugarova TP. The role of integrin alpha D beta2 (CD11d/CD18) in monocyte/macrophage migration. Exp Cell Res. 2008; 314: 2569-78. doi: 10.1016/j.yexcr.2008.05.016.

31. Uno Y, Momoi Y, Watari T, Goitsuka R, Tsujimoto H, Shimada T, Ono K, Goto N, Hasegawa A. Malignant histiocytosis with multiple skin lesions in a dog. J Vet Med Sci. 1993; 55: 1059-61. doi:

32. Skorupski KA, Clifford CA, Paoloni MC, Lara-Garcia A, Barber L, Kent MS, LeBlanc AK, Sabhlok A, Mauldin EA, Shofer FS, Couto CG, Sorenmo KU. CCNU for the treatment of dogs with histiocytic sarcoma. J Vet Intern Med. 2007; 21: 121-6. doi:

33. Hafeman S, London C, Elmslie R, Dow S. Evaluation of liposomal clodronate for treatment of malignant histiocytosis in dogs. Cancer Immunol Immunother. 2010; 59: 441-52. doi: 10.1007/s00262-009-0763-y.

34. Kezer KA, Barber LG, Jennings SH. Efficacy of dacarbazine as a rescue agent for histiocytic sarcoma in dogs. Vet Comp Oncol. 2017. doi: 10.1111/vco.12314.

35. Moore AS, Taylor DP, Reppas G, Frimberger AE. Chemotherapy for dogs with lymph node metastasis from histiocytic sarcomas. Aust Vet J. 2017; 95: 37-40. doi: 10.1111/avj.12522.

36. Rassnick KM, Moore AS, Russell DS, Northrup NC, Kristal O, Bailey DB, Flory AB, Kiselow MA, Intile JL. Phase II, open-label trial of single-agent CCNU in dogs with previously untreated histiocytic sarcoma. J Vet Intern Med. 2010; 24: 1528-31. doi:

37. Neal RE, Garcia PA, Rossmeisl JH, Davalos RV. A study using irreversible electroporation to treat large, irregular tumors in a canine patient. Conf Proc IEEE Eng Med Biol Soc. 2010; 2010: 2747-50. doi: 10.1109/iembs.2010.5626372.

38. Takahashi E, Nakamura S. Histiocytic sarcoma : an updated literature review based on the 2008 WHO classification. J Clin Exp Hematop. 2013; 53: 1-8. doi:

39. Pileri SA, Grogan TM, Harris NL, Banks P, Campo E, Chan JK, Favera RD, Delsol G, De Wolf-Peeters C, Falini B, Gascoyne RD, Gaulard P, Gatter KC, et al. Tumours of histiocytes

and accessory dendritic cells: an immunohistochemical approach to classification from the International Lymphoma Study Group based on 61 cases. Histopathology. 2002; 41: 1-29. doi:

40. Hornick JL, Jaffe ES, Fletcher CD. Extranodal histiocytic sarcoma: clinicopathologic analysis of 14 cases of a rare epithelioid malignancy. Am J Surg Pathol. 2004; 28: 1133-44. doi:

41. Lee D, Kim YB, Chung SH, Lee SR, Byun CS, Han SU, Han JH. Primary gastric histiocytic sarcoma reminiscent of inflammatory pseudotumor: a case report with review of the literature. Korean J Pathol. 2014; 48: 258-62. doi: 10.4132/KoreanJPathol.2014.48.3.258.

42. Wu W, Tanrivermis Sayit A, Vinters HV, Pope W, Mirsadraei L, Said J. Primary central nervous system histiocytic sarcoma presenting as a postradiation sarcoma: case report and literature review. Hum Pathol. 2013; 44: 1177-83. doi: 10.1016/j.humpath.2012.11.002.

43. Mongkonsritragoon W, Li CY, Phyliky RL. True malignant histiocytosis. Mayo Clin Proc. 1998; 73: 520-8. doi: 10.4065/73.6.520.

44. Gatalica Z, Bilalovic N, Palazzo JP, Bender RP, Swensen J, Millis SZ, Vranic S, Von Hoff D, Arceci RJ. Disseminated histiocytoses biomarkers beyond BRAFV600E: frequent expression of PD-L1. Oncotarget. 2015; 6: 19819-25. doi: 10.18632/oncotarget.4378.

45. Cao M, Eshoa C, Schultz C, Black J, Zu Y, Chang CC. Primary central nervous system histiocytic sarcoma with relapse to mediastinum: a case report and review of the literature. Arch Pathol Lab Med. 2007; 131: 301-5. doi: 10.1043/1543-2165(2007)131[301:pcnshs]2.0.co;2.

46. Sun W, Nordberg ML, Fowler MR. Histiocytic sarcoma involving the central nervous system: clinical, immunohistochemical, and molecular genetic studies of a case with review of the literature. Am J Surg Pathol. 2003; 27: 258-65. doi:

47. Risdall RJ, McKenna RW, Nesbit ME, Krivit W, Balfour HH, Jr., Simmons RL, Brunning RD. Virus-associated hemophagocytic syndrome: a benign histiocytic proliferation distinct from malignant histiocytosis. Cancer. 1979; 44: 993-1002. doi:

48. Audouin J, Vercelli-Retta J, Le Tourneau A, Adida C, Camilleri-Broet S, Molina T, Diebold J. Primary histiocytic sarcoma of the spleen associated with erythrophagocytic histiocytosis. Pathol Res Pract. 2003; 199: 107-12. doi: 10.1078/0344-0338-00362.

49. Shinoda H, Yoshida A, Teruya-Feldstein J. Malignant histiocytoses/disseminated histiocytic sarcoma with hemophagocytic syndrome in a patient with mediastinal germ cell tumor. Appl Immunohistochem Mol Morphol. 2009; 17: 338-44. doi: 10.1097/PAI.0b013e3181897e8e.

50. Feldman AL, Arber DA, Pittaluga S, Martinez A, Burke JS, Raffeld M, Camos M, Warnke R, Jaffe ES. Clonally related follicular lymphomas and histiocytic/dendritic cell sarcomas: evidence for transdifferentiation of the follicular lymphoma clone. Blood. 2008; 111: 5433-9. doi: 10.1182/blood-2007-11-124792.

51. Chen W, Lau SK, Fong D, Wang J, Wang E, Arber DA, Weiss LM, Huang Q. High frequency of clonal immunoglobulin receptor gene rearrangements in sporadic histiocytic/dendritic cell sarcomas. Am J Surg Pathol. 2009; 33: 863-73. doi: 10.1097/PAS.0b013e31819287b8.

52. Verma A, Shet T. Concomitant follicular lymphoma and histiocytic sarcoma: A rare progression, trans-differentiation or co-occurrence? Indian J Pathol Microbiol. 2015; 58: 537-9. doi: 10.4103/0377-4929.168860.

53. Fernandez-Pol S, Bangs CD, Cherry A, Arber DA, Gratzinger D. Two cases of histiocytic sarcoma with BCL2 translocations and occult or subsequent follicular lymphoma. Hum Pathol. 2016; 55: 39-43. doi: 10.1016/j.humpath.2016.04.004.

54. Hure MC, Elco CP, Ward D, Hutchinson L, Meng X, Dorfman DM, Yu H. Histiocytic sarcoma arising from clonally related mantle cell lymphoma. J Clin Oncol. 2012; 30: e49-53. doi: 10.1200/jco.2011.38.8553.

55. Shao H, Xi L, Raffeld M, Feldman AL, Ketterling RP, Knudson R, Rodriguez-Canales J, Hanson J, Pittaluga S, Jaffe ES. Clonally related histiocytic/dendritic cell sarcoma and chronic lymphocytic leukemia/small lymphocytic lymphoma: a study of seven cases. Mod Pathol. 2011; 24: 1421-32. doi: 10.1038/modpathol.2011.102.

56. Congyang L, Xinggui W, Hao L, Weihua H. Synchronous histiocytic sarcoma and diffuse large B cell lymphoma involving the stomach: a case report and review of the literature. Int J Hematol. 2011; 93: 247-52. doi: 10.1007/s12185-011-0773-3.

57. Carrasco DR, Fenton T, Sukhdeo K, Protopopova M, Enos M, You MJ, Di Vizio D, Nogueira C, Stommel J, Pinkus GS, Fletcher C, Hornick JL, Cavenee WK, et al. The PTEN and INK4A/ARF tumor suppressors maintain myelolymphoid homeostasis and cooperate to constrain histiocytic sarcoma development in humans. Cancer Cell. 2006; 9: 379-90. doi: 10.1016/j.ccr.2006.03.028.

58. Liu Q, Tomaszewicz K, Hutchinson L, Hornick JL, Woda B, Yu H. Somatic mutations in histiocytic sarcoma identified by next generation sequencing. Virchows Arch. 2016; 469: 233-41. doi: 10.1007/s00428-016-1965-2.

59. Michonneau D, Kaltenbach S, Derrieux C, Trinquand A, Brouzes C, Gibault L, North MO, Delarue R, Varet B, Emile JF, Brousse N, Hermine O. BRAF(V600E) mutation in a

histiocytic sarcoma arising from hairy cell leukemia. J Clin Oncol. 2014; 32: e117-21. doi: 10.1200/jco.2013.49.0078.

60. Go H, Jeon YK, Huh J, Choi SJ, Choi YD, Cha HJ, Kim HJ, Park G, Min S, Kim JE. Frequent detection of BRAF(V600E) mutations in histiocytic and dendritic cell neoplasms. Histopathology. 2014; 65: 261-72. doi: 10.1111/his.12416.

61. Idbaih A, Mokhtari K, Emile JF, Galanaud D, Belaid H, de Bernard S, Benameur N, Barlog VC, Psimaras D, Donadieu J, Carpentier C, Martin-Duverneuil N, Haroche J, et al. Dramatic response of a BRAF V600E-mutated primary CNS histiocytic sarcoma to vemurafenib. Neurology. 2014; 83: 1478-80. doi: 10.1212/wnl.0000000000000880.

62. Iwabuchi H, Kawashima H, Umezu H, Takachi T, Imamura M, Saitoh A, Ogose A, Imai C. Successful treatment of histiocytic sarcoma with cladribine and high-dose cytosine arabinoside in a child. Int J Hematol. 2017; 106: 299-303. doi: 10.1007/s12185-017-2202-8.

63. Mittal N, Aakalu V, Mehendele S, Setabutr P, Michals E, Schmidt ML. Primary Orbital Histiocytic Sarcoma in a Child Successfully Treated With Multiagent Chemotherapy. J Pediatr Hematol Oncol. 2016; 38: 653-7. doi: 10.1097/mph.0000000000000649.

64. Tsujimura H, Miyaki T, Yamada S, Sugawara T, Ise M, Iwata S, Yonemoto T, Ikebe D, Itami M, Kumagai K. Successful treatment of histiocytic sarcoma with induction chemotherapy consisting of dose-escalated CHOP plus etoposide and upfront consolidation auto-transplantation. Int J Hematol. 2014; 100: 507-10. doi: 10.1007/s12185-014-1630-y.

65. Gounder M, Desai V, Kuk D, Agaram N, Arcila M, Durham B, Keohan ML, Dickson MA, D'Angelo SP, Shukla N, Moskowitz C, Noy A, Maki RG, et al. Impact of surgery, radiation and systemic therapy on the outcomes of patients with dendritic cell and histiocytic sarcomas. Eur J Cancer. 2015; 51: 2413-22. doi: 10.1016/j.ejca.2015.06.109.

66. Coutermarsh-Ott S, Simmons A, Capria V, LeRoith T, Wilson JE, Heid B, Philipson CW, Qin Q, Hontecillas-Magarzo R, Bassaganya-Riera J, Ting JP, Dervisis N, Allen IC. NLRX1 suppresses tumorigenesis and attenuates histiocytic sarcoma through the negative regulation of NF-kappaB signaling. Oncotarget. 2016; 7: 33096-110. doi: 10.18632/oncotarget.8861.

67. Lei Y, Wen H, Ting JP. The NLR protein, NLRX1, and its partner, TUFM, reduce type I interferon, and enhance autophagy. Autophagy. 2013; 9: 432-3. doi: 10.4161/auto.23026.

68. Xia X, Cui J, Wang HY, Zhu L, Matsueda S, Wang Q, Yang X, Hong J, Songyang Z, Chen ZJ, Wang RF. NLRX1 negatively regulates TLR-induced NF-kappaB signaling by targeting TRAF6 and IKK. Immunity. 2011; 34: 843-53. doi: 10.1016/j.immuni.2011.02.022.

69. Tattoli I, Carneiro LA, Jehanno M, Magalhaes JG, Shu Y, Philpott DJ, Arnoult D, Girardin SE. NLRX1 is a mitochondrial NOD-like receptor that amplifies NF-kappaB and JNK pathways by inducing reactive oxygen species production. EMBO Rep. 2008; 9: 293-300. doi: 10.1038/sj.embor.7401161.

70. Soares F, Tattoli I, Rahman MA, Robertson SJ, Belcheva A, Liu D, Streutker C, Winer S, Winer DA, Martin A, Philpott DJ, Arnoult D, Girardin SE. The mitochondrial protein NLRX1 controls the balance between extrinsic and intrinsic apoptosis. J Biol Chem. 2014; 289: 19317-30. doi: 10.1074/jbc.M114.550111.

71. Singh K, Poteryakhina A, Zheltukhin A, Bhatelia K, Prajapati P, Sripada L, Tomar D, Singh R, Singh AK, Chumakov PM, Singh R. NLRX1 acts as tumor suppressor by regulating TNF-alpha induced apoptosis and metabolism in cancer cells. Biochim Biophys Acta. 2015; 1853: 1073-86. doi: 10.1016/j.bbamcr.2015.01.016.

72. Ito K, Kuroki S, Kobayashi M, Ono K, Washizu T, Bonkobara M. Identification of dasatinib as an in vitro potent growth inhibitor of canine histiocytic sarcoma cells. Vet J. 2013; 196: 536-40. doi: 10.1016/j.tvjl.2012.12.016.

73. Steinberg M. Dasatinib: a tyrosine kinase inhibitor for the treatment of chronic myelogenous leukemia and philadelphia chromosome-positive acute lymphoblastic leukemia. Clin Ther. 2007; 29: 2289-308. doi: 10.1016/j.clinthera.2007.11.005.

74. Talpaz M, Shah NP, Kantarjian H, Donato N, Nicoll J, Paquette R, Cortes J, O'Brien S, Nicaise C, Bleickardt E, Blackwood-Chirchir MA, Iyer V, Chen TT, et al. Dasatinib in imatinib-resistant Philadelphia chromosome-positive leukemias. N Engl J Med. 2006; 354: 2531-41. doi: 10.1056/NEJMoa055229.

75. Yamazaki H, Takagi S, Hoshino Y, Hosoya K, Okumura M. Inhibition of survivin influences the biological activities of canine histiocytic sarcoma cell lines. PLoS One. 2013; 8: e79810. doi: 10.1371/journal.pone.0079810.

76. Yamazaki H, Takagi S, Hosoya K, Okumura M. Influence of a survivin suppressor YM155 on the chemoresistance of canine histiocytic sarcoma cells. Vet J. 2015; 205: 375-80. doi: 10.1016/j.tvjl.2015.05.003.

77. Yamazaki H, Takagi S, Hosoya K, Okumura M. Survivin suppressor (YM155) enhances chemotherapeutic efficacy against canine histiocytic sarcoma in murine transplantation models. Res Vet Sci. 2015; 99: 137-44. doi: 10.1016/j.rvsc.2015.02.003.

Figures

Figure 1

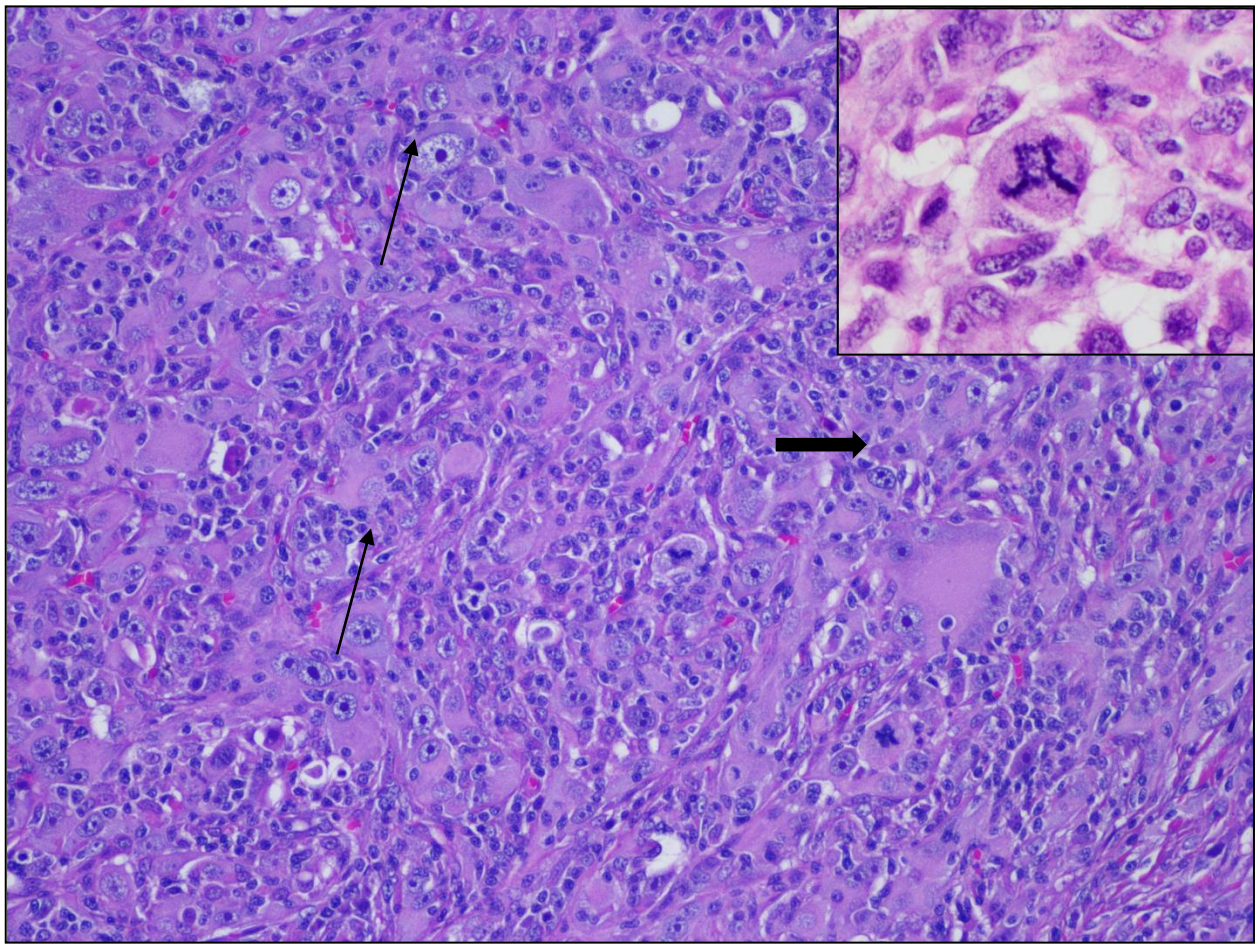

Figure 1. Histologically, canine histiocytic sarcoma is dominated by multiple criteria of malignancy. These include: marked pleomorphism, cyto- and karyomegaly (thin arrows), frequent and often bizarre mitoses (inset), and multinucleation (thick arrow). Image photographed at 200x, inset photographed at 400x.

Chapter 3

NLRX1 Suppresses Tumorigenesis and Attenuates Histiocytic Sarcoma through the Negative Regulation of NF-κB Signaling

This chapter was published in Oncotarget:

Coutermarsh-Ott S, Simmons A, Capria V, LeRoith T, Wilson JE, Heid B, Philipson CW, Qin Q, Hontecillas-Magarzo R, Bassaganya-Riera J, Ting JP, Dervisis N, Allen IC. NLRX1 suppresses tumorigenesis and attenuates histiocytic sarcoma through the negative regulation of NF-κB signaling. *Oncotarget.* 2016 May 31;7(22):33096-110. doi: 10.18632/oncotarget.8861. PMID: 27105514.

Abstract

Histiocytic sarcoma (HS) is an uncommon malignancy in both humans and veterinary species. Research exploring the pathogenesis of this disease is scarce; thus, diagnostic and therapeutic options for patients are limited. Recent publications have suggested a role for the NLR, NLRX1, in acting as a tumor suppressor. Based on these prior findings, we hypothesized that NLRX1 would function to inhibit tumorigenesis and thus the development of HS. To test this, we utilized *Nlrx1*$^{-/-}$ mice and a model of urethane-induced tumorigenesis. *Nlrx1*$^{-/-}$ mice exposed to urethane developed splenic HS that was associated with significant up-regulation of the NF-κB signaling pathway. Additionally, development of these tumors was also significantly associated with the increased regulation of genes associated with AKT signaling, cell death and autophagy. Together, these data show that NLRX1 suppresses tumorigenesis and reveals new genetic pathways involved in the pathobiology of HS.

Introduction

Histiocytic sarcoma (HS) is a rare, malignant neoplasm with a phenotypic profile consistent with an interstitial dendritic cell or macrophage origin. In human patients, this disease occurs most commonly in the intestinal tract, skin, soft tissue, and lymph nodes though case reports have also identified it in the central nervous system and stomach [1, 2]. Definitive diagnosis is often difficult due to its variable clinical presentation, as well as, its similarities to other histiocytic disorders such as hemophagocytic syndrome, malignant histiocytosis and monocytic leukemia. While still rare, this neoplasm is more common in veterinary medicine, where it is primarily a disease of dogs. Indeed, the bulk of studies of HS have arisen from cases in veterinary medicine. Treatment options in both human and veterinary medicine are limited and include complete surgical resection (when possible) coupled with chemotherapy or palliative radiation. However, in all species, treatment is often unsuccessful and the disease is typically fatal.

Pattern recognition receptors (PRRs) are important components of the innate immune system that are involved in the promotion and/or regulation of inflammation. These receptors recognize pathogen associated molecular patterns (PAMPs) and/or damage associated molecular patterns (DAMPs), which are products released by stressed or dying cells. PRRs that have been shown to significantly modulate the pathogenesis of neoplasia, include the Toll-like receptors (TLRs) and the NOD-like receptors (NLRs). TLRs are located on the surface of the cell, as well as, within endosomes and have been shown to play a role in lung cancer, breast cancer, and colon cancer [3-7]. NLRs are intracellular sensors and are well-studied in the context of colitis associated colorectal cancer [8, 9]. However, their involvement in other neoplasms is generally less defined and currently an area of intense research focus.

At least 34 NLR family members have been identified in mice and at least 22 in humans, the majority of which have yet to be functionally characterized [10]. Of the characterized NLRs, the majority appear to function as molecular effectors that form multi-protein complexes. For example, the most widely studied NLR family members form a multi-protein complex with the adaptor protein ASC and caspase-1, termed the inflammasome that is responsible for the production of the mature forms of the pro-inflammatory cytokines IL-1β and IL-18. However, a second sub-group of NLRs has recently been characterized that primarily function as non-inflammasome forming, regulatory NLRs. Members of this sub-group include NOD1 and NOD2, NLRX1 and NLRC3 (reviewed in [9]).

NLRX1 has been shown to be an important regulator of critical pathways associated with both inflammation and tumorigenesis. These include roles in the inhibition of NF-κB signaling, Type-I IFN production, and ROS production, as well as, the promotion of autophagy [11-15]. However, beyond these initial characterization studies, many questions remain unanswered regarding the function of this unique protein. The majority of studies investigating NLRX1 have focused on its role in host-pathogen interactions. However, the pathways modulated by NLRX1 are also typically dysregulated during tumorigenesis. Thus, we hypothesized that NLRX1 significantly inhibits tumorigenesis through regulating one or more of these previously characterized pathways. Here, we utilized *Nlrx1*$^{-/-}$ mice in a model of urethane induced tumorigenesis. Our data reveal that *Nlrx1*$^{-/-}$ mice are sensitive to urethane treatment and develop HS in the spleen that is associated with increased NF-κB signaling. We also identify a diverse range of genes associated with common cancer pathways, AKT signaling, cell death, and autophagy that are also significantly up-regulated in the *Nlrx1*$^{-/-}$ mice during HS. Collectively,

our results further confirm that NLRX1 functions as a tumor suppressor and extends these findings to HS, which is an understudied cancer with few biomarkers.

Materials and Methods

Experimental Animals

The generation and characterization of Nlrx1$^{-/-}$ mice have been previously described [14]. All experiments were conducted with 6 - 22 week old C57Bl/6 female mice. All animals were maintained under SPF conditions and received 5010 chow (LabDiet) and water ad libitum. All experiments were conducted in accordance with the NIH Guide for the Care and Use of Laboratory Animals and were conducted under institutional IACUC approval.

Bone Marrow Derived Macrophage Studies

Bone marrow derived macrophages (BMDMs) were isolated from the femurs of C57Bl/6 and *Nlrx1*$^{-/-}$ mice using standard procedures [16]. The cells were cultured in Dulbecco's modified Eagle's medium (DMEM) with 10% fetal bovine serum (FBS), 20% L929-conditioned cell culture supernatant, 1x L-glutamine, and 1x non-essential amino acids for 5-7 days. BMDMs were sub-cultured with or without serum overnight. Both live and dead cells were counted at designated intervals using either trypan blue and a hemacytometer or PI staining and quantification with an automated cell counter (Cellometer Vision from Nexcelom Bioscience) following the manufacturer's protocols. A minimum of 1000 cells for each genotype and treatment were counted using the automated system. Supernatants were removed for cytokine measurements and total RNA was collected for gene expression analysis.

Induction and Assessment of Histiocytic Sarcoma

To assess the pathobiological effects of urethane, all mice were subjected to once weekly, i.p. injections of urethane (Sigma) at 1 g/kg diluted in 1X PBS for a total of 7 weeks [17]. Body weight, physical condition, and behavior were assessed at least 3 days per week throughout the course of each study. Mice were harvested at 7 or 14 weeks post-urethane exposure or when moribund. On the day of harvest, mice were euthanized via CO_2 asphyxiation and approximately 1 ml of blood was collected by cardiac puncture. The lung, liver, and spleen were harvested from each animal. Portions of each tissue were placed either in formalin for histopathology or frozen and stored in the -80 for RNA/protein analysis. Samples of spleen were also prepared for flow cytometry.

Histopathologic Examination

Formalin-fixed tissues were routinely processed for histopathology. The paraffin-embedded tissues were sectioned at 5 μm and prepared for hematoxylin and eosin (H&E) staining. H&E stained sections were evaluated and scored by a board-certified veterinary pathologist (T.L.R.) while blinded to genotype and treatment. Immunohistochemistry for MAC387 (Abcam) was used to evaluate monocyte populations in the spleen.

Expression Profiling

Total RNA was harvested from spleens following mechanical homogenization, lysis and RNA extraction using a FastRNA Pro Green Kit and the manufacturer's protocols (MP Biomedicals). The purified RNA was quantified and 1μg of RNA was pooled from 3-5 individual mice prior to the cDNA reaction, for analysis using the RT2 Profiler PCR Array Platform (SABiosciences). Samples were evaluated using the manufacturer's protocols for the

following arrays: PAMM-033Z; PAMM-084Z; PAMM-011Z; PAMM-064Z; PAMM-025Z. Ingenuity Pathways Analysis (IPA) software was utilized to evaluate the array data. In addition to the profiling studies, RNA samples (5 µg) were also individually archived using a cDNA Archive Kit (ABI) and specifically targeted transcription products were quantified by real time PCR using commercially available primer/probe sets (ABI). All experimental samples were evaluated in triplicate and the relative expression was determined utilizing the ΔΔCt method by normalizing samples to the expression of the 18s rRNA housekeeping gene.

Human Metadata Analysis

Human *NLRX1* expression was evaluated using a publically accessible microarray meta-analysis search engine (http://www.nextbio.com/b/search/ba.nb), as previously described [18]. The following array data series were analyzed to generate the human patient data: GSE7553; GSE66354; GSE32490; GSE37470; GSE34823; GSE7339; GSE36474; GSE50579; GSE9750; GSE28511; GSE29431; GSE19750; GSE7553; GSE29491; GSE2719; GSE49972; GSE13898; and GSE36982 .

Statistical Analysis

Data are presented as the mean +/- standard error of the mean (SEM). Analysis Of Variance (ANOVA) followed by either Tukey-Kramer HSD or Newman-Keuls Post Test for multiple comparisons was performed on complex data sets for both individual experiments and composite data. Statistical significance for single data points were assessed by the Student's two-tailed t-test. Survival curves were generated utilizing the product limit method of Kaplan

and Meier and comparisons were made using the log rank test. In all cases, a p-value of less than 0.05 was considered statistically significant.

Results

NLRX1 is Differentially Regulated in Multiple Human Cancers

To gain broader insight into the contribution of NLRX1 in cancer, we conducted a retrospective evaluation of publically available gene expression metadata compiled from 18 human studies (**Figure 1A**). Each study focused on a specific type or sub-type of cancer and evaluated gene expression levels between the tumor specimen and either adjacent healthy tissue or specimens from comparable tissue in unaffected subjects. The change in *NLRX1* expression was deemed significant based on the parameters of each individual study. Our data analysis revealed that *NLRX1* is differentially regulated in a diverse range of human cancers (**Figure 1A**). For example, at the extremes, *NLRX1* was found to be up-regulated 2.72 fold in squamous cell carcinoma of the skin compared to normal skin, while being down-regulated 8.1 fold in high grade myxoid liposarcoma tumors compared to normal adipose tissue (**Figure 1A**). While no human HS studies have been conducted, *NLRX1* gene expression data was evaluated for malignant fibrous histiocytoma (**Figure 1A**). Malignant fibrous histiocytoma, like HS, is controversial in origin though histiocytic cells are thought to be a major contributor. In both humans and canines, this is a soft tissue sarcoma and, in dogs, occurs most commonly in the spleen and skin. The fact that NLRX1 is downregulated in this neoplasm may suggest a similar pattern in human HS. Together, these data reveal that NLRX1 plays a complex role in

tumorigenesis in humans and suggests that additional studies are needed to better define the contribution of this gene in patient populations.

NLRX1 Deficiency Results in Increased Cell Proliferation and Chemokine Production

The role of NLRX1 in the regulation of pathways associated with tumorigenesis is not well defined. A recent pair of studies have suggested that NLRX1 functions as a tumor suppressor through modulating apoptosis [19, 20]. In one study, NLRX1 expression was found to differentially regulate resistance to extrinsic and intrinsic apoptotic signals in transformed, but not primary murine embryonic fibroblasts [20]. In the other study, NLRX1 was found to function as a tumor suppressor by regulating TNF induced apoptosis in immortalized cell lines (18). In the same study, NLRX1 overexpression was found to compromise clonogenicity, growth and migration [19]. To complement these prior studies, we sought to directly evaluate the contribution of NLRX1 on cell proliferation and growth. Bone marrow derived macrophages were harvested from wild type and *Nlrx1*$^{-/-}$ mice and allowed to differentiate for 5-7 days following standard protocols [16]. Cells were quantified and re-plated at 275,000 cells/ml in standard growth media without the addition of FBS (**Figure 1B**). Over the course of 24 hours, cells were counted using both trypan blue and a hemacytometer, as well as, propidium iodide (PI) staining and assessments with an automated cell counter (**Figure 1B**). Both live cells and dead cells were counted using these techniques. Under these conditions, wild type macrophages did not increase in number over the 24 hour time course. However, we did observe significant expansion of *Nlrx1*$^{-/-}$ macrophages over the 24 hour time course (**Figure 1B**). The *Nlrx1*$^{-/-}$ macrophages more than doubled the number of wild type macrophages 16 hours after re-plating (**Figure 1B**). Further assessments of gene expression revealed that chemokines associated with

macrophage proliferation and recruitment, including *Ccl2* (MCP1) and *Csf3* (GCSF), were up-regulated in *Nlrx1*$^{-/-}$ macrophages compared to the wild type cells (**Figure 1C**). Unlike the prior studies, we did not observe differences in cell death. However, it should be noted that the prior studies induced apoptosis through TNF stimulation, glycolysis inhibition, increased cytosolic calcium flux, and endoplasmic reticulum stress [19, 20]. The current study evaluated cells with minimal stimulation beyond the overnight incubation in serum-free conditions. Thus, it is highly likely that the differences in cell death are associated with cell type, temporal, and stimulation specific mechanisms.

NLRX1 Attenuates Disease Pathogenesis following Urethane Exposure

To better characterize the role of NLRX1 in cancer, we subjected *Nlrx1*$^{-/-}$ mice to a urethane (ethyl carbamate)-induced tumor model (**Figure 2A**). Urethane induced tumor formation is a prototypical and highly reproducible animal model of carcinogenesis that is traditionally utilized to study lung cancer [17, 21, 22]. Repeated urethane exposure consistently results in pulmonary adenoma and adenocarcinoma formation [22]. Similar to some human adenocarcinomas, urethane induces specific mutations in *Kras* at codon 61 and mutations in p53 during later stages of disease progression [21]. Wild type and *Nlrx1*$^{-/-}$ mice were administered weekly intraperitoneal injections of 1g/kg body weight of urethane diluted in saline for a total of 7 weeks (**Figure 2A**). Survival, weight loss, and clinical parameters associated with disease progression were routinely monitored. We evaluated disease progression and tumorigenesis at weeks 7 and 14. We did not observe any significant pathological changes at week 7, following the final urethane injection (**Figure 3**). However, by week 14, 50% of the *Nlrx1*$^{-/-}$ mice had developed palpable masses in their peritoneal cavity and required euthanasia (**Figure 2B**).

Additionally, the urethane treated *Nlrx1*$^{-/-}$ mice failed to thrive throughout the duration of the study and demonstrated significantly decreased weight gain compared with the wild type animals starting 5 weeks after the initial exposure to urethane (**Figure 2C**). At necropsy, the palpable masses originally detected in the *Nlrx1*$^{-/-}$ animals were identified as markedly enlarged spleens (**Figure 2D**). Spleens from all animals were weighed and those from the urethane treated *Nlrx1*$^{-/-}$ mice were indeed significantly larger than all of the other genotypes and treatments (**Figure 2E**). No gross lesions were identified in any additional tissues or organs. Following urethane treatment, *Nlrx1* expression was increased in wild type animals that were resistant to HS (**Figure 2F**).

NLRX1 Suppresses the Development of Histiocytic Sarcoma

The increased urethane sensitivity observed in the *Nlrx1*$^{-/-}$ mice was directly correlated with splenomegaly. Subsequent histopathological assessments by two board certified veterinary pathologists (T.L.R. and S.C.O.) revealed that spleens from the urethane treated *Nlrx1*$^{-/-}$ mice were characterized by a significant expansion of the white pulp by high numbers of pleomorphic, mononuclear cells with frequent mitotic figures, thus consistent with a diagnosis of HS (**Figure 4A-B**). No significant pathology was observed in the spleens from the saline treated wild type and *Nlrx1*$^{-/-}$ mice or the urethane treated wild type animals (**Figure 4A**). A semi-quantitative assessment of spleen histopathology, based on number of lesions and percent area affected (scored on a scale of 0 – 3), revealed a significant increase in the spleen lesion score for the urethane treated *Nlrx1*$^{-/-}$ mice compared to all other genotypes and treatments (**Figure 4C**). Additional flow cytometry assessments of spleen cellularity, conducted at the time of harvest, confirmed the increased numbers of monocyte derived cells in the *Nlrx1*$^{-/-}$ spleens compared to

the wild type. T-cell, B-cell, and NK-cell populations were not significantly different between wild type and *Nlrx1*$^{-/-}$ spleens (**data not shown**). Immunohistochemistry for MAC387 was performed and neoplastic cells showed strong cytoplasmic positive staining (**Figure 4D**). Based on these results, our data suggests that macrophages are the dominate cell population associated with HS in the *Nlrx1*$^{-/-}$ mice. Together, these data suggest that NLRX1 functions to attenuate HS induced by urethane and further support a role for this unique NLR in tumor suppression.

NLRX1 Attenuates Urethane Induced Tumorigenesis in the Lung and Inflammation in the Liver

Typically, lung cancer progression is much slower in the urethane model, especially in C57Bl/6 mice and pathology is usually evaluated at least 24 weeks following the initial exposure. However, due to the sensitivity of the *Nlrx1*$^{-/-}$ mice to urethane and the rapid development of HS in the spleen, we evaluated lung histopathology 14 weeks following the initial exposure to urethane. In the wild type mice, we observed a small number of lesions in each treated animals consistent with urethane exposure (**Figure 5A**). Similar lesions were also observed in the *Nlrx1*$^{-/-}$ mice (**Figure 5A**). However, in the urethane treated *Nlrx1*$^{-/-}$ animals, we observed significantly higher numbers of tumor lesions (mean = 4.7 lesions) compared to the wild type animals (mean = 1.3) as well as a significant increase in bronchial associated lymphoid tissue (BALT) not seen in the wild type animals (**Figure 5B**). Thus, even at this earlier time-point in the urethane model, the wild type animals had begun forming the characteristic lung lesions associated with urethane exposure and, consistent with the morbidity data and findings in the spleen, the *Nlrx1*$^{-/-}$ mice were more sensitive. At necropsy, we also collected the liver for microscopic evaluation. Histopathologic assessments revealed that urethane exposure increased

liver extramedullary hematopoiesis (EMH) and perivascular inflammation in all of the treated animals when compared to untreated animals (**Figure 5C**). Moreover, we observed a significant increase in both parameters in the *Nlrx1*$^{-/-}$ mice compared to the wild type animals. In addition to the increased EMH and inflammation, we also observed a significant increase in liver necrosis in the urethane treated *Nlrx1*$^{-/-}$ mice (**Figure 5C**). This necrosis was not observed in the wild type animals. The increased mass formation in the lung and increased inflammation in the lung and liver observed in the urethane treated *Nlrx1*$^{-/-}$ mice is consistent with previous reports that identify NLRX1 as a negative regulator of inflammatory signaling pathways [23]. Likewise, the increased necrosis in the liver is consistent with previously reported findings in other models that suggest a role for NLRX1 in the modulation of cell death, autophagy, and cell metabolism [12, 19].

Genes Associated with Cancer, Cell Death and Autophagy are Significantly Up-Regulated in Histiocytic Sarcoma in *Nlrx1*$^{-/-}$ *Mice*

NLRX1 has been previously shown to modulate inflammatory signaling pathways, cell death, autophagy, and reactive oxygen species (ROS) production [8, 19]. To better address the signaling pathways that are dysregulated in the *Nlrx1*$^{-/-}$ mice during tumorigenesis, we profiled gene expression in the spleen following urethane exposure. Spleens were harvested from both urethane treated and untreated wild type and *Nlrx1*$^{-/-}$ animals and total RNA was extracted (**Figure 6**). The RNA from 3-5 randomly chosen spleens from each genotype and treatment were pooled in equal amounts and cDNA was generated (**Figure 6**). Different random pools of RNA were evaluated on each Superarray. The expression of 241 genes was evaluated using a panel of Superarrays (Qiagen) chosen to evaluate pathways associated with cancer, inflammation, cell

death, and autophagy using methods previously described by the authors [14]. Gene expression was determined following the manufacturer's protocols, which are based on the ΔΔCt method. The expression of each gene on the array was first normalized to a panel of 8 housekeeping genes and the change in gene expression between the respective urethane treated versus untreated wild type and *Nlrx1*$^{-/-}$ spleens was determined. The change in gene expression between the wild type and *Nlrx1*$^{-/-}$ spleens was then calculated and displayed as the fold change for each gene on the various arrays.

Because it is such a rare disease, very little data exists regarding gene expression or biochemical signaling pathways that are dysregulated in HS. Thus, we initially sought to evaluate genes commonly associated with cancer signaling. This initial evaluation revealed that 64 genes associated with tumorigenesis were significantly up-regulated in *Nlrx1*$^{-/-}$ spleens with HS compared to the wild type (**Figure 7A**). The genes with the greatest differences in expression (>1000 fold increase) included: *Dsp*, *Sox10*, *Ccl2*, *Ocln*, *Pgf*, *Epo*, *Foxc2*, and *Adm* (**Figure 7A**). Interestingly, all of these genes, with the exception of *Foxc2*, have been previously associated with various types of sarcoma in either human or rodent studies and increased *CCL2* gene expression has been directly correlated with HS in canine patients [24]. In addition to increased expression of cancer associated genes, we also observed increased expression of 76 genes associated with autophagy (**Figure 7A**). The genes with the greatest differences in expression (100-199 fold increase) included: *Rps6kb1*, *Tgfb1*, *Ctsb*, and *Hspa8* (**Figure 7A**). NLRX1 has been previously shown to positively regulate autophagy following virus exposure [13]. However, in the current study, NLRX1 deficiency was found to result in the elevation of several autophagy genes. This may suggest that under the conditions evaluated in this study, NLRX1 acts as a negative regulator of autophagy. However, it is important to note that changes in gene expression

do not necessarily correlate to changes in protein expression. Therefore, additional studies into protein expression would be necessary to better elucidate the effects of NLRX1 on autophagy in HS. We also observed increased expression of 44 genes associated with cell death (**Figure 7B**). These genes were further stratified based on general roles in either necrosis or apoptosis (**Figure 8**). Together, these data suggest that NLRX1 negatively regulates gene expression associated with autophagy, and more broadly cell death, during tumorigenesis. This finding is consistent with a previous study that found NLRX1 functions as a tumor suppressor through the regulation of TNF induced apoptosis [19].

Significant increases in serum CCL2 levels have been found in canine cases of disseminated HS [24]. Likewise, *Ccl2* appears to be up-regulated in macrophages from *Nlrx1*$^{-/-}$ mice and was identified as being one of the genes with the greatest level of up-regulation in the spleen during HS (**Figures 1C and 7A**). Thus, we evaluated serum protein levels of CCL2 by ELISA (**Figure 7B**). Consistent with the increased expression of *Ccl2* in the spleen, we observed a significant increase in serum CCL2 levels following urethane treatment in *Nlrx1*$^{-/-}$ mice compared to the wild type animals (**Figure 7B**). Prior studies have also evaluated other pro-inflammatory cytokines in the context of HS, including IL-6 [24]. While these studies did not find any correlation between IL-6 and tumor progression, this cytokine has been reported to be increased in the absence of NLRX1 [14]. Thus, we also evaluated serum protein levels of IL-6 by ELISA and found that the levels of this cytokine were significantly increased in urethane treated *Nlrx1*$^{-/-}$ mice compared to the wild type animals (**Figure 7C**). Together with the gene expression findings, these data show that NLRX1 attenuates inflammation and tumorigenesis through the negative regulation of genes associated with cancer, autophagy, and cell death during HS.

NLRX1 Negatively Regulates NF-κB and AKT Signaling in Histiocytic Sarcoma

In general, the genes and pathways that were found up-regulated were highly diverse and covered a broad spectrum of pathways associated with tumorigenesis. This suggests that NLRX1 likely indirectly regulates these pathways through its effects on one or more essential regulatory pathways up-stream from the genes evaluated. Prior studies have shown that NLRX1 negatively regulates the type-I interferon response and the NF-κB signaling cascade following virus exposure [14, 15]. While no prior data has associated IFN signaling with the urethane model, several lines of evidence indicate that the urethane model is potentiated by inflammation associated with increases in NF-κB signaling [17, 25]. Evaluation of the gene expression data did not reveal any significant differences in expression among genes generally associated with IFN signaling between the wild type and *Nlrx1*$^{-/-}$ spleens. Further analysis of pathways that were enriched in the spleen following urethane treatment also did not identify the IFN signaling pathway as being significantly dysregulated (**data not shown**). Thus, IFN signaling does not appear to play a role in either HS or NLRX1 function in this model. However, unlike the findings of IFN signaling, we did observe significant differences in genes associated with the NF-κB signaling cascade (**Figure 9A**). Our analysis revealed that 54 genes associated with NF-κB signaling were significantly up-regulated (≥ 2-fold increase in expression) in the spleens from urethane treated *Nlrx1*$^{-/-}$ mice compared to the wild type animals (**Figure 9A**). Two genes, *Csf2* and *Csf3*, were found to have the highest fold change in expression (>1000 fold) (**Figure 9A**). Seven additional genes had greater than 100-fold changes in expression between the *Nlrx1*$^{-/-}$ and wild type spleens, including *Agt, Fos, Tnfrsf10b, Il10, Ccl2, Egr1,* and *Egfr* (**Figure 9A**). All expression data was analyzed using Ingenuity Pathway Analysis (IPA) to identify relationships and pathways that were enriched in the urethane treated *Nlrx1*$^{-/-}$ spleens compared to the wild

type spleens. The IPA analysis confirmed that the NF-κB signaling pathway was significantly up-regulated during HS in the *Nlrx1*$^{-/-}$ mice (**Figure 9B**). These data are consistent with prior studies supporting a role for NLRX1 in the negative regulation of NF-κB [14]. The IPA analysis also revealed a significant increase in TNF signaling (**Figure 9B**), which is consistent with the recent study that suggested NLRX1 functions as a tumor suppressor through modulating this pathway in cancer cells [19]. Our IPA analysis further revealed a significant increase in the AKT signaling pathway (**Figure 9B**). This was unexpected, as no prior studies have shown an association between NLRX1 function and AKT signaling. Each pathway downstream of AKT signaling was found to be up-regulated in the absence of NLRX1 during HS (**Figure 9B**). While more studies are clearly necessary, these findings suggest that NLRX1 may also function, either directly or indirectly, to negatively regulate AKT signaling during cancer. Together, these data suggest that the sensitivity of the *Nlrx1*$^{-/-}$ mice to urethane is at least in part associated with the up-regulation of gene transcription associated with increased NF-κB and AKT signaling.

Discussion

Traditionally, the roles of NLRX1 have predominately been studied in the context of host-pathogen interactions. However, recent studies have expanded the function of this unique NLR to include roles in the regulation of metabolism, cell death, and cancer [12, 19, 20]. The results obtained in the present study support previous findings and strongly suggest that NLRX1 functions to attenuate tumor progression. Mechanistically, our data suggest that this is through the downregulation of NF-κB signaling, as this pathway is significantly up-regulated in the *Nlrx1*$^{-/-}$ mice following urethane exposure. Thus, in the current study, we have identified NLRX1 as an important tumor suppressor and characterized a group of genes downstream of NF-κB

signaling that are significantly up-regulated in the *Nlrx1*$^{-/-}$ animals that contribute to the development of HS.

In addition to our current findings, prior studies have also evaluated NLRX1 in cancer utilizing either xenograft models or models of inflammation driven colorectal cancer [19, 20, 26, 27]. In the xenograft study, nude mice were injected with RKO colon carcinoma cells, where NLRX1 was either stably knocked down or overexpressed [19]. In the presence of TNF, NLRX1 knockdown resulted in significantly increased tumor volume, whereas overexpression attenuated tumor growth [19]. To evaluate the role of NLRX1 in CAC, tumorigenesis was induced in wild type and *Nlrx1*$^{-/-}$ mice by treating the animals with the chemical carcinogen azoxymethane (AOM) immediately prior to dextran sulfate sodium (DSS) exposure [20, 26, 27]. In this model, inflammation associated with DSS exposure functions as a tumor promoter. The results show that *Nlrx1*$^{-/-}$ mice were significantly more sensitive to inflammation driven tumorigenesis compared to similarly treated wild type animals [20, 26, 27]. Significantly higher numbers and larger-sized polyps were observed in the *Nlrx1*$^{-/-}$ mice [20]. The *Nlrx1*$^{-/-}$ mice were also found to have increased colon inflammation associated with DSS exposure [20]. In both the xenograft as well as the AOM/DSS models, the loss of NLRX1 was suggested to have implications in cell death leading to tumorigenesis, which is supported by our data as well. Findings from the xenograft study suggest that NLRX1 appears to sensitize the cells to TNF induced cell death through a Caspase-8 dependent mechanism and maintains ATP levels through the regulation of mitochondrial Complex I and Complex III activities [19]. A similar mechanism is described in the colitis associated cancer (CAC) studies [20]. In the CAC studies, *in vivo* tumorigenesis data was supported by correlations to murine embryonic fibroblast data that suggested NLRX1

expression mediates resistance to extrinsic apoptotic signals, while also conferring susceptibility to intrinsic apoptotic signals [20].

The results of the current study support a role for NLRX1 in mediating cell death under neoplastic conditions, but not in primary macrophages. Our study identified 44 genes associated with cell death that were upregulated in the spleens of *Nlrx1*$^{-/-}$ mice with HS. Interestingly, the majority of cell death genes upregulated in these mice were related to apoptosis; however, no clear link to either intrinsic or extrinsic apoptosis was identified. It is also unclear if the up-regulation of genes associated with cell death was directly associated with the neoplastic macrophages or associated with the general tissue damage that occurred in the spleen during HS progression. To expand upon these findings, we conducted basic assessments of cell death associated with our proliferation studies using primary bone marrow derived macrophages. Under our experimental conditions, we did not observe a significant difference in cell death between the wild type and *Nlrx1*$^{-/-}$ macrophages. Rather, we noted a significant increase in *Nlrx1*$^{-/-}$ cell proliferation. It is certainly possible that the increase in cell numbers that we observed could also be correlated with reduced cell death. In fact, increased cell proliferation and reduced cell death are commonly observed when essential pathways associated with tumorigenesis are disrupted [28]. The increased *Nlrx1*$^{-/-}$ macrophage proliferation is consistent with the increased splenic macrophage proliferation observed by histopathology in the spleens during HS. Likewise, the increase in expression of genes, such as *Ccl2* and *Csf3*, which are NF-κB regulated cytokines associated with macrophage proliferation and recruitment, are also consistent with our *in vivo* findings. Thus, the role of NLRX1 in regulating cell death (and proliferation) in normal versus neoplastic cells warrants further study.

In the present study, we sought to extend the assessments of NLRX1 and evaluate additional pathways modulated by this unique NLR in the context of tumorigenesis. Prior studies have shown that NLRX1 is a member of the regulatory NLR sub-group and functions to inhibit inflammatory signaling cascades, including IFN and NF-κB signaling (reviewed in [8]). While we did not observe any role for dysregulated IFN signaling in the development of HS in the *Nlrx1*$^{-/-}$ mice, we did find a strong correlation between tumorigenesis and the up-regulation of genes associated with NF-κB signaling. Prior mechanistic studies have shown that NLRX1 interacts with TRAF6 to negatively regulate NF-κB signaling [14]. The NF-κB signaling pathway directly regulates a wide range of biological functions beyond inflammation and is associated with almost every hallmark of cancer [28]. In the context of HS, there is a paucity of data pertaining to NF-κB signaling. Beyond a few incidental observations, no detailed studies have comprehensively evaluated this signaling pathway in HS. However, NF-κB signaling has been evaluated in other types of sarcoma. For example, in human hemangioma and angiosarcoma lesions, high levels of RelA and strong activation of the NF-κB/IL-6/STAT3 signaling axis has been previously reported [29]. These human data were complemented by studies using *Ink4a/Arf* deficient mice, which recapitulate genetic traits observed in human angiosarcoma patients and xenograft mice. In these models, animals developed angiosarcoma in the lung, liver, and spleen and systemic inhibition of Ikkβ, IL-6 or STAT3 significantly inhibited angiosarcoma growth [29]. In other sarcomas, inhibition of the NF-κB pathway has also been shown to significantly attenuate tumorigenesis. In a study utilizing a myxoid liposarcoma cell line, inhibition of the NF-κB signaling pathway was shown to decrease cell viability, reduce phosphorylation of NF-κB proteins, and attenuate caspase-3 regulated apoptosis [30]. Interestingly, the human metadata analysis described in the current study found the greatest

decrease in NLRX1 expression in myxoid liposarcoma (**Figure 1**). This suggests a possible link between reduced NLRX1 levels and increased NF-κB signaling in this neoplasm.

In addition to up-regulation of the NF-κB cascade, we also observed increased AKT signaling during HS in the *Nlrx1*$^{-/-}$ mice. This result was quite unexpected as no prior studies have associated NLRX1 with AKT signaling. However a related protein, AIM2, has recently been shown to attenuate the progression of colon tumorigenesis, in part, through reducing AKT activation [31]. In this study, *Aim2*$^{-/-}$ mice were found to be highly sensitive to colitis associated colorectal cancer. The increased tumor burden in these mice was significantly attenuated in those animals treated with an AKT inhibitor, suggesting that up-regulation of this pathway is associated with tumorigenesis [31]. Unlike the NF-κB pathway, the contribution of AKT signaling in HS has been previously reported [32]. In human specimens, immunohistochemistry revealed high levels of p-AKT expression in 9 of 10 HS samples [32]. These human data were further supported using a novel *Pten*$^{+/-}$ *Ink4a/Arf*$^{-/-}$ double mutant mouse model of HS. In this model, loss of PTEN results in aberrant activation of the PI3K/AKT signaling pathway, as well as, the RAS/MAPK pathway [32]. Ultimately, this results in increased AKT, ERK1 and ERK2 phosphorylation and the eventual development of HS [32]. Interestingly, lymphomas arising in the *Ink4a/Arf*$^{-/-}$ mice did not show this increase in AKT signaling compared with normal tissue from wild type animals, suggesting that increased AKT signaling is specific to HS in this model [32].

We identified 194 genes up-regulated in the *Nlrx1*$^{-/-}$ mice following urethane administration that were associated with cancer signaling, autophagy and NF-κB signaling. Many interesting targets were identified that have not been previously associated with either HS or NLRX1 function. Of the individual genes and proteins that were found to be significantly

dysregulated, IL-6 and CCL2 are highly interesting. We observed increased systemic levels of IL-6 in the serum of the *Nlrx1*$^{-/-}$ mice (**Figure 7**). In canine patients, previous reports have observed significant increases in IL-6 in metastatic splenic hemophagocytic HS [33]. Likewise, as mentioned above in human patients and mouse models, prior studies evaluating the NF-κB/IL-6/STAT3 axis in other types of sarcoma have reported increased IL-6 signaling and attenuation of tumorigenesis following treatment with IL-6 inhibitors [29]. Together, these findings suggest a major role for IL-6 in disease pathogenesis. Increased IL-6 levels have been previously reported in the *Nlrx1*$^{-/-}$ mice in other models associated with pathogen infection [14]. The direct association between NLRX1 and IL-6 signaling is presumed to result from increased NF-κB signaling found in the absence of NLRX1. A recent paper showed that enhanced IL-6 in *Nlrx1*$^{-/-}$ mice is consequential, as anti-IL6R therapy completely reduced colon polyps in these animals [26]. However, it is also important to note that increased IL-6 could also be an indirect response to the animal's clinical decline, rather than a direct effect of NLRX1 function on tumorigenesis. Additional mechanistic insight will be necessary to better define the relationship between NLRX1, IL-6 and HS pathogenesis. The increase in CCL2 (MCP-1), both *ex vivo* and *in vitro* is also an intriguing observation. Transcription of *CCL2* is highly regulated by NF-κB and the cytokine displays potent monocyte chemotactic activity. Increased CCL2 has been previously reported in veterinary patients with HS [24]. In this prior study, serum levels of CCL2 were significantly increased in dogs diagnosed with disseminated HS compared to healthy control animals [24]. While we focused on IL-6 and CCL2, many of the other genes identified are also highly interesting and should provide significant insight related to HS pathogenesis.

NLRX1 is a novel member of a unique regulatory sub-group of NLR family members that functions to negatively regulate diverse biochemical signaling cascades. Members of this

regulatory sub-group function to control aberrant inflammation and other biologically relevant pathways associated with a variety of human diseases, including cancer. Here, we have shown that NLRX1 functions to suppress tumorigenesis, in part, through the negative regulation of NF-κB signaling. These findings are consistent with previous studies that have characterized NLRX1 as a tumor suppressor in other cancer models. We anticipate that future studies will better define the role of NLRX1 in cancer. Additionally, we have uncovered an extensive number of genes and pathways that have not previously been associated with HS. Thus, further studies of these pathways and dysregulated genes should identify novel targets for future therapeutic strategies to attenuate HS progression.

Acknowledgements

We would like to thank Dr. Gregory R. Robins (UNC Chapel Hill) for providing technical assistance.

References

1. Laviv Y, Zagzag D, Fichman-Horn S, Michowitz S. Primary central nervous system histiocytic sarcoma. Brain Tumor Pathol. 2013; 30: 192-5. doi: 10.1007/s10014-012-0123-z.

2. Lee D, Kim YB, Chung SH, Lee SR, Byun CS, Han SU, Han JH. Primary gastric histiocytic sarcoma reminiscent of inflammatory pseudotumor: a case report with review of the literature. Korean J Pathol. 2014; 48: 258-62. doi: 10.4132/KoreanJPathol.2014.48.3.258.

3. Chatterjee S, Crozet L, Damotte D, Iribarren K, Schramm C, Alifano M, Lupo A, Cherfils-Vicini J, Goc J, Katsahian S, Younes M, Dieu-Nosjean MC, Fridman WH, et al. TLR7 promotes tumor progression, chemotherapy resistance, and poor clinical outcomes in non-small cell lung cancer. Cancer Res. 2014; 74: 5008-18. doi: 10.1158/0008-5472.can-13-2698.

4. Samara KD, Antoniou KM, Karagiannis K, Margaritopoulos G, Lasithiotaki I, Koutala E, Siafakas NM. Expression profiles of Toll-like receptors in non-small cell lung cancer and idiopathic pulmonary fibrosis. Int J Oncol. 2012; 40: 1397-404. doi: 10.3892/ijo.2012.1374.

5. Xu L, Wen Z, Zhou Y, Liu Z, Li Q, Fei G, Luo J, Ren T. MicroRNA-7-regulated TLR9 signaling-enhanced growth and metastatic potential of human lung cancer cells by altering the phosphoinositide-3-kinase, regulatory subunit 3/Akt pathway. Mol Biol Cell. 2013; 24: 42-55. doi: 10.1091/mbc.E12-07-0519.

6. Bhatelia K, Singh K, Singh R. TLRs: linking inflammation and breast cancer. Cell Signal. 2014; 26: 2350-7. doi: 10.1016/j.cellsig.2014.07.035.

7. Sipos F, Furi I, Constantinovits M, Tulassay Z, Muzes G. Contribution of TLR signaling to the pathogenesis of colitis-associated cancer in inflammatory bowel disease. World J Gastroenterol. 2014; 20: 12713-21. doi: 10.3748/wjg.v20.i36.12713.

8. Allen IC. Non-Inflammasome Forming NLRs in Inflammation and Tumorigenesis. Front Immunol. 2014; 5: 169. doi: 10.3389/fimmu.2014.00169.

9. Davis BK, Philipson C, Hontecillas R, Eden K, Bassaganya-Riera J, Allen IC. Emerging significance of NLRs in inflammatory bowel disease. Inflamm Bowel Dis. 2014; 20: 2412-32. doi: 10.1097/mib.0000000000000151.

10. Bryant CE, Monie TP. Mice, men and the relatives: cross-species studies underpin innate immunity. Open Biol. 2012; 2: 120015. doi: 10.1098/rsob.120015.

11. Arnoult D, Soares F, Tattoli I, Castanier C, Philpott DJ, Girardin SE. An N-terminal addressing sequence targets NLRX1 to the mitochondrial matrix. J Cell Sci. 2009; 122: 3161-8. doi: 10.1242/jcs.051193.

12. Lei Y, Wen H, Ting JP. The NLR protein, NLRX1, and its partner, TUFM, reduce type I interferon, and enhance autophagy. Autophagy. 2013; 9: 432-3. doi: 10.4161/auto.23026.

13. Lei Y, Wen H, Yu Y, Taxman DJ, Zhang L, Widman DG, Swanson KV, Wen KW, Damania B, Moore CB, Giguere PM, Siderovski DP, Hiscott J, et al. The mitochondrial proteins NLRX1 and TUFM form a complex that regulates type I interferon and autophagy. Immunity. 2012; 36: 933-46. doi: 10.1016/j.immuni.2012.03.025.

14. Allen IC, Moore CB, Schneider M, Lei Y, Davis BK, Scull MA, Gris D, Roney KE, Zimmermann AG, Bowzard JB, Ranjan P, Monroe KM, Pickles RJ, et al. NLRX1 protein attenuates inflammatory responses to infection by interfering with the RIG-I-MAVS and TRAF6-NF-kappaB signaling pathways. Immunity. 2011; 34: 854-65. doi: 10.1016/j.immuni.2011.03.026.

15. Moore CB, Bergstralh DT, Duncan JA, Lei Y, Morrison TE, Zimmermann AG, Accavitti-Loper MA, Madden VJ, Sun L, Ye Z, Lich JD, Heise MT, Chen Z, et al. NLRX1 is a

regulator of mitochondrial antiviral immunity. Nature. 2008; 451: 573-7. doi: 10.1038/nature06501.

16. Davis BK. Isolation, culture, and functional evaluation of bone marrow-derived macrophages. Methods Mol Biol. 2013; 1031: 27-35. doi: 10.1007/978-1-62703-481-4_3.

17. Bauer AK, Cho HY, Miller-Degraff L, Walker C, Helms K, Fostel J, Yamamoto M, Kleeberger SR. Targeted deletion of Nrf2 reduces urethane-induced lung tumor development in mice. PLoS One. 2011; 6: e26590. doi: 10.1371/journal.pone.0026590.

18. Kupershmidt I, Su QJ, Grewal A, Sundaresh S, Halperin I, Flynn J, Shekar M, Wang H, Park J, Cui W, Wall GD, Wisotzkey R, Alag S, et al. Ontology-based meta-analysis of global collections of high-throughput public data. PLoS One. 2010; 5. doi: 10.1371/journal.pone.0013066.

19. Singh K, Poteryakhina A, Zheltukhin A, Bhatelia K, Prajapati P, Sripada L, Tomar D, Singh R, Singh AK, Chumakov PM, Singh R. NLRX1 acts as tumor suppressor by regulating TNF-alpha induced apoptosis and metabolism in cancer cells. Biochim Biophys Acta. 2015; 1853: 1073-86. doi: 10.1016/j.bbamcr.2015.01.016.

20. Soares F, Tattoli I, Rahman MA, Robertson SJ, Belcheva A, Liu D, Streutker C, Winer S, Winer DA, Martin A, Philpott DJ, Arnoult D, Girardin SE. The mitochondrial protein NLRX1 controls the balance between extrinsic and intrinsic apoptosis. J Biol Chem. 2014; 289: 19317-30. doi: 10.1074/jbc.M114.550111.

21. Horio Y, Chen A, Rice P, Roth JA, Malkinson AM, Schrump DS. Ki-ras and p53 mutations are early and late events, respectively, in urethane-induced pulmonary carcinogenesis in A/J mice. Mol Carcinog. 1996; 17: 217-23. doi: 10.1002/(sici)1098-2744(199612)17:4<217::aid-mc5>3.0.co;2-a.

22. Shimkin MB, Polissar MJ. Some quantitative observations on the induction and growth of primary pulmonary tumors in strain A mice receiving urethan. J Natl Cancer Inst. 1955; 16: 75-97. doi:

23. Xia X, Cui J, Wang HY, Zhu L, Matsueda S, Wang Q, Yang X, Hong J, Songyang Z, Chen ZJ, Wang RF. NLRX1 negatively regulates TLR-induced NF-kappaB signaling by targeting TRAF6 and IKK. Immunity. 2011; 34: 843-53. doi: 10.1016/j.immuni.2011.02.022.

24. Nikolic Nielsen L, Kjelgaard-Hansen M, Kristensen AT. Monocyte chemotactic protein-1 and other inflammatory parameters in Bernese Mountain dogs with disseminated histiocytic sarcoma. Vet J. 2013; 198: 424-8. doi: 10.1016/j.tvjl.2013.07.030.

25. Stathopoulos GT, Sherrill TP, Cheng DS, Scoggins RM, Han W, Polosukhin VV, Connelly L, Yull FE, Fingleton B, Blackwell TS. Epithelial NF-kappaB activation promotes urethane-induced lung carcinogenesis. Proc Natl Acad Sci U S A. 2007; 104: 18514-9. doi: 10.1073/pnas.0705316104.

26. Koblansky AA, Truax AD, Liu R, Montgomery SA, Ding S, Wilson JE, Brickey WJ, Muhlbauer M, McFadden RT, Hu P, Li Z, Jobin C, Lund PK, et al. The Innate Immune Receptor NLRX1 Functions as a Tumor Suppressor by Reducing Colon Tumorigenesis and Key Tumor-Promoting Signals. Cell Rep. 2016; 14: 2562-75. doi: 10.1016/j.celrep.2016.02.064.

27. Tattoli I, Killackey SA, Foerster EG, Molinaro R, Maisonneuve C, Rahman MA, Winer S, Winer DA, Streutker CJ, Philpott DJ, Girardin SE. NLRX1 Acts as an Epithelial-Intrinsic Tumor Suppressor through the Modulation of TNF-Mediated Proliferation. Cell Rep. 2016; 14: 2576-86. doi: 10.1016/j.celrep.2016.02.065.

28. Hanahan D, Weinberg RA. Hallmarks of cancer: the next generation. Cell. 2011; 144: 646-74. doi: 10.1016/j.cell.2011.02.013.

29. Yang J, Kantrow S, Sai J, Hawkins OE, Boothby M, Ayers GD, Young ED, Demicco EG, Lazar AJ, Lev D, Richmond A. INK4a/ARF [corrected] inactivation with activation of the NF-kappaB/IL-6 pathway is sufficient to drive the development and growth of angiosarcoma. Cancer Res. 2012; 72: 4682-95. doi: 10.1158/0008-5472.can-12-0440.

30. Willems SM, Schrage YM, Bruijn IH, Szuhai K, Hogendoorn PC, Bovee JV. Kinome profiling of myxoid liposarcoma reveals NF-kappaB-pathway kinase activity and casein kinase II inhibition as a potential treatment option. Mol Cancer. 2010; 9: 257. doi: 10.1186/1476-4598-9-257.

31. Wilson JE, Petrucelli AS, Chen L, Koblansky AA, Truax AD, Oyama Y, Rogers AB, Brickey WJ, Wang Y, Schneider M, Muhlbauer M, Chou WC, Barker BR, et al. Inflammasome-independent role of AIM2 in suppressing colon tumorigenesis via DNA-PK and Akt. Nat Med. 2015; 21: 906-13. doi: 10.1038/nm.3908.

32. Carrasco DR, Fenton T, Sukhdeo K, Protopopova M, Enos M, You MJ, Di Vizio D, Nogueira C, Stommel J, Pinkus GS, Fletcher C, Hornick JL, Cavenee WK, et al. The PTEN and INK4A/ARF tumor suppressors maintain myelolymphoid homeostasis and cooperate to constrain histiocytic sarcoma development in humans. Cancer Cell. 2006; 9: 379-90. doi: 10.1016/j.ccr.2006.03.028.

33. Soare T, Noble PJ, Hetzel U, Fonfara S, Kipar A. Paraneoplastic syndrome in haemophagocytic histiocytic sarcoma in a dog. J Comp Pathol. 2012; 146: 168-74. doi: 10.1016/j.jcpa.2011.05.006.

Figures

Figure 1.

A.

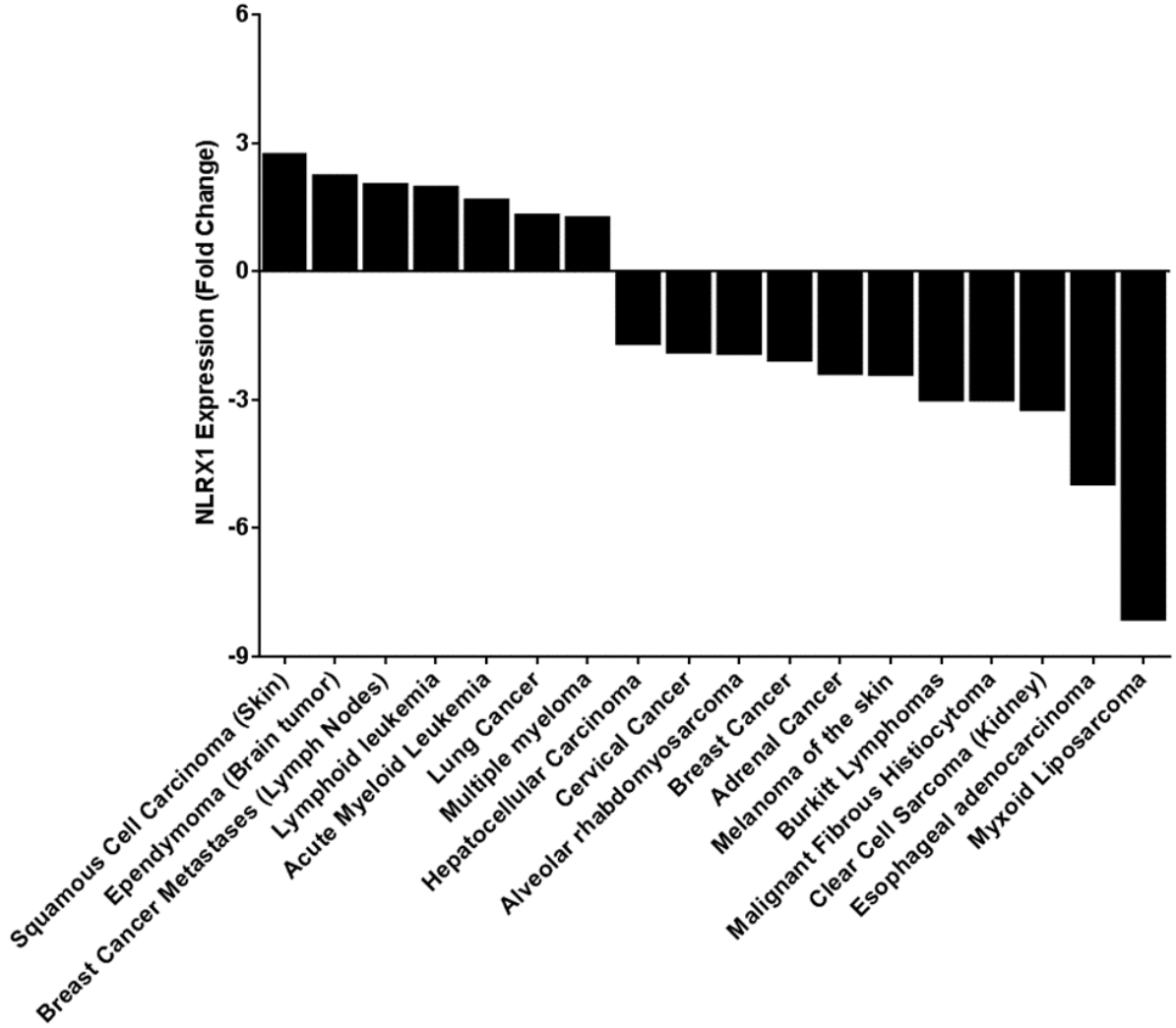

B.

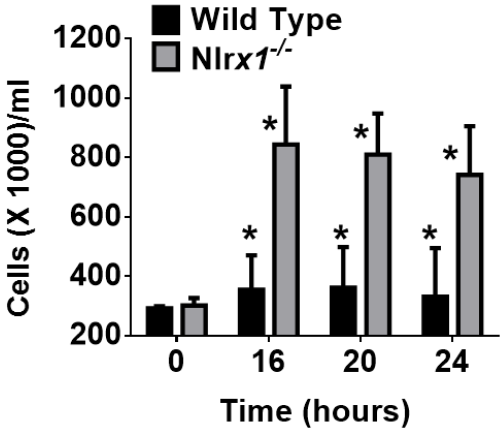

C.

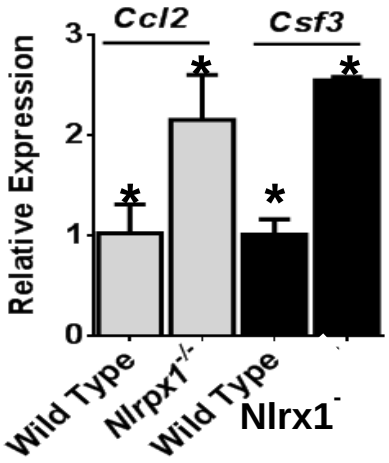

Figure 1: *NLRX1* Gene Expression is Significantly Dysregulated in Diverse Human Neoplasms. (A) A retrospective analysis of gene expression metadata from samples collected from human subjects revealed that *NLRX1* expression was significantly dysregulated in a diverse range of cancer subtypes. Data shown were determined to be significant changes in *NLRX1* expression between the tumor sample and either adjacent tissue from the same subject or a comparable tissue from an unaffected control subject based on the specific parameters established in each individual study. (B-C) Macrophages from *Nlrx1*$^{-/-}$ mice rapidly proliferate and release increased cytokines associated with cell growth and migration. (B) Bone marrow derived macrophages from *Nlrx1*$^{-/-}$ mice significantly expand under standard tissue culture conditions. (C) Significant increases in *Ccl2* (Monocyte Chemotactic Protein-1) and *Csf3* (GCSF) gene expression were observed in *Nlrx1*$^{-/-}$ macrophages compared to wild type macrophages. Data are representative of 5 independent studies. *$p<0.05$.

Figure 2.

A.

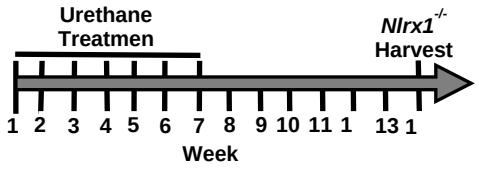

B.

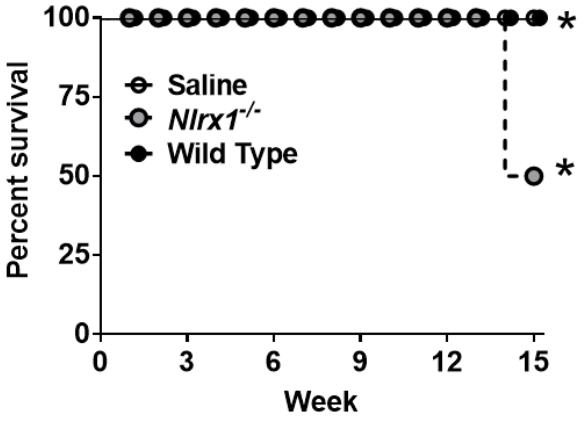

C.

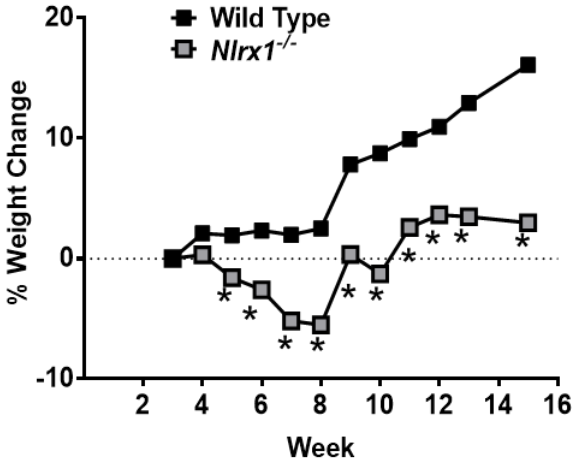

D.

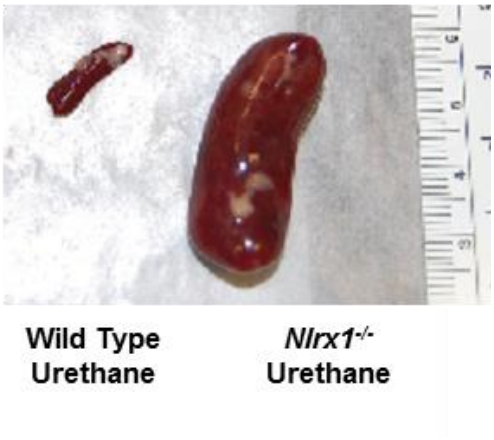

E.

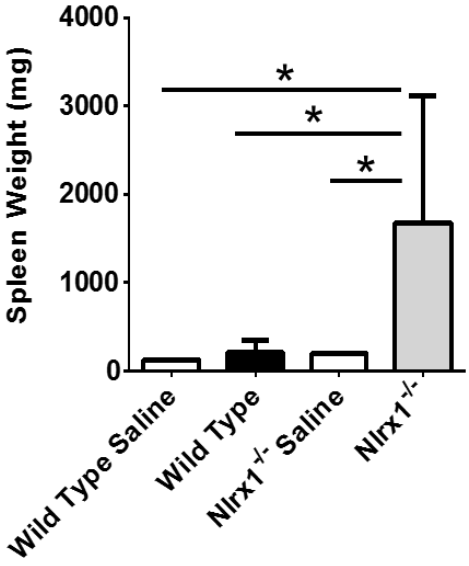

F.

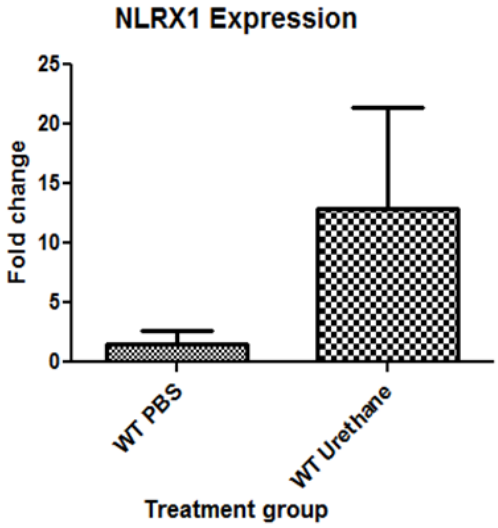

Figure 2: NLRX1 Improves Survival and Morbidity Following Urethane Exposure. (A) Schematic of the urethane model. *Nlrx1*$^{-/-}$ and wild type mice received 7 injections of 1g/kg body weight of urethane in saline over the course of 7 weeks. (B) Kaplan-Meier plot of *Nlrx1*$^{-/-}$ and wild type mouse survival. (C) *Nlrx1*$^{-/-}$ mice demonstrated a significant decrease in weight gain over the course of the model compared to the wild type animals. (D) Necropsy revealed palpable masses in the peritoneal cavity associated with hypersplenomegaly in the *Nlrx1*$^{-/-}$ mice. (E) Urethane treatment resulted in significant increases in spleen weight in the *Nlrx1*$^{-/-}$ mice compared to wild type animals. (F) Urethane treatment increases *Nlrx1* expression in wild type mice. Data are representative of 3 independent studies. *Nlrx1*$^{-/-}$ urethane, n=10; wild type urethane, n=28; *Nlrx1*$^{-/-}$ saline, n=3; wild type saline, n=3. *$p<0.05$.

Figure 3.

A.

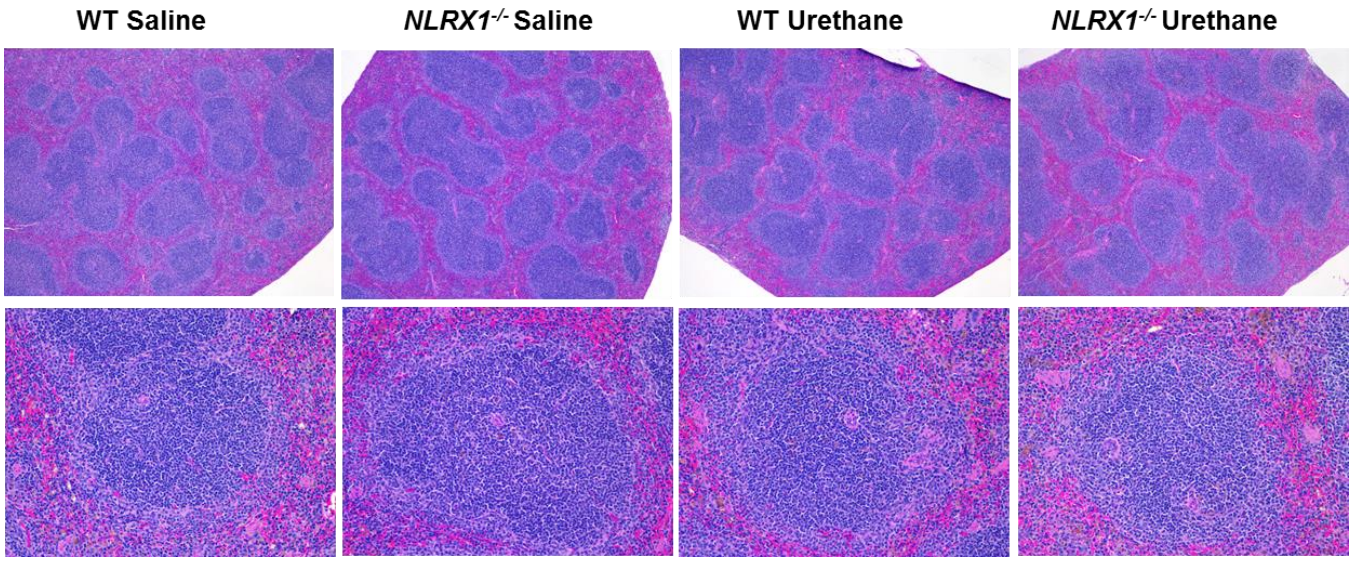
WT Saline
NLRX1-/- Saline
WT Urethane
NLRX1-/- Urethane

B.

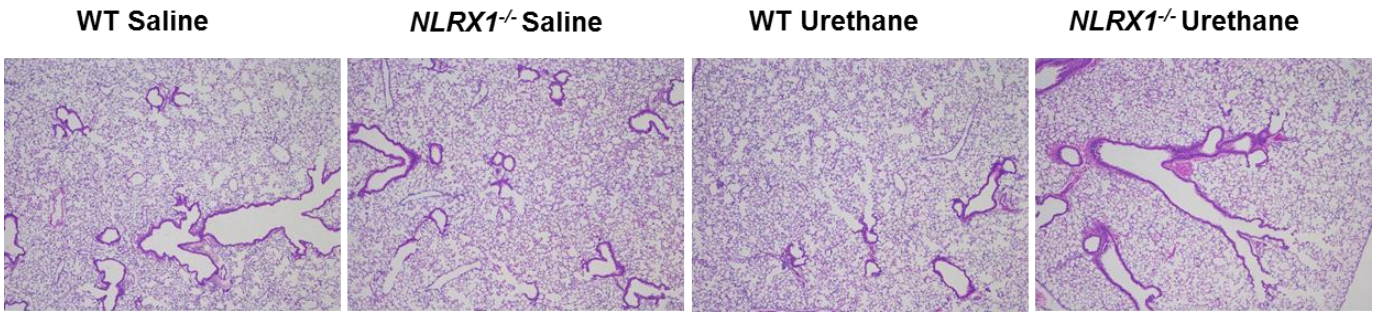
WT Saline
NLRX1-/- Saline
WT Urethane
NLRX1-/- Urethane

C.

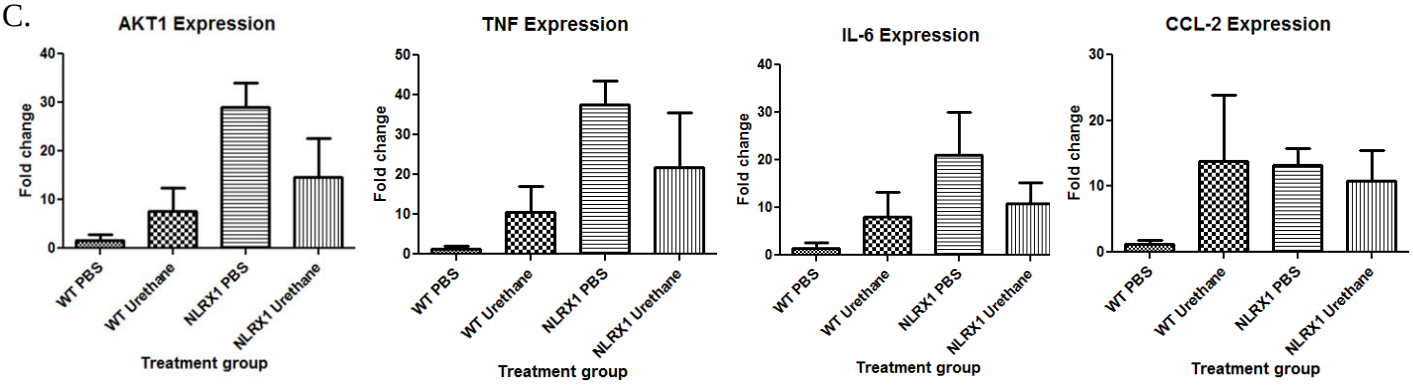
AKT1 Expression
TNF Expression
IL-6 Expression
CCL-2 Expression
Fold change
WT PBS
WT Urethane
NLRX1 PBS
NLRX1 Urethane
Treatment group

Figure 3. Disease Progression and Changes in Gene Expression Identified at 14 Weeks are not Evident at 7 Weeks. (A-B) Additional mouse studies evaluated at week 7 revealed no gross or histologic evidence of splenomegaly or tumorigenesis in the (A) spleen or (B) lung. (C) No significant differences in gene expression of *Akt1*, *Tnf*, *Il-6*, *Nlrx1*, and *Ccl-2* were identified between the experimental and control groups. Analysis was based on the ΔΔCt method, where all data was standardized to the average gene expression for 18s and normalized to the respective untreated wild type spleens.

Figure 4.

A.

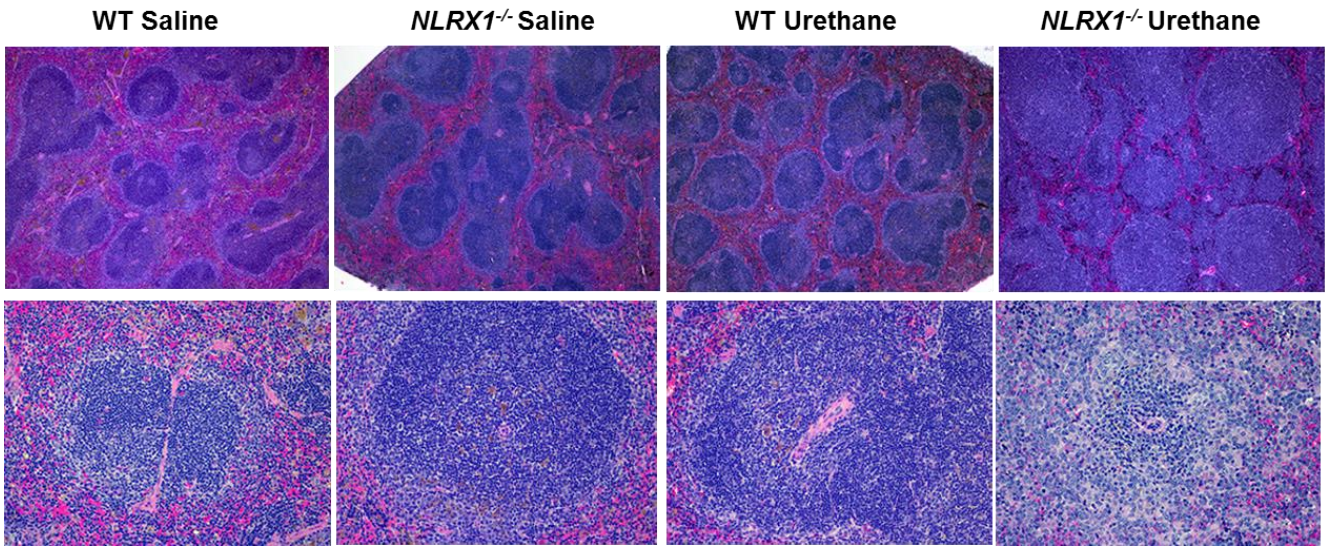

B.

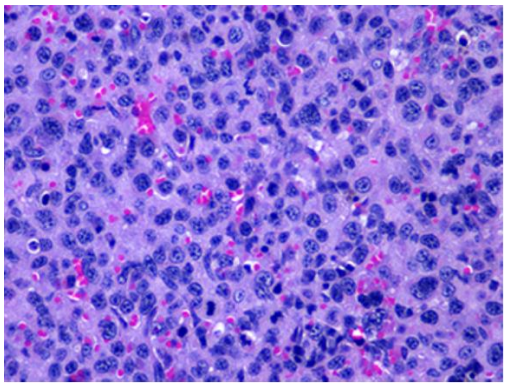

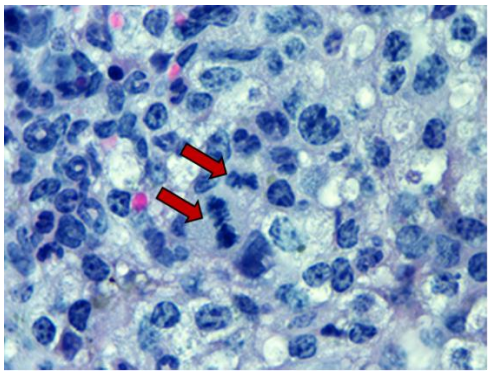

C.

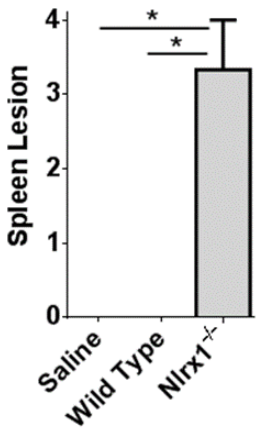

D.

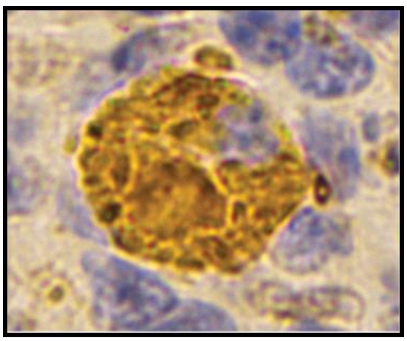

Figure 4: NLRX1 Attenuates the Development and Progression of Histiocytic Sarcoma. Evaluation of histopathology revealed that urethane treatment resulted in the development of histiocytic sarcoma in *Nlrx1*$^{-/-}$ mice. (A) Evaluation of H&E stained sections revealed a significant expansion of the white pulp and increased monocyte populations in spleens from urethane treated *Nlrx1*$^{-/-}$ mice compared to the saline treated and urethane treated wild type animals. (B) Higher magnification evaluation revealed that all of the lesions contained high-grade malignancies consisting of markedly pleomorphic monocytes containing multiple mitotic figures (arrow). (C) Semi-quantitative scoring of histopathology revealed a significant increase in spleen lesions in the *Nlrx1*$^{-/-}$ mice compared to the wild type animals following urethane treatment. (D) Immunohistochemistry using MAC387 (Abcam) was utilized to better classify the pre-dominate cell populations present in the spleen. All of the monocytes associated with spleen lesions were strongly positive for MAC387, suggesting that they are predominately macrophages. Data are representative of 3 independent studies. *Nlrx1*$^{-/-}$ urethane, n=10; wild type urethane, n=28; *Nlrx1*$^{-/-}$ saline, n=3; wild type saline, n=3. *$p < 0.05$.

Figure 5.

A.

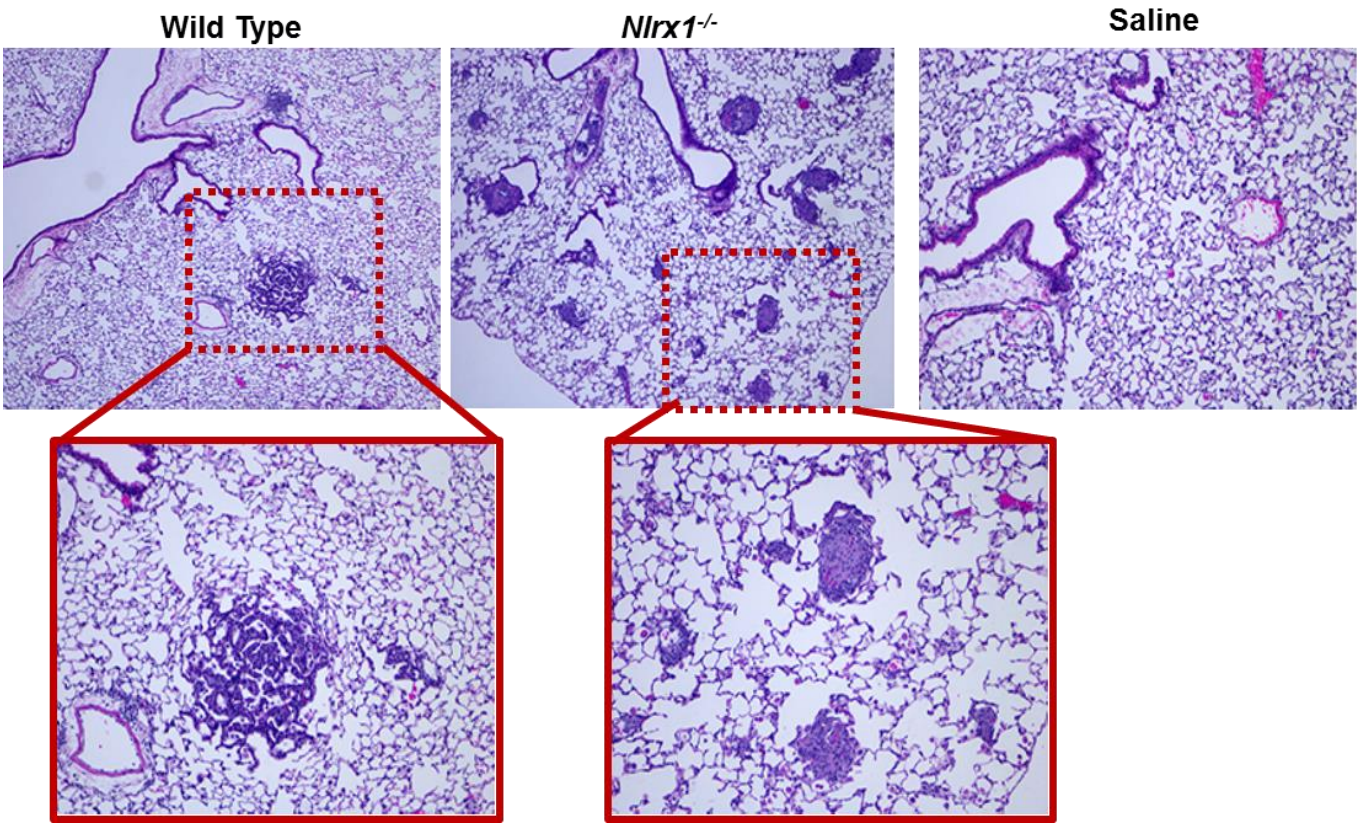
Wild Type
Nlrx1-/-
Saline

B.

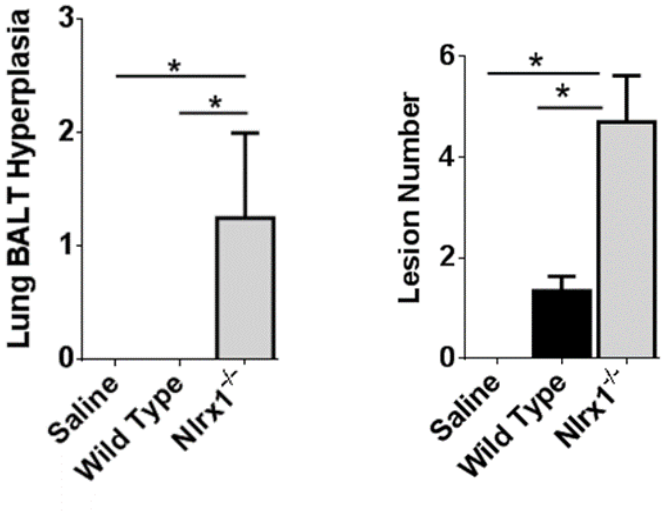
Lung BALT Hyperplasia
3
2
1
0
*
*
Saline
Wild Type
Nlrx1-/-
Lesion Number
6
4
2
0
*
*
Saline
Wild Type
Nlrx1-/-

C.

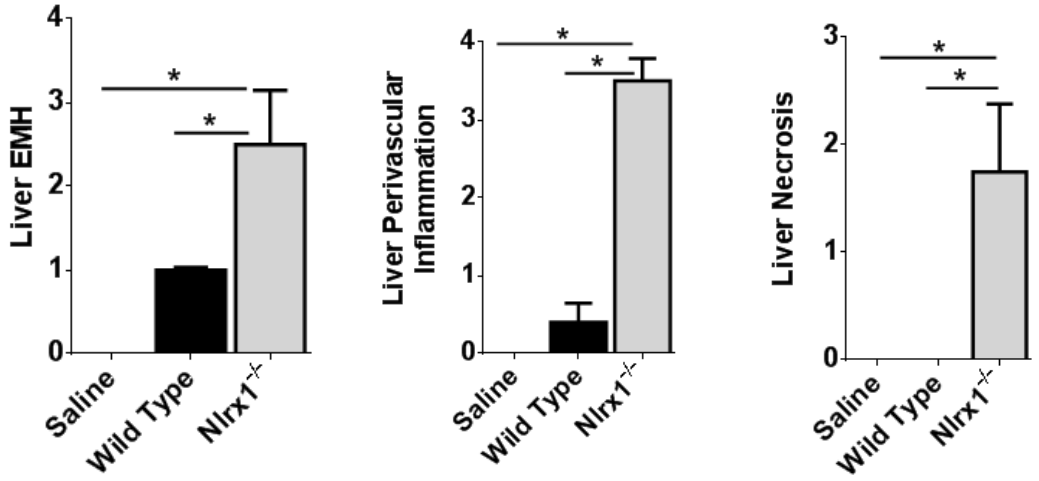

Figure 5: NLRX1 Attenuates Urethane Induced Lesions in the Lung and Liver. (A) Evaluation of histopathology revealed that urethane exposure increased lung lesions in both *Nlrx1*$^{-/-}$ and wild type mice. (B) Semi-quantitative scoring revealed a significant increase in bronchial associated lymphoid tissue (BALT) hyperplasia and the number of lesions in lungs harvested from urethane treated *Nlrx1*$^{-/-}$ mice. (C) In addition to the lungs, urethane exposure also resulted in increased liver lesions in the wild type and *Nlrx1*$^{-/-}$ mice. *Nlrx1*$^{-/-}$ mice developed significant increases in extramedullary hematopoiesis, perivascular inflammation, and necrosis compared to wild type animals. Data are representative of 3 independent studies. *Nlrx1*$^{-/-}$ urethane, n=10; wild type urethane, n=28; *Nlrx1*$^{-/-}$ saline, n=3; wild type saline, n=3. *$p<0.05$.

Figure 6.

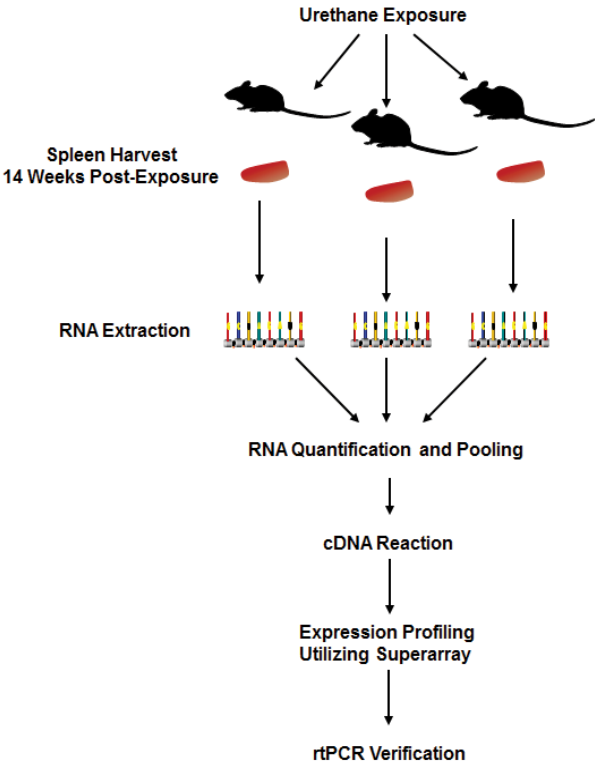

Figure 6. Schematic Illustrating the Experimental Design for Expression Profiling. Multiple mice from each genotype and condition were exposed to urethane. Spleens were harvested 14 weeks following the initial urethane exposure. The total spleen RNA from each mouse was quantified and pooled in equal amounts. The pooled RNA was converted into cDNA and expression profiling was conducted using a panel of Superarrays (Qiagen). Expression data was verified by evaluation of gene expression changes of a subset of individual genes using rtPCR from both pooled and un-pooled samples.

Figure 7.

A.

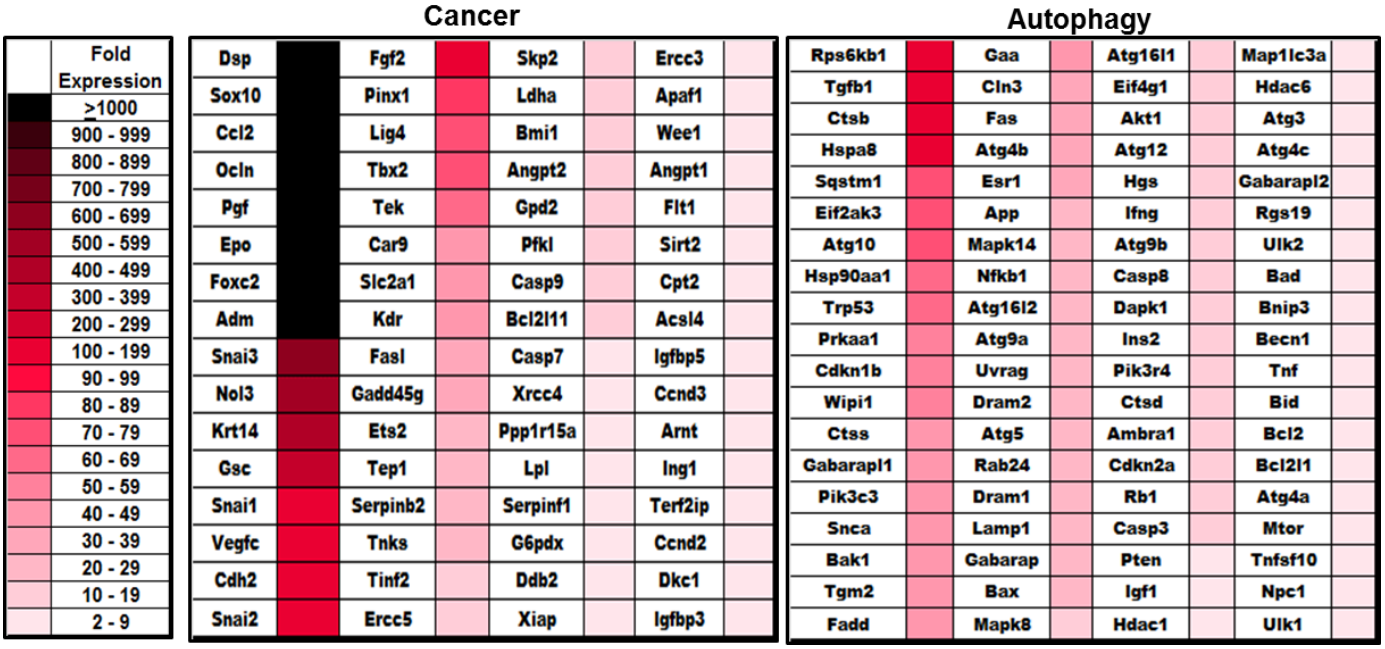

B.

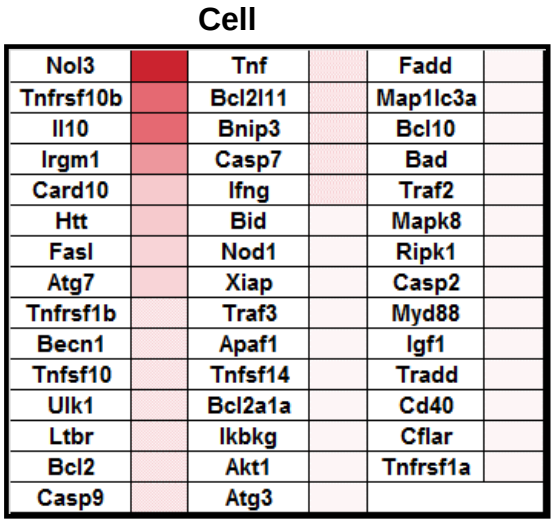

C.

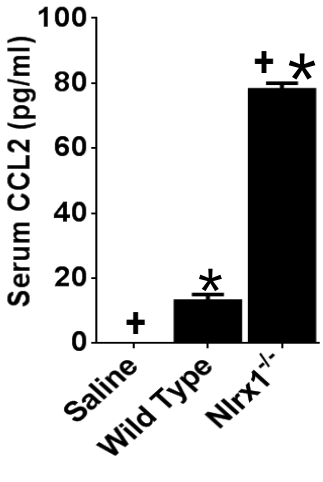

D.

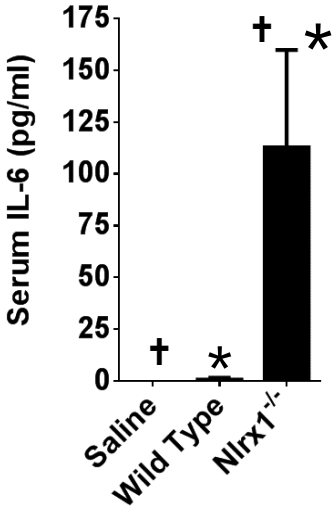

Figure 7: Genes Associated with Cancer, Autophagy, and Cell Death Are Significantly Up-Regulated in NLRX1 Deficient Mice during Histiocytic Sarcoma. Gene transcription was profiled from RNA collected from wild type and *Nlrx1*$^{-/-}$ spleens 14 weeks following the initial

saline or urethane exposure. (A-B) Heatmap reflecting the change in gene expression of all genes associated with common cancer pathways, autophagy, and cell death that were identified as being significantly up-regulated in the spleen following urethane treatment of *Nlrx1*$^{-/-}$ mice compared to the urethane treated wild type animals. Analysis was based on the ΔΔCt method, where all data was standardized to the average gene expression for a panel of 8 housekeeping genes and normalized to the respective untreated *Nlrx1*$^{-/-}$ and untreated wild type spleens. Greater than a 2-fold change in gene expression was considered significant. Three - five randomly selected spleens from each genotype and treatment group were selected and pooled for profiling studies. (C) A significant increase in serum IL-6 and CCL2 levels were detected in the *Nlrx1*$^{-/-}$ mice compared to wild type animals 14 weeks after the initial urethane injection. Cytokine levels were determined by ELISA. *Nlrx1*$^{-/-}$ urethane, n=6; wild type urethane, n=10; *Nlrx1*$^{-/-}$ saline, n=3; wild type saline, n=3. *$p<0.05$.

Figure 8.

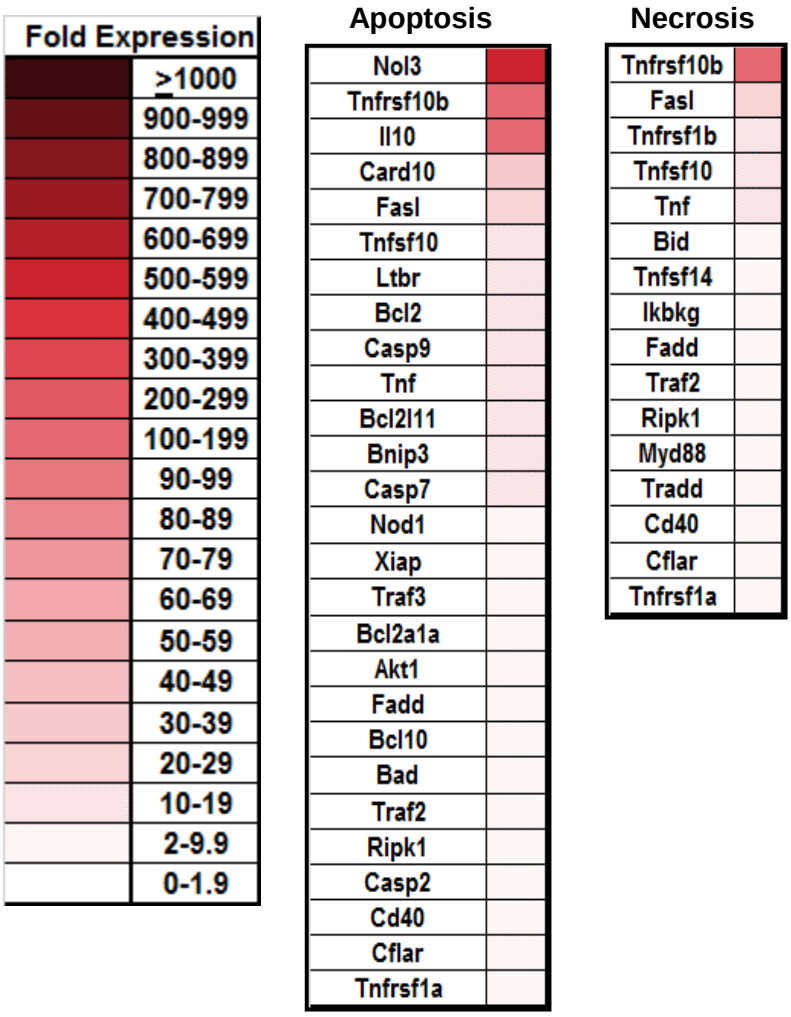

Figure 8. Genes Associated with Both Apoptosis and Necrosis are Up-regulated During Tumorigenesis. Heatmap reflecting the change in gene expression of genes associated with cell death segregated into those associated with apoptosis versus necrosis. These genes were identified as being significantly up-regulated in the spleen following urethane treatment of *Nlrx1*$^{-/-}$ mice compared to the urethane treated wild type animals. Analysis was based on the ΔΔCt method, where all data was standardized to the average gene expression for a panel of 8 housekeeping genes and normalized to the respective untreated *Nlrx1*$^{-/-}$ and untreated wild type

spleens. Greater than a 2-fold change in gene expression was considered significant. Three - five randomly selected spleens from each genotype and treatment group were selected and pooled for profiling studies.

Figure 9.

A.

Csf2	2295.11	Smad3	16.34	Raf1	7.54
Csf3	1670.90	Relb	15.72	Tnfsf14	7.10
Agt	951.79	Ltbr	15.41	Ikbkb	6.99
Fos	377.43	Nfkb2	14.62	Traf6	6.97
Tnfrsf10b	169.20	Fadd	14.58	Bcl3	6.89
Il10	163.94	Zap70	13.84	Tollip	6.78
Ccl2	117.01	Elk1	12.33	Bcl2a1a	6.51
Egr1	111.84	Lta	12.02	Ikbkg	6.39
Egfr	105.74	Eif2ak2	11.63	Csf1	5.97
Ifng	47.19	Tbk1	10.44	Mapk3	4.73
Il1a	43.96	Tnf	10.37	Bcl10	4.41
Card10	34.82	Akt1	10.36	Tlr3	4.05
Ikbke	23.57	Nod1	9.34	Cd27	3.76
Fasl	22.77	Tnfsf10	8.61	Jun	3.72

B.

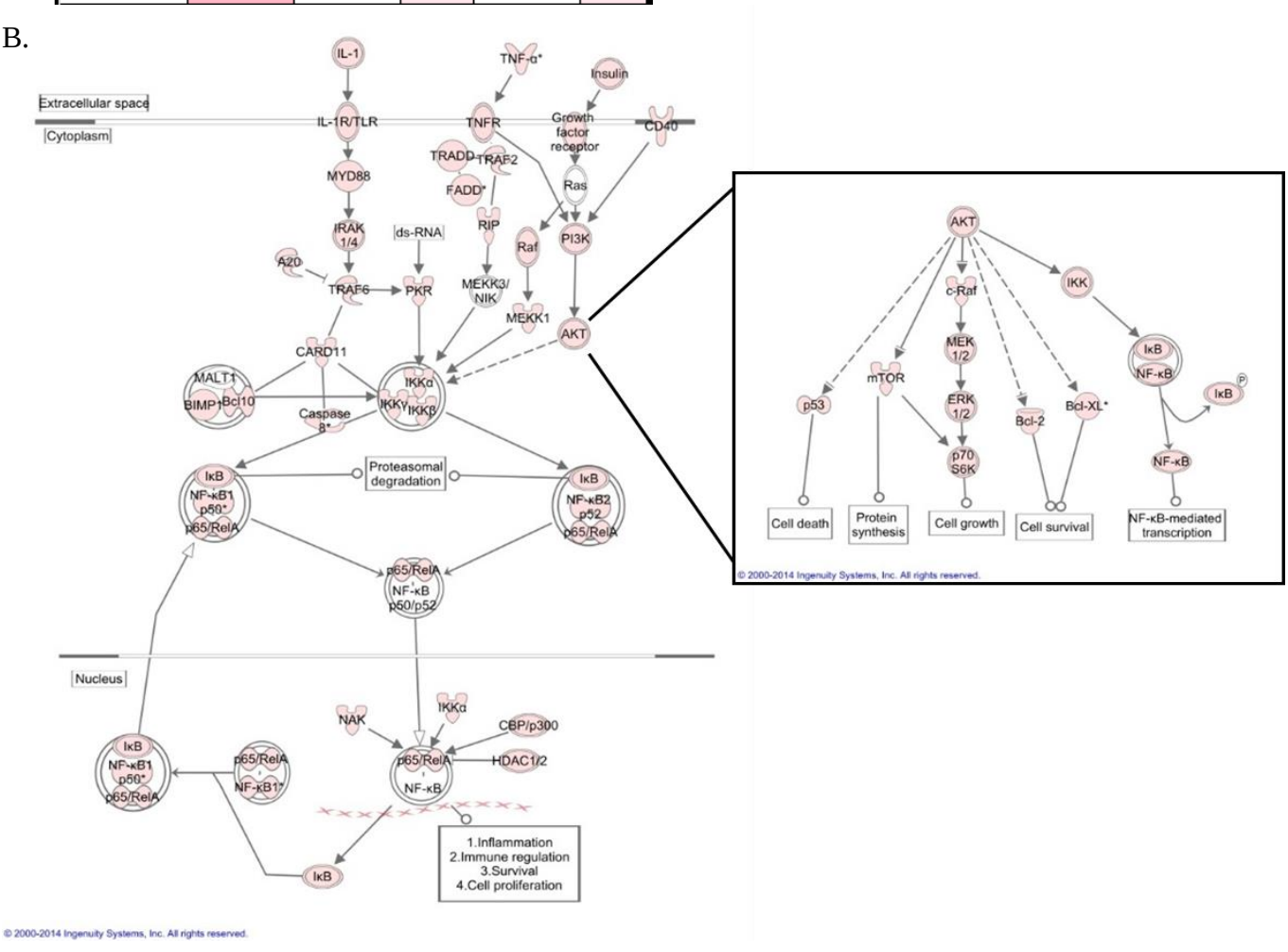

Figure 9: NLRX1 Negatively Regulates NF-κB and AKT Signaling during Tumorigenesis. (A) Heatmap and fold change in expression of all genes associated with NF-κB signaling that were identified as being significantly up-regulated in the spleen following urethane treatment of *Nlrx1*$^{-/-}$ mice compared to the urethane treated wild type animals. Analysis was based on the ΔΔCt method, where all data was standardized to the average gene expression for a panel of 8 housekeeping genes and normalized to the respective untreated *Nlrx1*$^{-/-}$ and untreated wild type spleens. Greater than a 2-fold change in gene expression was considered significant. Three – five randomly selected spleens from each genotype and treatment group were selected and pooled for profiling studies. (B) Evaluation of all gene expression data using Ingenuity Pathway Analysis revealed a significant increase in NF-κB and AKT signaling in *Nlrx1*$^{-/-}$ spleens following urethane exposure compared to wild type. Pink icons represents genes that were significantly up-regulated (≥2 fold change in expression) in the *Nlrx1*$^{-/-}$ spleens compared to the change in expression observed in the wild type spleens following urethane treatment. *Nlrx1*$^{-/-}$ urethane, n=5; wild type urethane, n=5; *Nlrx1*$^{-/-}$ saline, n=5; wild type saline, n=5.

Chapter 4

NF-κB Signaling and AKT Signaling Contribute to the Pathogenesis of Canine Histiocytic Sarcoma

Coutermarsh-Ott, SL, Dervisis, NG, Klahn, SL, Parys, M, Gregory-Bryson, E, Kiupel, M, Yuzbasiyan-Gurkan, V, Eden, K, Lahmers, K, Allen, IC

Abstract

Histiocytic sarcoma (HS) is a highly malignant neoplasm of macrophage or dendritic cell origin. It is a rare tumor in humans and uncommonly found in dogs. In dogs, it can originate in a variety of different organs including spleen, lung, skin, and others. In all species, treatment options are limited and often unsuccessful. Despite this, very little is known about the pathogenesis of this disease. Previous studies in our lab have suggested a role for both NF-κB and AKT signaling in HS development in mice. The current study aimed to test the hypothesis that those pathways found to be important in mice would also contribute to the disease in canines. To test this, we used a combination of qRT-PCR and microarray analysis on canine patient samples to evaluate the expression of notable genes within both the NF-κB and AKT signaling pathways. Interestingly, our initial results reveal a significant increase in the expression of *IL-1B, IL-6, TNF, MTOR, AKT1,* and *PIK3R* in canine patients diagnosed with HS whose primary tumor arises in the spleen but no changes in gene expression in those patients whose tumor arises within the lung. To further this, we evaluated a second population of dogs diagnosed with either histiocytic sarcoma of dendritic cell origin or the hemophagocytic sub-type of HS of macrophage origin using microarray analysis. Relative gene expression in these patients show that multiple genes in the NF-κB and AKT signaling pathways are increased in patients diagnosed with the hemophagocytic sub-type whereas similar increases are not seen in

those with non-hemophagocytic HS. Collectively, these data suggest that the two tumors have significantly different pathogeneses and that being able to differentiate between the two clinically will provide meaningful prognostic significance.

Introduction

Histiocytic sarcoma (HS) is a malignant tumor of macrophage or dendritic cell origin. Case reports of the tumor in humans are exceptionally rare, however, it is slightly more common in veterinary patients. Because of this, the majority of characterization studies have been conducted in veterinary patients. In veterinary medicine, HS is primarily a tumor of dogs though there are case reports in other species [1-6]. It can occur in any breed, age, or sex of dog, but is most common in older, large breed canines. Clinical presentations are variable, often non-specific, and highly dependent on the location of the tumor. There are two forms of the disease, a localized form and a disseminated form [1]. The localized form typically arises as a solitary tumor located in the spleen, subcutis, areas surrounding joints, and/or the lung [1]. The disseminated form is characterized by a diffuse infiltration of neoplastic cells in multiple organs. Though recent literature has suggested that solitary tumors arising in the periarticular soft tissues are associated with a better prognosis, the majority of these tumors often metastasize and do not respond to treatment [7, 8]. Most of these tumors arise from tissue-specific interstitial dendritic cells. These will stain positive for immunohistochemical markers such as CD18, Cd11c, Iba-1, and CD204 [1, 9]. There is a subset of these tumors arising from CD11d+ macrophages (splenic and bone marrow macrophages) that are termed hemophagocytic histiocytic sarcoma (HHS) [10]. These tumors are associated with a grave prognosis and multiple paraneoplastic syndromes such as thrombocytopenia, anemia, and hemorrhage [7].

Despite the poor prognosis in both dogs and humans, few studies have been published investigating the pathogenesis of this disease. One of the earliest studies was done using knockout mice deficient in the tumor suppressors *Pten* and *Ink4a/Arf* [11]. Mice partially deficient in *Pten* and completely deficient in *Ink4a/ARF* were found to spontaneously develop neoplastic proliferations of histiocytic cells identified as macrophages via immunohistochemistry [11]. Subsequent evaluation of human HS samples also showed a similar inactivation of these tumor suppressor genes [11]. Additional genetic studies in dogs have shown that mutations in the tumor suppressor genes *CDKN2A/B, RB1*, and *PTEN* are associated with breed predispositions to HS in Bernese mountain dogs and Flat-coated retrievers [12].

More recently, our research team has implicated an emerging tumor suppressor, NLRX1, in murine HS [13]. NLRX1 is an intracellular receptor in the NLR family responsible for recognizing cytosolic pathogen-associated molecular patterns (PAMPs) and damage associated molecular patterns (DAMPs) and subsequently modulating numerous downstream signaling pathways including NF-κB signaling, and others [14-17]. In our studies, mice lacking this gene developed marked splenomegaly 14 weeks following exposure to the carcinogen urethane. Subsequent histopathologic evaluation showed effacement of the normal splenic architecture by cells consistent with HS [13]. We further showed that the development of these tumors was associated with increases in gene expression in a multiple pathways involved in cancer, cell death, and autophagy [13]. Most notably, increases in expression of genes within the NF-κB and AKT signaling pathways were identified [13].

The role of NF-κB signaling in tumorigenesis is well-established and studies have shown it to play a role in multiple tumor types [18-23]. It has been shown to promote tumorigenesis specifically by activating gene expression in cancer cells, but also by promoting inflammation

within the local tumor microenvironment [18]. This central, pro-inflammatory, cell signaling pathway can be initiated by ligands binding different types of cellular receptors including: T-cell receptors (TCRs), tumor necrosis factor receptors (TNFRs), Toll-like receptors (TLRs), NOD-like receptors (NLRs), Interleukin-1 receptors (IL-1Rs) and others. Once these receptors are bound, a cascade of events takes place ultimately leading to the phosphorylation of IκB and release of transcription factors RelA and p50 to enter the nucleus. Once these enter the nucleus, they bind to multiple target genes and initiate increased expression of a variety of substances including pro-inflammatory cytokines such as IL-6, TNF, and IL-1β as well as cell survival and proliferation pathways.

Like NF-κB signaling, AKT signaling has also been shown to play a pivotal role in neoplastic transformation and progression [24]. In fact, mutations of components of this pathway are among the most commonly identified in cancer in human and veterinary patients [25-32]. AKT signaling is initiated by the binding of growth factors to their subsequent receptor tyrosine kinase. This initiates a cascade of phosphorylation events by the kinases AKT1, PDK1, and MTOR ultimately ending in the phosphorylation of downstream targets that promote cell growth, cell cycle progression, and limit apoptosis. Unlike NF-κB signaling, this pathway has been previously implicated in HS in both dogs and humans [11, 12]. PTEN is an important tumor suppressor that is mutated in both species. It is a phosphatase involved in the regulation of AKT signaling by acting on phosphoinositide substrates, such as PIP3. PIP3 is a critical substrate in the progression of AKT signaling. Thus PTEN acts to mitigate signaling through the reduction of this substrate.

The current study aims to further our initial studies and investigate the clinical relevance of NF-κB and AKT signaling pathways in canine HS. We utilized patient tumor samples and

both qRT-PCR and microarray analysis to evaluate the expression of relevant genes in both pathways. Indeed we do show that primary HS of the spleen and patients diagnosed with HHS do exhibit increases in expression of genes in both signaling pathways, wherea , those patients with primary lung HS and/or non-hemophagocytic HS do not. These results further our understanding of the pathogenesis of HS and suggest that differentiating between HS and HHS in patients could provide meaningful clinical and prognostic significance.

Materials and Methods

Study population for gene expression analysis.

Medical records produced in the VA-MD College of Veterinary Medicine (VMCVM) teaching hospital were searched for patients admitted or seen between January 2008 and June 2016 in which the keyword "histiocytic" was identified with their visit. These cases were reviewed and those patients diagnosed with HS via histopathology from a biopsy or necropsy were selected. All slides were reviewed by a second board certified veterinary pathologist (SCO). Additionally, all cases without associated immunohistochemistry (IHC) were submitted for CD18 IHC confirmation. After confirming the diagnosis of HS, only those patient groups with primary splenic or primary pulmonary HS were included in the study. This was due to the fact that numbers of cases in other tissue types with adequate tissue sample were low. Tissue controls for spleen and lung were chosen by randomly identifying dogs submitted for necropsy with no historical or histologic evidence of disease in the organ of interest (spleen and lung respectively) or presence of HS anywhere else in the body.

Gene expression.

For each sample, two, unstained slides were cut at a thickness of 20 µm from the archived FFPE tissues. For tumor samples, only tumor tissue was isolated and, for control

samples, all available spleen or lung tissue was isolated. The tissues were then deparaffinized using xylene and RNA was extracted using a Quick-RNA™ MiniPrep (Plus) (Zymo Research, R1057). 0.5-0.7 µg of RNA was then diluted in RNAse free water and utilized in a cDNA reaction. The resulting cDNA was used in a qRT-PCR reaction using the following canine probes: *18S, AKT1, PIK3R, MTOR, NLRX1, TNF, IL-1B,* and *IL-6*. Relative fold change was calculated using the ΔΔCt method using *18S* as an intrinsic control and normal tissue samples (spleen and lung respectively) as experimental controls.

Microarray data.

Tumor samples from dogs presenting to the Center for Comparative Oncology, Michigan State University (MSU), were selected. The diagnosis was confirmed via standard H&E and immunohistochemistry against CD18 (histiocytic sarcoma) and CD11d (hemophagocytic histiocytic sarcoma) by a single pathologist (MK). Samples were collected at the time of biopsy or surgery with the written consent of the owners (between 2007 and 2012), flash-frozen in liquid nitrogen and stored at -80°C. Samples were homogenized, extracted with Trizol reagent (Invitrogen, Carlsbad, CA, USA) and purified with RNeasy clean up (Qiagen, Valencia, CA, USA) per the manufacturers' protocols. Resultant RNA was quantified via spectrophotometry and assayed for quality on Agilent (Santa Clara, CA, USA) bioanalyzer at the Research Support Technology Facility (RSTF) at MSU. A total of 30 samples were selected for array analysis with GeneChip Canine 2.0 Genome Arrays (Affymetrix, Santa Clara, CA, USA). The analysis was performed in a single batch, in a randomized manner at MSU's RSTF per Affymetrix protocols. Briefly, the MessageAmp Premier RNA amplification kit (Invitrogen, Carlsbad, CA, USA) was used to synthesize cDNA from total RNA. cDNA which was then used for synthesis of biotin-labeled aRNA. aRNA was purified, quantified and fragmented before hybridization with the

GeneChips. Hybridized chips were washed, stained using streptavidin-conjugated phycoerythrin dye (Invitrogen, Carlsbad, CA, USA) and enhanced with biotinylated goat antistreptavidin antibody (Vector Laboratories, Burlingame, CA, USA) using an Affymetrix GeneChip Fluidics Station 450 and Genechip Operating Software. The Affymetrix GeneChip scanner 7G was used to acquire images. Relative gene expression was calculated by normalizing all samples to *BACTIN* as an endogenous control and canine dendritic cells or macrophages as experimental controls for HS and HHS respectively. Data was then analyzed using Ingenuity Pathway Analysis (IPA) software.

Statistical analysis.

Statistical analyses were performed using GraphPad Prism 5. For gene expression calculations on patient samples, significant outliers ($p \leq 0.05$) for each gene were identified using GraphPad Quick-calcs (an on-line tool) and removed. Each relative fold change was evaluated using a non-parametric Mann-Whitney test and deemed to be significant at $p \leq 0.05$.

Results

Clinicopathologic findings

We identified 41 cases of confirmed or suspected canine HS diagnosed through biopsy or necropsy from the VMCVM VTH between January 2008 and June 2016 (data not shown). In order to facilitate statistical analysis and have adequate patient numbers for gene expression studies, we chose to focus on those patients diagnosed with primary splenic HS or primary lung HS. We identified 10 patients with primary splenic HS (**Table 1**). The average age of these patients was 9.8 ± 2.8 years with a range from 4 to 14 years old. 7/10 of these patients were neutered males and 3/10 were spayed females. No intact animals were identified in this population. Six breeds were represented and included: Mixed breed (3/10), Labrador retriever

(2/10), Golden retriever (2/10), Pitbull (1/10), German shepherd (1/10), and Boston terrier (1/10). The majority of these patients had localized disease (7/10) while the remainder (3/10) had evidence of metastasis to the liver or other organs. Eight control samples were used (**Table 2**). The average age of these animals was 8.4 $\pm$ 5.1 years with a range from <1 to 14 years old. The population included 4/8 neutered males, 2/8 spayed females, 1/8 intact males, and 1/8 intact females. Five breeds were represented and included: Mixed breed (4/8), Pitbull (1/8), Boxer (1/8), and Australian shepherd (1/8).

For our second group, we identified 4 patients with primary lung HS (**Table 1**). The average age of these patients was 10.8 $\pm$ 1.3 year of age with a range from 9 to 12 years old. 3/4 patients were neutered males and the remaining patient was a spayed female. Again, no intact canines were identified in this population. Four breeds were represented and included Golden retriever (1/4), Staffordshire terrier (1/4), Beagle (1/4) and English sheepdog (1/4). 3/4 patients had disease localized to the lung while the remaining patient had evidence of metastasis to the eye and kidney. There were 4 samples of lung tissue used as controls (**Table 2**). The average age was 8.5 years $\pm$ 4.9 years with a range of 3 to 14 years. 2/4 dogs were neutered males, 1/4 dogs was an intact male, and 1/10 dogs was an intact female. All dogs were mixed breed (4/4).

Pathologic findings

Microscopically, these patients had an unencapsulated, densely cellular, infiltrative neoplasm composed of sheets of round to spindle cells on scant or pre-existing fibrovascular stroma that effaced normal tissue architecture (**Figure 1**). These cells were characterized by mild to marked pleomorphism. Cells ranged from round to spindle and were characterized by moderate to abundant amounts of cytoplasm and round to reniform to elongate nuclei with variably condensed chromatin. These neoplasms often exhibited nuclear and/or cellular

gigantism, multinucleation, and bizarre mitotic figures. All cases were subjected to CD18 IHC at the time of diagnosis or retrospectively for this study. Cases were considered positive if neoplastic cells exhibited membranous or cytoplasmic staining (**Figure 1**).

Gene expression profiling for NF-κB signaling

Previous work in our lab has suggested that NF-κB signaling may be increased in murine HS, thus we chose to focus our initial investigations on this pathway [13]. Therefore, we extracted RNA from FFPE tissues housed in the VMCVM VTH archives and conducted qRT-PCR. Because our samples were limited to FFPE tissue, our analysis was limited to gene expression studies. We used the expression of key targets of NF-κB transcription factors, *TNF*, *IL-6*, and *IL-1β*, as surrogates to detect pathway activation. We compared relative gene expression in those patients with splenic HS to the expression of these genes in normal spleens (**Figure 2**). We found that in tumor tissue from spleens, there was a statistically significant increase in both *IL-1β* and *IL-6*. Additionally, there was an increasing trend for *TNF* but this did not reach statistical significance (**Figure 2**). We did not, however, see similar changes in tumor tissue from the lungs. When tumor tissue from the lung was compared to normal lung tissue no statistically significant changes or strong trends in any of the genes evaluated were identified (**Figure 2**). Interestingly, *TNF* did show a mild increase in tumor tissue relative to normal lung tissue, but with fold changes far less than those identified in the spleen (**Figure 2**).

Gene expression profiling for AKT signaling

In addition to finding increases in expression of *TNF*, *IL-6*, and *IL-1β*, our previous studies also showed increases in genes reflecting AKT signaling [13]. Therefore, to evaluate this in our patient samples, we utilized primer probes for *AKT1*, *PIK3R*, and *MTOR* and compared relative gene expression in those patients with splenic HS to the expression of these genes in

normal spleens (**Figure 3**). *AKT1*, *PIK3R*, and *MTOR* are genes that encode for kinases integral to the activation and progression of this pathway and thus increases in expression of these genes were used as a surrogate to detect activation of the AKT signaling pathway. In our splenic patients we observed statistically significant increases in the expression of all three genes (**Figure 3**). When we evaluated these primer probes to compare relative gene expression in those patients with pulmonary HS to the expression of these genes in normal lung tissue, we did not see any significant changes or consistent trends (**Figure 3**).

Microarray data

Genes in the NF-κB and AKT signaling pathways were previously identified in our rodent models to be increased and thus our initial experiments were designed to evaluate these specific genes in canine tumors. In the previously described experiments, we were limited by the number of archived cases that fit our criteria and the number of primer probes we could use. Additionally, we chose to focus our efforts on tumors arising in specific tissues to be able to compare the levels of gene expression to what is present normally in the tissue. Results from these studies suggest that there are different pathways involved in tumors arising in different tissues.

Canine HS is thought to arise from interstitial dendritic cells while a subset of these tumors, termed HHS are thought to arise from splenic macrophages. Non-hemophagocytic HS can be localized or disseminated and arise in a number of different tissues whereas HHS is mostly limited to the spleen with potential secondary dissemination. Therefore, we hypothesized that since our genes of interest reflecting NF-κB and AKT activation were elevated in canine histiocytic tumors arising from the spleen and not the lung, that these may represent the hemophagocytic sub-type and be of different cell origin with different pathogenetic mechanisms.

To test this, we utilized microarray analysis on 25 canine patients diagnosed with HS and 5 patients diagnosed with the hemophagocytic sub-type (**Table 3**). Fold change in fluorescence values were calculated after all values were normalized to *B-ACTIN*. The resulting fluorescence was used to determine the relative expression of all genes evaluated in tumors compared to controls. In an attempt to refine our controls, we isolated canine peripheral blood mononuclear cells (PBMC) and subsequently differentiated them into either dendritic cells or macrophages. Dendritic cells were used as controls for tumors diagnosed as HS and macrophages were used as controls for tumors diagnosed as the hemophagocytic sub-type. We then used IPA analysis to identify important pathways that differed between the tumors and the controls. Interestingly, we identified similar trends in the data for HHS as we did in our splenic samples (**Figure 4**). 7 out of 12 genes evaluated were increased in expression in HHS tumor samples compared to canine PBMC-derived macrophages and included: *IL1R1, MYD88, NFKB1, IRAK1, TRAF6, TNF,* and *IL-1β* (**Figure 4**). These are all genes encoding proteins necessary for NF-κB signaling suggesting an overall increase in the activation of this pathway. The remaining 5 genes included *IKBKB, NFKBIA, RELA, and IL6* which exhibited no changes in expression, and *IL1A* which was decreased in expression (**Figure 4**). IL1A is a pro-inflammatory protein that is not only produced as a result of NF-κB signaling, but, it is also an important cytokine that can initiate NF-κB signaling. Studies in humans have shown that mutations in *IL1A* that reduce the ability of miRNAs to bind and negatively regulate gene expression are associated with the development of hepatocellular carcinomas and gastric carcinomas [33, 34]. The reason for this has been postulated to be related to IL1A playing a more significant role in anti-tumor immunity [35]. Thus, our findings of decreases in expression of this gene in HHS patients is supportive of tumor development. In HS, however, when compared to PBMC-derived dendritic cells, there was no

clear increase or decrease in the overall pathway. In these samples, 4 out of 12 genes showed increased expression and included *IL-6, TRAF6, IKBKB, and NFKBIA* (**Figure 4**). 1 out of 14 genes was decreased and included: *TNF* (**Figure 4**). The remaining 7 genes showed no changes in overall expression (**Figure 4**). For AKT signaling, 8 genes were evaluated that reflected expression of the AKT signaling pathway and included: *EGFR, PI3CA, MTOR, PDK1, PTEN, BCL2L1*, AKT1 and *CDKN1A* (**Figure 5**). Similarly, HHS samples when compared to macrophages showed increases in 6 out of 8 genes and included: *EGFR, PI3CA, MTOR, PDK1, PTEN*, and *BCL2L1* (**Figure 5**). *BCL2L1* encodes for Bcl-xl, a member of the anti-apoptotic Bcl-2 family of proteins while *CDKN1A* encodes for P21, a cyclin-dependent kinase inhibitor and involved in cell cycle arrest. The remaining genes showed no changes in expression (**Figure 5**). For HS, 3 out of 8 genes were elevated and included: *PI3CA, PDK1,* and *PTEN* (**Figure 5**). 1 out of 7 genes showed a decrease in expression and included: *CDKN1A* (**Figure 5**) while the remaining genes exhibited no changes in expression.

DISCUSSION

The current study adds to the paucity of literature evaluating the pathogenesis of canine HS and suggests mechanistic differences between different tumor types. Our initial gene expression studies focused on comparing tumors arising in specific tissues to non-diseased, essentially normal tissue from that same organ in a control dog population. These results showed increases in expression in genes reflecting both NF-κB and AKT signaling in tumors arising from the spleen but not those arising in the lung. This was initially unexpected. However, canine HS is accepted to arise from two possible cell types. HS (non-hemophagocytic) arises from resident tissue dendritic cells. These tumors develop wherever dendritic cells are found and thus have been diagnosed in many different tissue types. HHS, however, is considered a sub-

type of HS and arises from splenic macrophages. This tumor develops in the spleen and has several unique features when compared to HS. First, it is often associated with a much worse prognosis and second, is often associated with paraneoplastic syndromes such as thrombocytopenia and anemia due to the active phagocytosis of patient blood cells by neoplastic cells [7, 10]. Since HHS is characterized as a sub-type of HS, further characterization studies are not often pursued following the initial diagnosis of HS. However, previous studies have shown significant differences in the histologic and clinical behavior of these two tumors. Our results further show mechanistic differences and thus implicate a necessity to differentiate the two.

Our initial expression studies and our microarray analysis suggest that a central pro-inflammatory cell signaling pathway, NF-κB signaling, may be important in canine HHS. We chose to evaluate NF-κB signaling by using the expression of *IL-6, TNF*, and *IL-1β* as surrogate markers of pathway activation. Levels of *TNF* and *IL-6* have been previously evaluated in a single case of HHS in a Golden retriever [36]. Similar to our initial methods, this study compared gene expression of *TNF* and *IL-6* from tumor tissue versus splenic tissue from a normal control dog. However, they identified increases in *IL-6* but decreases in *TNF* [36]. This significantly differs from our results that identified no changes in *IL6* and increases in *TNF* in our HHS patients. Since there is often marked variation in patient samples as evidenced by our own patient population, our evaluation includes higher patient numbers and is thus more robust and likely reveals trends more reflective of the general canine population. Another study evaluated levels of various pro-inflammatory cytokines including IL-6 and TNF in the serum of Bernese mountain dogs diagnosed with disseminated HS [37]. Results of this study showed no significant differences in serum IL-6 or TNF compared to levels in control dogs [37]. This study differs significantly from our study in that they evaluated circulating levels of these cytokines.

This is a more accurate reflection of systemic levels of inflammation, however, we were most interested in evaluating what may be coming directly from tumor tissue. A single study evaluating serum levels of inflammatory cytokines was performed in humans [38]. Three human patients diagnosed with malignant histiocytosis were included in the study and cytokines measured included TNF, IL-1β, and IL-6 [38]. Aside from increases in IL-6 (relative to reference ranges), the authors found no consistent changes in circulating cytokine levels among these patients [38]. Like the previous study in dogs, this study was designed to evaluate systemic levels of these cytokines and is not an accurate reflection of levels present in tumor tissue alone.

We also found significant increases in the expression of key genes in the AKT signaling pathway. Historically, previous studies have linked this pathway to HS in mice, dogs, and humans [11, 12]. In fact, some of the first studies looking at the pathogenesis of HS were done in mice. These studies found that mice genetically modified to have reduced *Pten* and absent *Ink4a* expression developed biphasic neoplasms composed of both a lymphoid and a histiocytic compartment [11]. Further analysis of these tumors illustrated a complete loss of *Pten* in tumor cells and a subsequent increase in phosphorylation of AKT [11]. Using immunohistochemistry, they were able to also evaluate the presence of PTEN in human HS samples. Here they showed that tumor cells did not stain positively thus suggesting a loss of PTEN protein in tumor cells [11]. Additionally, mutations in *PTEN* have been identified in the Bernese mountain dog, a breed predisposed to the development of the tumor [12]. Despite this, our results show that, in both our HS and HHS populations of dogs, *PTEN* expression is slightly increased (**Figure 5**). One explanation for this could relate to how we defined our cases. In our patients, we were interested in differences between those cases diagnosed as HS versus those diagnosed as HHS whereas the previous studies made no distinction between the two. Moreover, we attempted to

more accurately reflect changes in gene expression of these tumors by utilizing PBMC-derived dendritic cells or macrophages as controls. Despite finding increases in the expression of *PTEN*, we were able to show increases in expression in multiple genes reflecting AKT signaling suggesting an overall increase in expression of the pathway of our HHS patients. Moreover, we were also able to show that, in HHS patients, there are increases in the expression *BCL2L1*, a target gene of AKT signaling. *BCL2L1* encodes for the anti-apoptotic protein BCL-XL. Previous studies using knockout mice have shown that loss of this protein reduces susceptibility to colorectal cancer [39].

Gene expression studies are somewhat limiting as they only reveal what is happening at the transcription level. Ideally, we would like to be able to evaluate protein levels as translation and post-translational modifications can have significant impacts on the levels and amounts of protein. However, this tumor is exceptionally rare and thus our ability to accumulate fresh tissues is often the biggest limiting factor. Additionally, HS is not easily diagnosed prior to surgical biopsy and thus it can become cumbersome to sample every tumor where HS is a differential. Therefore, in order to begin making conclusions using the tissues that are currently available, we chose to evaluate archived FFPE tissues. Future studies will be needed to evaluate if similar patterns are identifiable at the protein level.

Another consideration when measuring relative gene expression is the identification of accurate control samples. In our initial gene expression studies, we chose to profile gene expression at the level of the tissue. In this way we clearly showed that in tumors arising in the spleen, there is a relative increase in expression in genes involved in both NF-κB and AKT signaling when compared to non-neoplastic, non-diseased, histologically quiescent splenic tissue. However, the argument could be made that these quiescent tissues are composed of a variety of

different cell types which have a variety of different baseline signaling. Therefore, in subsequent studies we attempted to evaluate gene expression changes using the tumor's cell of origin. Tumors identified as HHS were compared to canine macrophages and those identified as HS were compared to canine dendritic cells. Interestingly, we were able to show similar trends in our data despite the different criteria which suggests that both may be valid controls.

Though the use of patient samples has significantly more clinical relevance than, for example, tumors developed in mouse models or cell lines grown in culture, there are some limitations. Because these samples are from actual patients, there are many confounding variables that may affect our results. For example, these tumors represent tissues from multiple breeds. Though the Bernese mountain dog and Flat-coated retriever have been the only breeds to date to show specific clinical and genetic predispositions to certain types and locations of HS, there is a possibility that other purebred dogs may have specific clinical and genetic manifestations that may skew our overall data. Similar limitations exist in the use of patient tissues as controls. Additionally, differences in lifestyles such as diet and home environment, as well as, the possibility of concurrent disease and/or use of medications also contribute to the population heterogeneity.

This report summarizes our investigation of inflammatory pathways important in canine HS. We utilized gene expression studies and evaluated key genes as surrogate markers of NF-κB and AKT signaling activation. Indeed we found that not only are these pathways increased in tumor samples compared to tissue controls, but that these changes appear to be specific for those canine patients with HHS. Currently, HHS is considered a sub-type of HS and thus a distinction between the two is not often pursued. Our results suggest that differentiating between them will

provide meaningful clinical and prognostic significance and, thus, new and better diagnostics are critically needed.

Acknowledgements

We would like to acknowledge the Michigan State Diagnostic Lab and all personnel involved in acquiring and processing patient samples used for the microarray analysis.

References

1. Moore PF. A review of histiocytic diseases of dogs and cats. Vet Pathol. 2014; 51: 167-84. doi: 10.1177/0300985813510413.

2. Scurrell E, Trott A, Rozmanec M, Belford CJ. Ocular histiocytic sarcoma in a cat. Vet Ophthalmol. 2013; 16 Suppl 1: 173-6. doi: 10.1111/vop.12052.

3. Warschau M, Hoffmann M, Dziallas P, Hansmann F, Baumgartner W, Mischke R, Cichowski S, Fehr M. Invasive histiocytic sarcoma of the lumbar spine in a ferret (Mustela putorius furo). J Small Anim Pract. 2017; 58: 115-8. doi: 10.1111/jsap.12632.

4. Ishimori M, Michishita M, Yoshimura H, Azakami D, Ochiai K, Ishiwata T, Takahashi K. Disseminated histiocytic sarcoma with hemophagocytosis in a rabbit. J Vet Med Sci. 2017; 79: 1503-6. doi: 10.1292/jvms.17-0297.

5. Paciello O, Passantino G, Costagliola A, Papparella S, Perillo A. Histiocytic sarcoma of the nasal cavity in a horse. Res Vet Sci. 2013; 94: 648-50. doi: 10.1016/j.rvsc.2013.01.005.

6. Ogihara K, Itoh T, Mizuno Y, Tamukai K, Madarame H. Disseminated Histiocytic Sarcoma in an African Hedgehog (Atelerix albiventris). J Comp Pathol. 2016; 155: 361-4. doi: 10.1016/j.jcpa.2016.09.001.

7. Dervisis NG, Kiupel M, Qin Q, Cesario L. Clinical prognostic factors in canine histiocytic sarcoma. Vet Comp Oncol. 2016. doi: 10.1111/vco.12252.

8. Klahn SL, Kitchell BE, Dervisis NG. Evaluation and comparison of outcomes in dogs with periarticular and nonperiarticular histiocytic sarcoma. J Am Vet Med Assoc. 2011; 239: 90-6. doi: 10.2460/javma.239.1.90.

9. Kato Y, Murakami M, Hoshino Y, Mori T, Maruo K, Hirata A, Nakagawa TL, Yanai T, Sakai H. The class A macrophage scavenger receptor CD204 is a useful immunohistochemical

marker of canine histiocytic sarcoma. J Comp Pathol. 2013; 148: 188-96. doi: 10.1016/j.jcpa.2012.06.009.

10. Moore PF, Affolter VK, Vernau W. Canine hemophagocytic histiocytic sarcoma: a proliferative disorder of CD11d+ macrophages. Vet Pathol. 2006; 43: 632-45. doi: 10.1354/vp.43-5-632.

11. Carrasco DR, Fenton T, Sukhdeo K, Protopopova M, Enos M, You MJ, Di Vizio D, Nogueira C, Stommel J, Pinkus GS, Fletcher C, Hornick JL, Cavenee WK, et al. The PTEN and INK4A/ARF tumor suppressors maintain myelolymphoid homeostasis and cooperate to constrain histiocytic sarcoma development in humans. Cancer Cell. 2006; 9: 379-90. doi: 10.1016/j.ccr.2006.03.028.

12. Hedan B, Thomas R, Motsinger-Reif A, Abadie J, Andre C, Cullen J, Breen M. Molecular cytogenetic characterization of canine histiocytic sarcoma: A spontaneous model for human histiocytic cancer identifies deletion of tumor suppressor genes and highlights influence of genetic background on tumor behavior. BMC Cancer. 2011; 11: 201. doi: 10.1186/1471-2407-11-201.

13. Coutermarsh-Ott S, Simmons A, Capria V, LeRoith T, Wilson JE, Heid B, Philipson CW, Qin Q, Hontecillas-Magarzo R, Bassaganya-Riera J, Ting JP, Dervisis N, Allen IC. NLRX1 suppresses tumorigenesis and attenuates histiocytic sarcoma through the negative regulation of NF-kappaB signaling. Oncotarget. 2016; 7: 33096-110. doi: 10.18632/oncotarget.8861.

14. Allen IC, Moore CB, Schneider M, Lei Y, Davis BK, Scull MA, Gris D, Roney KE, Zimmermann AG, Bowzard JB, Ranjan P, Monroe KM, Pickles RJ, et al. NLRX1 protein attenuates inflammatory responses to infection by interfering with the RIG-I-MAVS and

TRAF6-NF-kappaB signaling pathways. Immunity. 2011; 34: 854-65. doi: 10.1016/j.immuni.2011.03.026.

15. Xia X, Cui J, Wang HY, Zhu L, Matsueda S, Wang Q, Yang X, Hong J, Songyang Z, Chen ZJ, Wang RF. NLRX1 negatively regulates TLR-induced NF-kappaB signaling by targeting TRAF6 and IKK. Immunity. 2011; 34: 843-53. doi: 10.1016/j.immuni.2011.02.022.

16. Tattoli I, Carneiro LA, Jehanno M, Magalhaes JG, Shu Y, Philpott DJ, Arnoult D, Girardin SE. NLRX1 is a mitochondrial NOD-like receptor that amplifies NF-kappaB and JNK pathways by inducing reactive oxygen species production. EMBO Rep. 2008; 9: 293-300. doi: 10.1038/sj.embor.7401161.

17. Lei Y, Wen H, Ting JP. The NLR protein, NLRX1, and its partner, TUFM, reduce type I interferon, and enhance autophagy. Autophagy. 2013; 9: 432-3. doi: 10.4161/auto.23026.

18. DiDonato JA, Mercurio F, Karin M. NF-kappaB and the link between inflammation and cancer. Immunol Rev. 2012; 246: 379-400. doi: 10.1111/j.1600-065X.2012.01099.x.

19. Koblansky AA, Truax AD, Liu R, Montgomery SA, Ding S, Wilson JE, Brickey WJ, Muhlbauer M, McFadden RM, Hu P, Li Z, Jobin C, Lund PK, et al. The Innate Immune Receptor NLRX1 Functions as a Tumor Suppressor by Reducing Colon Tumorigenesis and Key Tumor-Promoting Signals. Cell Rep. 2016; 14: 2562-75. doi: 10.1016/j.celrep.2016.02.064.

20. Zhang L, Shao L, Creighton CJ, Zhang Y, Xin L, Ittmann M, Wang J. Function of phosphorylation of NF-kB p65 ser536 in prostate cancer oncogenesis. Oncotarget. 2015; 6: 6281-94. doi: 10.18632/oncotarget.3366.

21. He W, Jiang Y, Zhang X, Zhang Y, Ji H, Zhang N. Anticancer cardamonin analogs suppress the activation of NF-kappaB pathway in lung cancer cells. Mol Cell Biochem. 2014; 389: 25-33. doi: 10.1007/s11010-013-1923-0.

22. He G, Karin M. NF-kappaB and STAT3 - key players in liver inflammation and cancer. Cell Res. 2011; 21: 159-68. doi: 10.1038/cr.2010.183.

23. Piao HL, Yuan Y, Wang M, Sun Y, Liang H, Ma L. alpha-catenin acts as a tumour suppressor in E-cadherin-negative basal-like breast cancer by inhibiting NF-kappaB signalling. Nat Cell Biol. 2014; 16: 245-54. doi: 10.1038/ncb2909.

24. Yuan TL, Cantley LC. PI3K pathway alterations in cancer: variations on a theme. Oncogene. 2008; 27: 5497-510. doi: 10.1038/onc.2008.245.

25. Ciruelos Gil EM. Targeting the PI3K/AKT/mTOR pathway in estrogen receptor-positive breast cancer. Cancer Treat Rev. 2014; 40: 862-71. doi: 10.1016/j.ctrv.2014.03.004.

26. Clark AR, Toker A. Signalling specificity in the Akt pathway in breast cancer. Biochem Soc Trans. 2014; 42: 1349-55. doi: 10.1042/bst20140160.

27. Cardoso AP, Pinto ML, Pinto AT, Oliveira MI, Pinto MT, Goncalves R, Relvas JB, Figueiredo C, Seruca R, Mantovani A, Mareel M, Barbosa MA, Oliveira MJ. Macrophages stimulate gastric and colorectal cancer invasion through EGFR Y(1086), c-Src, Erk1/2 and Akt phosphorylation and smallGTPase activity. Oncogene. 2014; 33: 2123-33. doi: 10.1038/onc.2013.154.

28. Danielsen SA, Eide PW, Nesbakken A, Guren T, Leithe E, Lothe RA. Portrait of the PI3K/AKT pathway in colorectal cancer. Biochim Biophys Acta. 2015; 1855: 104-21. doi: 10.1016/j.bbcan.2014.09.008.

29. Mundi PS, Sachdev J, McCourt C, Kalinsky K. AKT in cancer: new molecular insights and advances in drug development. Br J Clin Pharmacol. 2016; 82: 943-56. doi: 10.1111/bcp.13021.

30. Robbins HL, Hague A. The PI3K/Akt Pathway in Tumors of Endocrine Tissues. Front Endocrinol (Lausanne). 2015; 6: 188. doi: 10.3389/fendo.2015.00188.

31. Maniscalco L, Iussich S, de Las Mulas JM, Millan Y, Biolatti B, Sasaki N, Nakagawa T, De Maria R. Activation of AKT in feline mammary carcinoma: a new prognostic factor for feline mammary tumours. Vet J. 2012; 191: 65-71. doi: 10.1016/j.tvjl.2010.12.016.

32. Uva P, Aurisicchio L, Watters J, Loboda A, Kulkarni A, Castle J, Palombo F, Viti V, Mesiti G, Zappulli V, Marconato L, Abramo F, Ciliberto G, et al. Comparative expression pathway analysis of human and canine mammary tumors. BMC Genomics. 2009; 10: 135. doi: 10.1186/1471-2164-10-135.

33. Gao Y, He Y, Ding J, Wu K, Hu B, Liu Y, Wu Y, Guo B, Shen Y, Landi D, Landi S, Zhou Y, Liu H. An insertion/deletion polymorphism at miRNA-122-binding site in the interleukin-1alpha 3' untranslated region confers risk for hepatocellular carcinoma. Carcinogenesis. 2009; 30: 2064-9. doi: 10.1093/carcin/bgp283.

34. Zeng XF, Li J, Li SB. A functional polymorphism in IL-1A gene is associated with a reduced risk of gastric cancer. Tumour Biol. 2014; 35: 265-8. doi: 10.1007/s13277-013-1034-2.

35. Song X, Voronov E, Dvorkin T, Fima E, Cagnano E, Benharroch D, Shendler Y, Bjorkdahl O, Segal S, Dinarello CA, Apte RN. Differential effects of IL-1 alpha and IL-1 beta on tumorigenicity patterns and invasiveness. J Immunol. 2003; 171: 6448-56. doi:

36. Soare T, Noble PJ, Hetzel U, Fonfara S, Kipar A. Paraneoplastic syndrome in haemophagocytic histiocytic sarcoma in a dog. J Comp Pathol. 2012; 146: 168-74. doi: 10.1016/j.jcpa.2011.05.006.

37. Nikolic Nielsen L, Kjelgaard-Hansen M, Kristensen AT. Monocyte chemotactic protein-1 and other inflammatory parameters in Bernese Mountain dogs with disseminated histiocytic sarcoma. Vet J. 2013; 198: 424-8. doi: 10.1016/j.tvjl.2013.07.030.

38. Imashuku S, Okuda T, Yoshihara T, Ikushima S, Hibi S. Cytokine levels in aggressive natural killer cell leukemia and malignant histiocytosis. Br J Haematol. 1991; 79: 132-3. doi:

39. Scherr AL, Gdynia G, Salou M, Radhakrishnan P, Duglova K, Heller A, Keim S, Kautz N, Jassowicz A, Elssner C, He YW, Jaeger D, Heikenwalder M, et al. Bcl-xL is an oncogenic driver in colorectal cancer. Cell Death Dis. 2016; 7: e2342. doi: 10.1038/cddis.2016.233.

TABLES and FIGURES

Table 1

Dog	Age (years)	Sex	Breed	Primary tumor location	Additional sites	CD18 IHC Positivity
1	14	MN	Labrador retriever	Spleen	Liver, lung, heart, LN	Y
2	4	MN	Pitbull	Spleen	Liver	Y
3	10	MN	Mixed	Spleen	Liver	Y
4	10	FS	Golden retriever	Spleen	None	Y
5	10	FS	German shepherd	Spleen	None	Y
6	10	MN	Mixed	Spleen	None	Y
7	8	MN	Boston terrier	Spleen	None	Y
8	13	FS	Mixed	Spleen	None	Y
9	8	MN	Labrador Retriever	Spleen	None	Y
10	11	MN	Golden retriever	Spleen	None	Y
11	11	MN	English sheepdog	Lung	None	Y
12	9	MN	Beagle	Lung	LN	Y
13	11	MN	Golden retriever	Lung	Kidney, eye	Y
14	12	FS	Staffordshire terrier	Lung	None	Y

Table 1: Ten splenic histiocytic sarcoma patients and four pulmonary histiocytic sarcoma patients were utilized in gene expression analysis. Data for patients diagnosed with histiocytic sarcoma and used for relative gene expression analysis using tumor tissue compared to tissue specific controls.

Table 2

Dog	Age (years)	Sex	Breed	Tissue used	Cause of death/euthanasia
1	>1	F	Pitbull	Spleen	ARD, unknown death
2	9	MN	Boxer	Spleen	Heart failure
3	14	FS	Mixed	Spleen	Hepatic neoplasia
4	11	MN	Mixed	Spleen	Meningioma
5	4	M	Bulldog	Spleen	Renal disease
6	3	MN	Mixed	Spleen	Mandibular osteomyelitis
7	11	MN	Mixed	Spleen	Hemorrhagic gastroenteritis
8	14	FS	Australian shepherd	Spleen	Degenerative myelopathy
9	3	MN	Mixed	Lung	Mandibular osteomyelitis
10	6	F	Mixed	Lung	Granulomatous meningoencephalitis
11	14	FS	Mixed	Lung	Hepatic neoplasia
12	11	MN	Mixed	Lung	Meningioma

Table 2: Eight samples of spleen and four samples of lung were available for use as tissue controls. Data for patients chosen as control tissues in gene expression analysis comparing tumor tissue to tissue specific controls.

Table 3

Dog	Breed	HHS vs. HS
1	Bernese mountain dog	HHS
2	Bernese mountain dog	HHS
3	Bernese mountain dog	HHS
4	Bernese mountain dog	HHS
5	Bernese mountain dog	HHS
6	Bernese mountain dog	HS
7	Bernese mountain dog	HS
8	Bernese mountain dog	HS
9	Bernese mountain dog	HS
10	Bernese mountain dog	HS
11	Bernese mountain dog	HS
12	Other	HS
13	Bernese mountain dog	HS
14	Other	HS
15	Other	HS
16	Other	HS
17	Other	HS
18	Other	HS
19	Other	HS
20	Bernese mountain dog	HS
21	Other	HS
22	Other	HS
23	Other	HS
24	Other	HS

25	**Other**	**HS**
26	**Other**	**HS**
27	**Other**	**HS**
28	**Other**	**HS**
29	**Bernese mountain dog**	**HS**
30	**Other**	**HS**

Table 3: Patient data for microarray analysis. Patients were identified as being a Bernese mountain dog or other breed and diagnosed with histiocytic sarcoma (HS) or hemophagocytic histiocytic sarcoma (HHS).

Figure 1

A.

B.

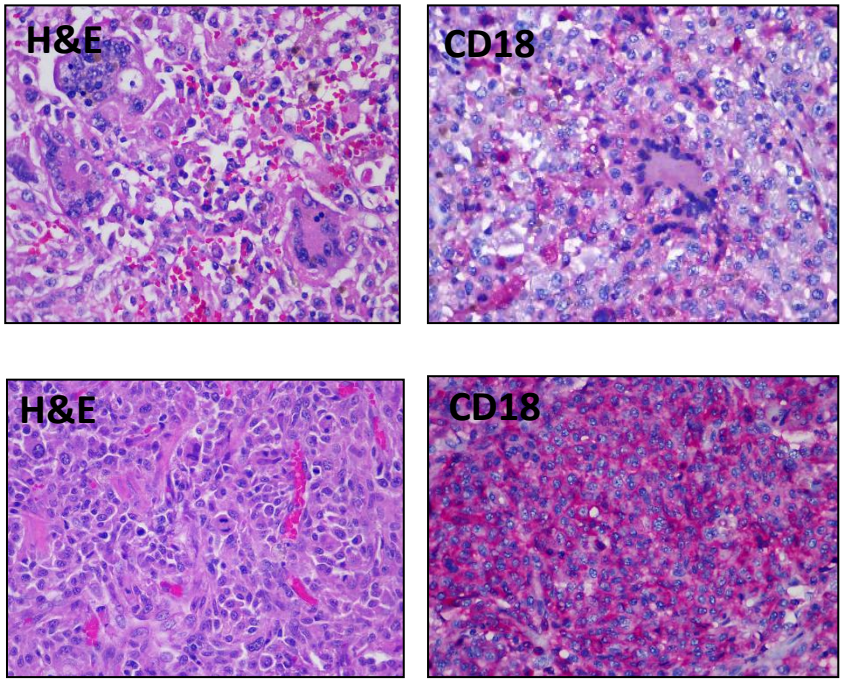

Figure 1. All canine samples were confirmed to be histiocytic sarcoma. Tumor tissue from patients with primary splenic (A) and pulmonary (B) HS was histologically similar and composed of pleomorphic histiocytic cells that effaced normal tissue architecture and stained positively with CD18 immunohistochemistry. Images are at 400x magnification.

Figure 2

A.

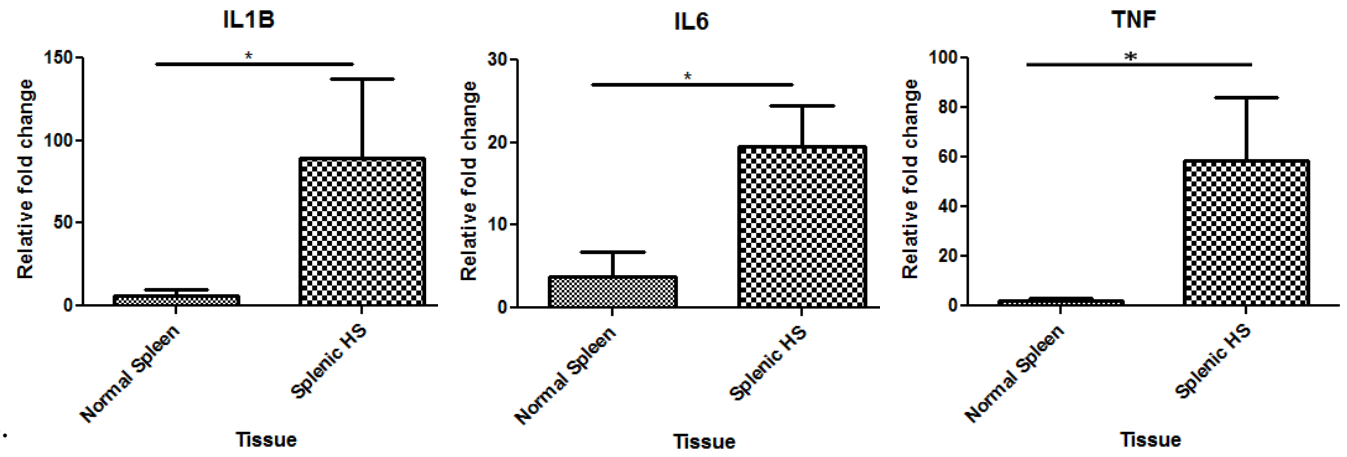

B.

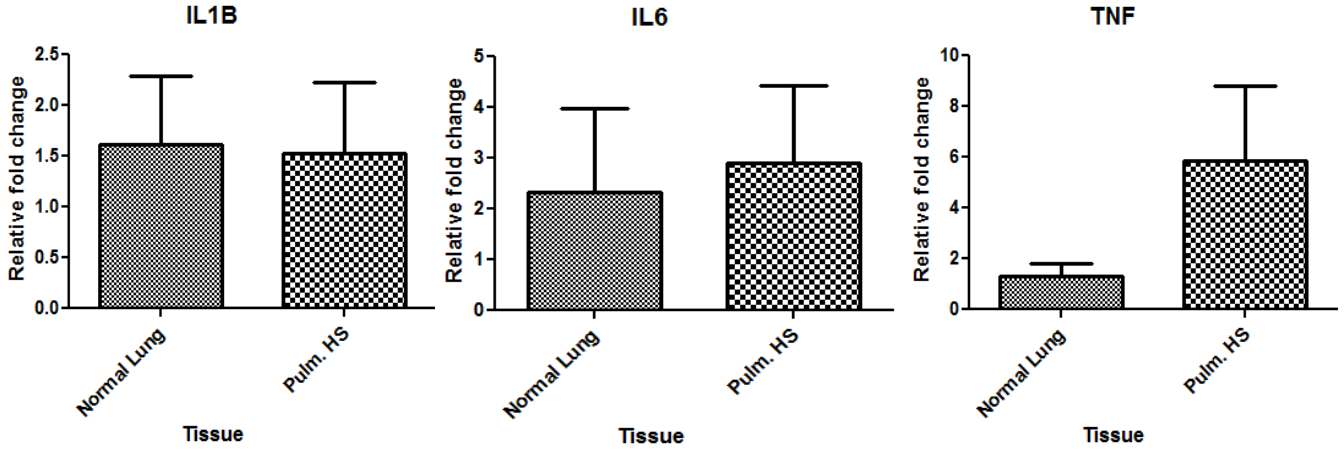

Figure 2: Genes reflecting NF-κB signaling exhibited differing relative expression between splenic and pulmonary tumors. (A) Gene expression changes in splenic histiocytic sarcoma when compared to normal splenic tissue. *Il-1β* and *Il-6* show statistically significant increases in expression, n=10. (B) Gene expression changes in pulmonary histiocytic sarcoma when compared to normal lung tissue. No statistically significant changes are identified, n= 4. *=$p<0.05$.

Figure 3

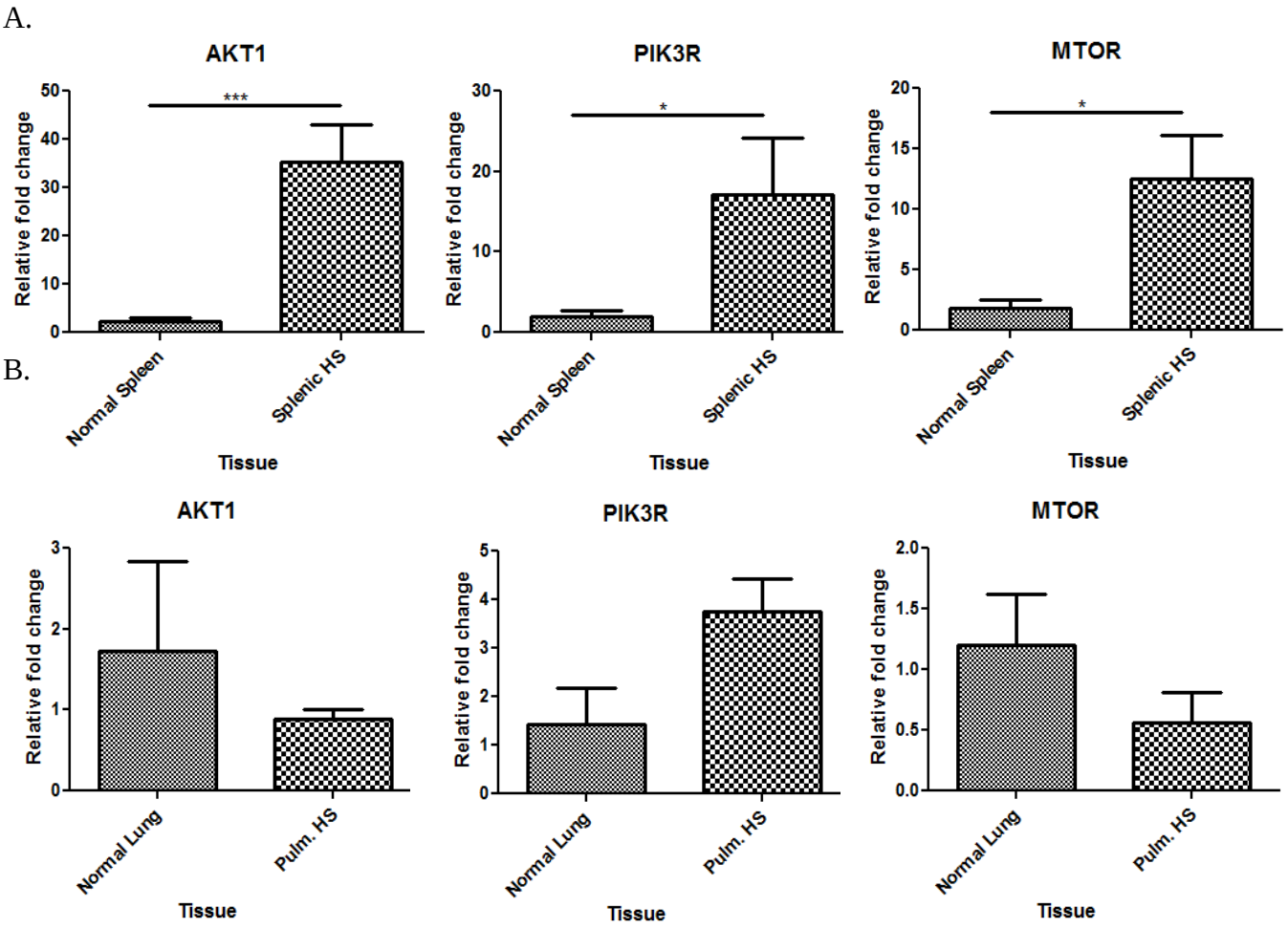

Figure 3: Genes reflecting AKT signaling exhibited differing relative expression between splenic and pulmonary tumors. (A) Gene expression changes in splenic histiocytic sarcoma when compared to normal splenic tissue. *Akt1*, *Pik3r*, and *Mto*r show statistically significant increases, n=10. (B) Gene expression changes in pulmonary histiocytic sarcoma compared to normal lung tissue. No statistically significant changes are identified, n=4. ***=$p<0.0005$ *=$p<0.05$.

Figure 4

A.

HHS	
IL1R1	39.11
TNF	10.98
NFKB1	9.20
IL1B	8.44
MYD88	5.26
IRAK1	3.84
TRAF6	3.66
IKBKB	1.53
NFKBIA	1.44
RELA	1.42
IL6	-1.21
IL1A	-12.09

Min Max

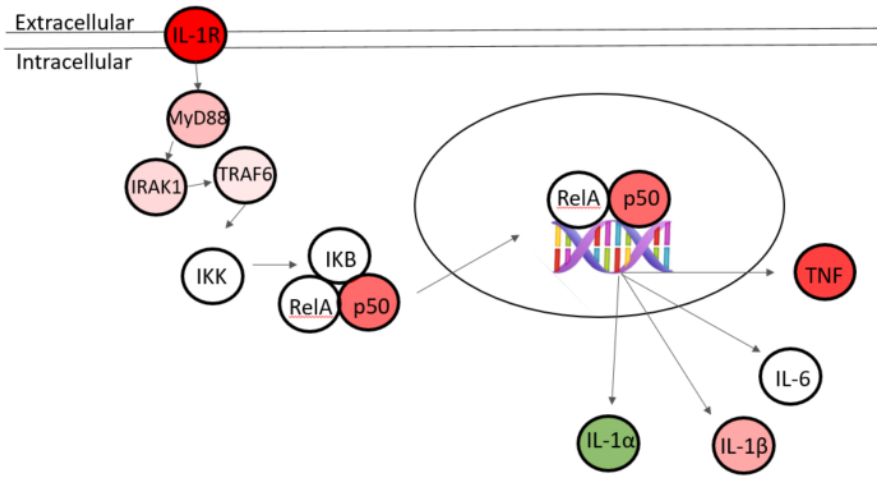

B.

HS	
IL6	22.00
TRAF6	4.46
NFKBIA	2.59
IKBKB	2.03
IL1A	1.81
MYD88	1.69
NFKB1	1.66
IL1R1	1.54
RELA	1.25
IRAK1	1.04
IL1B	-1.52
TNF	-3.85

Min Max

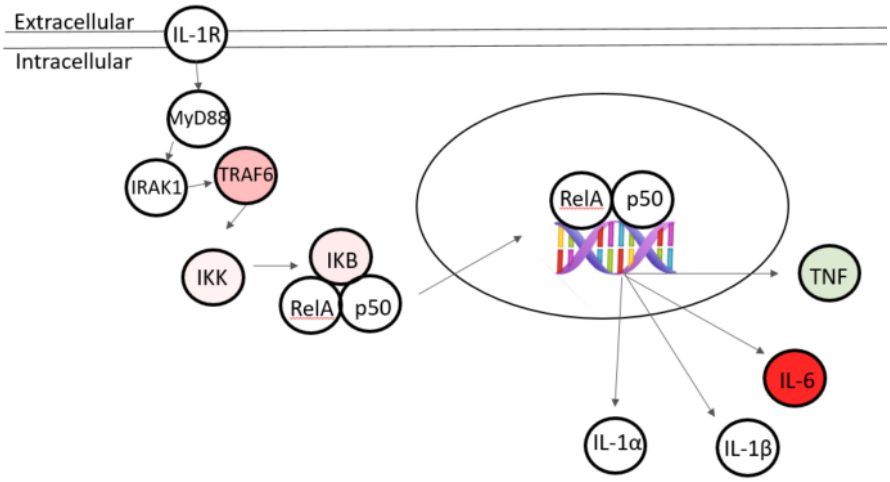

Figure 4: Genes reflecting NF-κB signaling exhibited differing relative expression between hemophagocytic histiocytic sarcoma (A) and histiocytic sarcoma (B). Heat maps and signaling pathways show relative fold changes in genes evaluated where red represents a 2 fold or greater increase in expression and green a 2 fold or greater decrease in expression when compared to controls. HS, n=25, HHS, n=5.

Figure 5

A.

HHS	
EGFR	20.53
PIK3CA	8.91
MTOR	8.35
PDK1	6.76
BCL2L1	3.93
PTEN	2.07
AKT1	1.81
CDKN1A	-1.70

Min Max

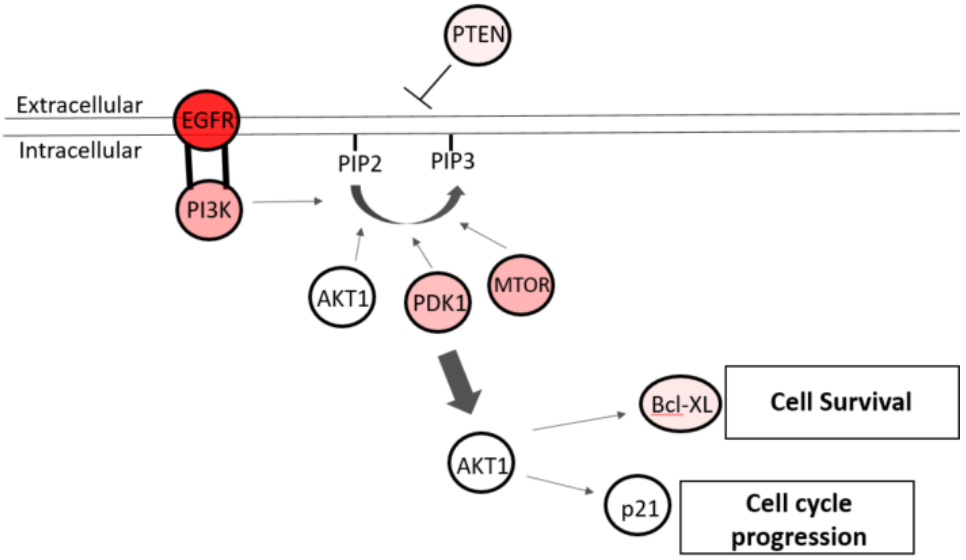

B.

HHS	
EGFR	20.53
PIK3CA	8.91
MTOR	8.35
PDK1	6.76
BCL2L1	3.93
PTEN	2.07
AKT1	1.81
CDKN1A	-1.70

Min Max

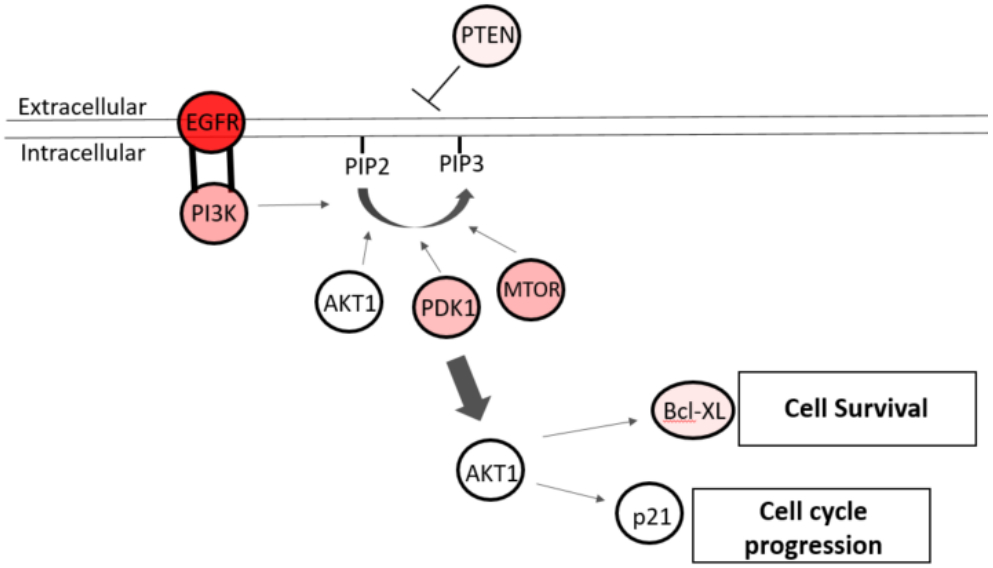

Figure 5: Genes reflecting AKT signaling exhibited differing relative expression between hemophagocytic histiocytic sarcoma (A) and histiocytic sarcoma (B). Heat maps and signaling pathways show relative fold changes in genes evaluated where red represents a 2 fold or greater increase in expression and green a 2 fold or greater decrease in expression when compared to controls. HS, n=25, HHS, n=5.

Chapter 5

Generation of a Murine Xenograft Model to Study Histiocytic Sarcoma

Coutermarsh-Ott, SL, Qin, Q, Dervisis, NG, Allen, IC.

Abstract

Histiocytic sarcoma (HS) is an aggressive tumor in both human and veterinary species. It is exceptionally rare in humans and only slightly more common in dogs. Due to its rarity, there is a paucity of literature evaluating mechanisms of disease. Moreover, therapeutic options in both humans and dogs are minimal and have limited efficacy. Current models for evaluating the disease have relied heavily on genetically modified mice and spontaneous tumor development in canines. Because of its rarity and its limited therapeutic options, additional models are needed. In our lab, we developed a xenograft model by injecting an immortalized canine HS cell line, DH82, into an immunocompromised strain of mouse, NOD scid gamma. Doing this, we successfully grew HS tumors that had negligible effects on the health of the mice. Additionally we found that these tumors are able to metastasize to the lungs of these mice. We were able to perform pilot studies using the PI3 kinase inhibitor, LY294002, in our model and found that a 24 hour exposure to the drug does not appear to significantly impact AKT signaling within tumor tissue.

Introduction

Histiocytic sarcoma (HS) is a malignant tumor that occurs rarely in humans and infrequently in veterinary species. In humans, it can be diagnosed in the lymph node, gastrointestinal tract, soft tissues, and skin [1-3]. In veterinary patients, primarily dogs, it is most common in the spleen, lung, skin, periarticular soft tissues, and, more recently, the central nervous system [4]. Most of these tumors arise from tissue-specific interstitial dendritic cells while a subset of these tumors arise from CD11d+ splenic macrophages and are termed hemophagocytic histiocytic sarcoma (HHS). In all species, HS is generally associated with a poor prognosis, high rates of metastasis, and limited treatment options. Because of this, the ability to study molecular pathways involved in the development and progression of HS as well as the efficacy of new treatment modalities is important.

Though animal models for studying HS are limited, the majority of the current literature focuses on the naturally-occurring disease in dogs. This has several advantages. HS in canines is a good model for the disease in humans. It happens slightly more frequently in dogs and has been associated with many of the same mutations identified in humans [5]. However, the naturally occurring disease in dogs still has many drawbacks. Though it does occur more frequently than in humans, the overall incidence is still relatively low in canine cancer patients. Additionally, ethical treatment of patients allow limited opportunity for experimental manipulation or the use of true experimental controls. This is important for both mechanistic and therapeutic studies as molecular techniques like manipulating gene and protein expression are important. Moreso, factors like owner compliance, home environment, age, sex, nutritional status, concurrent disease, and previous treatments can all create additional variables that may confound results and obscure important trends.

To address these shortcomings, multiple cell lines have been developed for *in vitro* experiments. Both immortalized and primary cell lines can be useful in studying disease mechanisms but also allow for some experimental manipulation. One of the earliest developed lines is the DH82 cell line. This is an immortalized canine cell line derived from a single, spontaneous case of malignant histiocytosis in a 10 year-old, male Golden retriever (ATCC). These cells were originally characterized as histiocytic by the presence of Fc-receptors, phagocytosis of latex particles, and plastic adherence in cell culture as well as their consistent histologic and ultrastructural morphology [6]. The advantage of these cell lines is that they provide access to a relatively constant flow of cells that are easy to grow, easy to manipulate, and easy to sample for experimental results. The shortcomings of these *in vitro* models are the inability of the cell growth vessel to neither recapitulate the 3-D environment of a biological tumor nor account for the biological interactions between the tumor and the host. A variety of host derived factors including the tumor stroma, blood vessels, immune cells, etc. can play a significant role in how tumors grow and develop. To address this, we developed a xenograft model using DH82 cells implanted into the immunocompromised mouse line, NOD scid gamma. In this model, we were able to successfully grow HS tumors that metastasized but did not affect the overall health of the mouse. Moreover, we have been able to use this model in testing the therapeutic efficacy of novel treatment strategies. Because HS is a malignant disease with a poor prognosis, improved models are necessary to investigate important mechanisms of disease that may have potential therapeutic implications in both human and veterinary patients.

Materials and Methods

Animals

All experiments were conducted according to the NIH Guide for the Care and Use of Laboratory Animals and were conducted under the approval of the Virginia Tech Institutional Animal Care and Use Committee (IACUC). All animals used for tumor injection experiments were 4-6 week-old, female, NOD scid gamma (NSG) mice derived from animals acquired from Jackson Laboratories. Once received, animals were allowed to acclimate at least seven days prior to experiments. These animals were housed under specific pathogen free (SPF) conditions with autoclaved housing and materials, fed irradiated mouse chow *ad libitum*, and offered autoclaved water *ad libitum*.

Tumor injections

Cells were originally purchased from ATCC (ATCC® CRL-10389™) and maintained as frozen stocks. DH82 cells were grown under standard cell culture conditions in Eagle's Minimum Essential medium (EMEM) supplemented with 15% fetal bovine serum (FBS), 1% non-essential amino acids, 100 units/ml penicillin, and 100 ug/ml streptomycin. Prior to injection, cells were enumerated for 2-4 generations, washed, and re-suspended in Matrigel. Mice were anesthetized with 2-5% Isoflurane and 2.25×10^6 cells/100 ul Matrigel were injected subcutaneously into the right caudal flank. All animals were recovered on room air. Following injections, mice were weighed and monitored twice weekly for health and tumor status. Once tumors were visible (6-8 weeks after injection), animals were weighed and tumors measured three times weekly. Animals were euthanized when tumors reached a calculated diameter of 1.4-1.6 cm. At necropsy, samples of tumor, lung, and spleen were placed into formalin. Samples of tumor were also taken for fresh frozen for downstream RNA analysis. Formalin fixed samples were processed routinely for H&E staining, as well as, submitted for canine CD18 immunohistochemistry.

Acute LY294002 study

Tumor injections were performed as described above. Once tumors reached 0.75-1.0 cm calculated diameter, mice were intraperitoneally (i.p.) injected with 100 µl of a 25 mg/kg LY294002 (Sigma) solution. Prior to injection, lyophilized LY294002 was dissolved in DMSO and then reconstituted to the appropriate dose in sterile phosphate buffered saline (PBS). Mice were euthanized 24 hours following injection. Samples of tumor and lung were placed into formalin and submitted for routine histologic processing. Samples of fresh tumor were utilized for protein extraction and Western blotting.

Results

Mice develop subcutaneous masses that do not appear to be associated with weight loss.

To develop an experimental model of canine HS, we injected 2.25 x 10^6 cells resuspended in Matrigel subcutaneously into the right flank of NSG mice. To assess tumor size, we utilized a method previously utilized in a breast cancer model [7]. Briefly, two perpendicular diameters are taken and the square root of the multiplication of these two numbers is calculated. Mice developed palpable tumors approximately 6-8 weeks following injection. The development of these tumors did not appear to have any significant effects on overall animal health as the animals continued to gain weight over the course of the study (**Figure 1**). Additionally, no overt clinical evidence of morbidity was identified nor were any animals lost during the experiment. Upon necropsy, we identified pale tan, soft to firm masses within the subcutis (**Figure 2A**). On cut section, they were homogenous and pale tan. Tumors located on the flank showed no evidence of involvement with adjacent structures. Few tumors grew slightly

caudally and ended up over the right hip joint or leg musculature. Rarely in these tumors there was infiltration into the adjacent skeletal muscle.

Tumors are morphologically and immunohistochemically consistent with canine histiocytic sarcoma.

Samples of the primary tumor were fixed in formalin and evaluated by routine histopathology. Tumors were characterized by an unencapsulated, infiltrative, densely cellular neoplasm composed of sheets of malignant histiocytic cells expanding the subcutis (**Figure 2B**). These cells were markedly pleomorphic and characterized by moderate to abundant amounts of eosinophilic cytoplasm with large round to irregular nuclei with a large magenta nucleolus. They exhibited numerous features of malignancy similar to the tumor in canines including cytomegaly and karyomegaly **(Figure 2B)**. Mitotic figures were frequent and often bizarre. These are all features that are commonly identified in canine HS. To rule out the possibility of a neoplasm induced by our initial injection and confirm that these cells were indeed canine in origin, we utilized immunohistochemistry. CD18 is a receptor found on most leukocytes and is commonly used in the initial identification of HS in canines. Therefore we performed IHC using a canine CD18 antibody and, indeed, tumor cells exhibited diffuse cytoplasmic and/or membranous positivity (**Figure 2C**). No adjacent mouse tissues exhibited staining.

Mice develop pulmonary metastases that are morphologically and immunohistochemically consistent with canine histiocytic sarcoma.

At necropsy, scattered areas of pulmonary hemorrhage were identified grossly (**Figure 3A)**. Therefore, lung tissues were fixed in formalin and submitted for routine H&E staining. Scattered throughout alveolar septa were few clusters of neoplastic cells (**Figure 3B**). These

cells exhibited histologic features similar to those identified in the primary tumor. There was marked pleomorphism and nuclear gigantism. To identify the cell of origin of these clusters of neoplastic cells, canine CD18 was again performed. The large, abnormal neoplastic cells exhibited diffuse positivity (**Figure 3C**). No adjacent mouse tissue exhibited staining.

No changes in protein expression were identified following treatment with LY294002

Previous studies have shown than AKT signaling is an important pathway involved in the development of HS in mice, humans, and dogs [5, 8, 9]. Therefore, we were interested in utilizing our model in a small pilot study to evaluate the use of LY294002, a PI3 kinase inhibitor, to treat HS tumors. We hypothesized that treatment of these mice with this drug would lead to decreases in AKT signaling within 24 hours following treatment. Therefore, we allowed tumors to grow to 0.75-1.0 cm and i.p. injected all mice with 25 mg/kg of LY294002. Twenty-four hours following treatment, the animals were euthanized and fresh tumor samples were submitted for protein extraction and Western blot for AKT, p-AKT, GSK3β, and p- GSK3β. B-actin was performed for normalization. No significant differences in the expression of proteins were identified between animals treated with the drug or vehicle (**Figure 4**).

Discussion

Our lab is one of a handful of labs utilizing this model to study HS. Yamazaki et al has utilized a xenograft model of canine HS to evaluate the efficacy of YM155, a drug that promotes apoptosis through the inhibition of survivin, as a treatment for HS. In these studies, three previously characterized canine HS cell lines were injected subcutaneously into nude mice and tumors were allowed to develop [10]. Similar to our studies, these authors describe no significant morbidities, such as weight loss, associated specifically with the development and

growth of these tumors, and they also describe the development of lung metastases from the primary tumor in all cell lines [10]. More recently, Pfankuche et al has utilized a xenograft model of canine HS to study the potential use of Morbillivirus as an oncolytic agent [11]. These studies injected DH82 cells into SCID mice. Though they did not directly report on weight change or other measures of morbidity, they do describe tumor necrosis as a measure of tumor regression. In tumors not infected with Morbillivirus, there is minimal necrosis of the tumor which is consistent with our findings as well [11]. Collectively, the results of our studies and these studies have shown that this model is relatively safe in terms of the overall health of the research animal and is practical for use in scientific experimentation.

Xenograft models are an important tool used by many researchers to study cancer pathogenesis. However, consideration needs to be given to both their benefits and limitations. They are certainly advantageous over *in vitro* culture methods as they provide for a 3-D environment and more realistic biological interactions. They are also advantageous over utilizing naturally occurring disease in veterinary species, such as dogs, which are limited by ethical considerations as well as the potential for uncontrollable variables producing confounding results. However, xenograft models do require the use of significantly immunocompromised mice to prevent tumor rejection. Our model uses NOD scid gamma mice (Prkdc^{scid} Il2rg^{tm1Wjl}/SzJ), but, as the previously mentioned studies have shown, other immune compromised strains can be used as well [10, 11]. Regardless of the strain, these mice all have significant defects in their cellular and humoral immunity. This is important as the immune system has been shown to play very important roles in tumor growth and promotion [12]. Additionally, housing these animals requires more diligent husbandry than traditional SPF mice.

They require autoclaved bedding and materials, autoclaved water, and irradiated food to prevent infection by opportunistic pathogens in the environment.

The results of our pilot study using LY294002 revealed no significant differences in AKT signaling between tumors treated with drug versus those treated with vehicle. However, this study had some limitations. We found that the LY294002 drug was very difficult to solubilize under our conditions. Due to the nature of the drug, it requires solubilization with a solvent such as DMSO. However, DMSO can be toxic to animals and thus we needed to keep our concentrations injected into the animals at less than 5% of the total injection dose. In order to do this, we solubilized the drug in small amounts of DMSO and then resuspended that solution in PBS. Using this method, the drug formed a heavy precipitate that was difficult to equalize across injections. Because of this, we are pursuing collaborations to use this model in investigations of novel drug delivery vehicles such as nanoparticles and nanobots.

We are among some of the first reports of the use of DH82 cells in xenograft models and one of few using this cell line to study cancer therapeutics. These xenograft models provide an important alternative tool to studying rare diseases, such as HS, where patient samples and resources are limited. We were able to not only successfully generate our model, but also utilize it in an experimental situation to test a therapeutic not previously evaluated for the use in HS. Additionally, the model allows for the added benefit of studying the events of spontaneous metastasis. We anticipate the continued use of this model in the hopes of furthering our knowledge of the pathogenesis of this disease as well as the repertoire of potential therapeutics available for patient treatment. We anticipate using this model for future studies evaluating the use of novel drug delivery vehicles as well as novel treatment strategies such as high-frequency irreversible electroporation.

References

1. Zhang X, Kryston JJ, Michalak WA, Zhang K, Lin F, Schuerch C. Histiocytic sarcoma in the small intestine: a case report with flow cytometry study and review of the literature. Pathol Res Pract. 2008; 204: 763-70. doi: 10.1016/j.prp.2008.03.009.

2. Hornick JL, Jaffe ES, Fletcher CD. Extranodal histiocytic sarcoma: clinicopathologic analysis of 14 cases of a rare epithelioid malignancy. Am J Surg Pathol. 2004; 28: 1133-44. doi:

3. Schnettler K, Salomone C, Valbuena JR. [Cutaneous histiocytic sarcoma: report of one case]. Rev Med Chil. 2009; 137: 547-51. doi: /S0034-98872009000400014.

4. Affolter VK, Moore PF. Localized and disseminated histiocytic sarcoma of dendritic cell origin in dogs. Vet Pathol. 2002; 39: 74-83. doi: 10.1354/vp.39-1-74.

5. Hedan B, Thomas R, Motsinger-Reif A, Abadie J, Andre C, Cullen J, Breen M. Molecular cytogenetic characterization of canine histiocytic sarcoma: A spontaneous model for human histiocytic cancer identifies deletion of tumor suppressor genes and highlights influence of genetic background on tumor behavior. BMC Cancer. 2011; 11: 201. doi: 10.1186/1471-2407-11-201.

6. Wellman ML, Krakowka S, Jacobs RM, Kociba GJ. A macrophage-monocyte cell line from a dog with malignant histiocytosis. In Vitro Cell Dev Biol. 1988; 24: 223-9. doi:

7. Pulaski BA, Ostrand-Rosenberg S. Mouse 4T1 breast tumor model. Curr Protoc Immunol. 2001; Chapter 20: Unit 20.2. doi: 10.1002/0471142735.im2002s39.

8. Coutermarsh-Ott S, Simmons A, Capria V, LeRoith T, Wilson JE, Heid B, Philipson CW, Qin Q, Hontecillas-Magarzo R, Bassaganya-Riera J, Ting JP, Dervisis N, Allen IC. NLRX1 suppresses tumorigenesis and attenuates histiocytic sarcoma through the negative regulation of NF-kappaB signaling. Oncotarget. 2016; 7: 33096-110. doi: 10.18632/oncotarget.8861.

9. Carrasco DR, Fenton T, Sukhdeo K, Protopopova M, Enos M, You MJ, Di Vizio D, Nogueira C, Stommel J, Pinkus GS, Fletcher C, Hornick JL, Cavenee WK, et al. The PTEN and INK4A/ARF tumor suppressors maintain myelolymphoid homeostasis and cooperate to constrain histiocytic sarcoma development in humans. Cancer Cell. 2006; 9: 379-90. doi: 10.1016/j.ccr.2006.03.028.

10. Yamazaki H, Takagi S, Hosoya K, Okumura M. Survivin suppressor (YM155) enhances chemotherapeutic efficacy against canine histiocytic sarcoma in murine transplantation models. Res Vet Sci. 2015; 99: 137-44. doi: 10.1016/j.rvsc.2015.02.003.

11. Pfankuche VM, Spitzbarth I, Lapp S, Ulrich R, Deschl U, Kalkuhl A, Baumgartner W, Puff C. Reduced angiogenic gene expression in morbillivirus-triggered oncolysis in a translational model for histiocytic sarcoma. J Cell Mol Med. 2017; 21: 816-30. doi: 10.1111/jcmm.13023.

12. Hanahan D, Weinberg RA. Hallmarks of cancer: the next generation. Cell. 2011; 144: 646-74. doi: 10.1016/j.cell.2011.02.013.

Figures

Figure 1

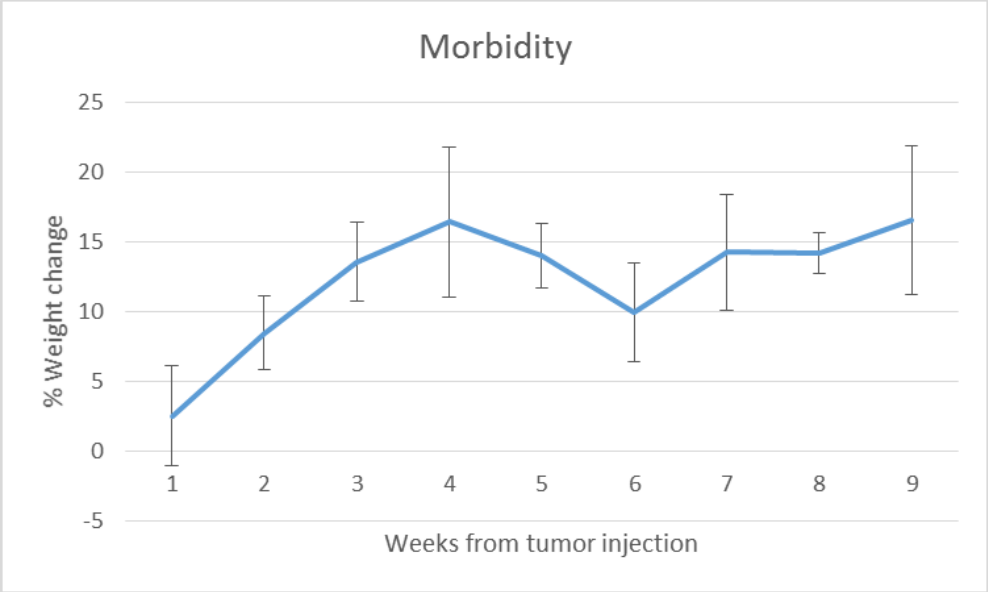

Figure 1. Implantation and growth of tumor cells does not have significant effects on overall health of the mice. Over the course of the study, mice continue to steadily gain weight with no evidence of weight loss.

Figure 2

A.

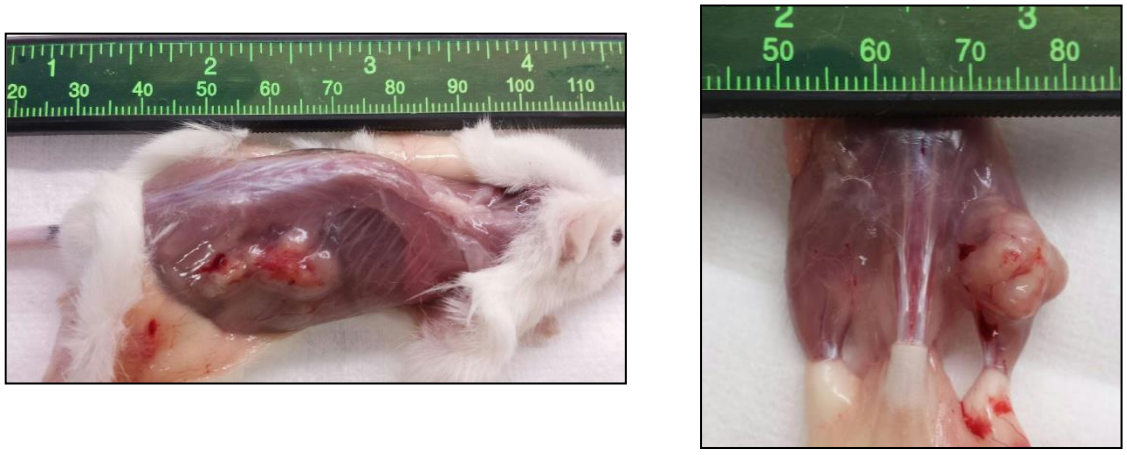

B.

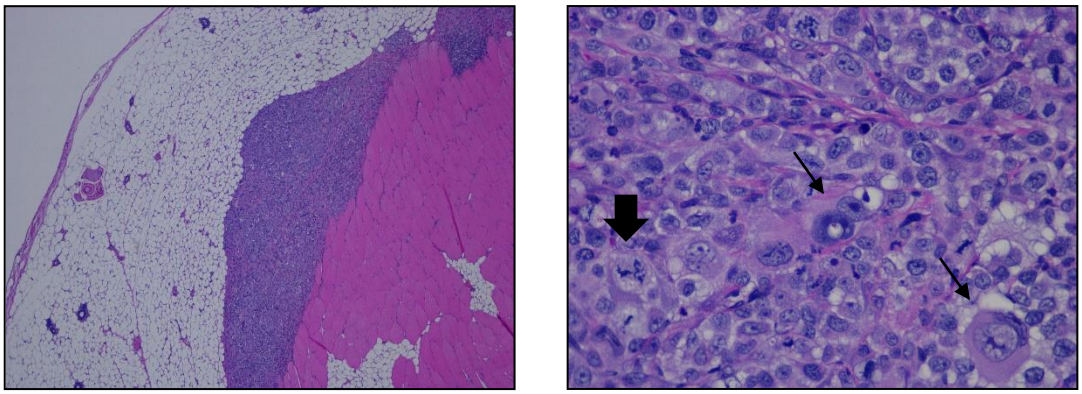

C.

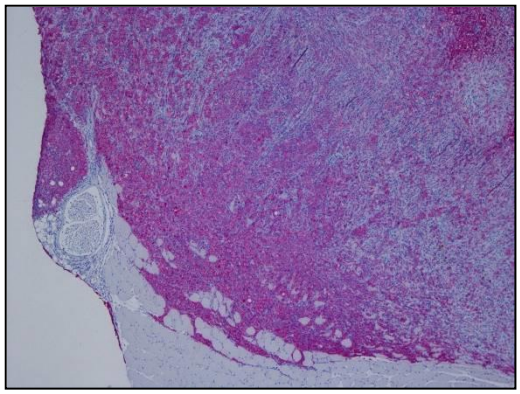

Figure 2. Tumors were grossly, histologically, and immunohistochemically consistent with canine HS. (A) Grossly, tumors were soft to firm, pale white masses within the subcutis. (B) Histologically, neoplastic cells were pleomorphic and often characterized by both cyto- and karyomegaly (thin arrow). Mitotic figures were frequent and often bizarre (thick arrow). (C) Staining with canine CD18 antibody revealed diffuse cytoplasmic staining within neoplastic cells.

Figure 3

A.

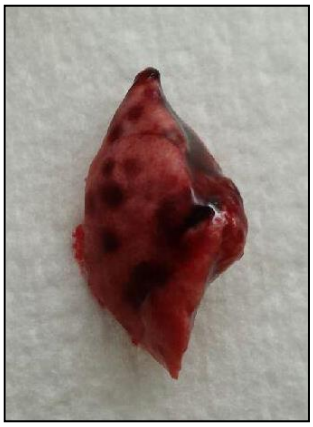

B.

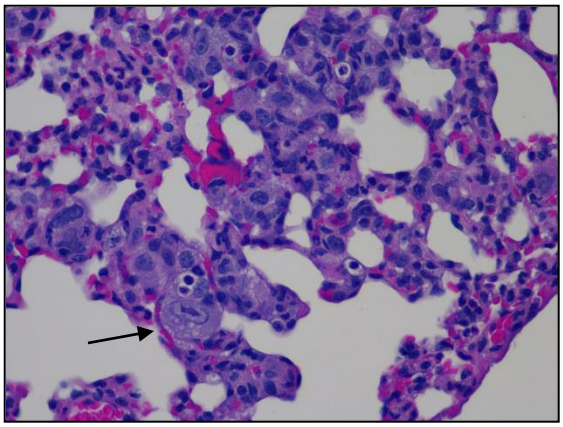

C.

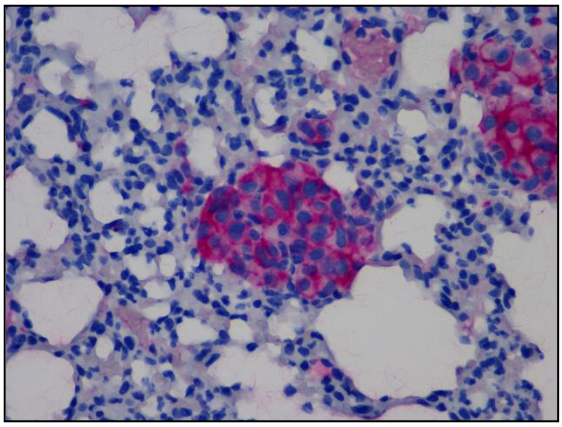

Figure 3. Tumors metastasized to the lungs. (A) Grossly there were areas of hemorrhage on the surface of the lungs. (B) Histologically, there were neoplastic cells within alveolar septa (thin arrow). (C) Staining with canine CD18 antibody revealed diffuse cytoplasmic staining within neoplastic cells.

Figure 4

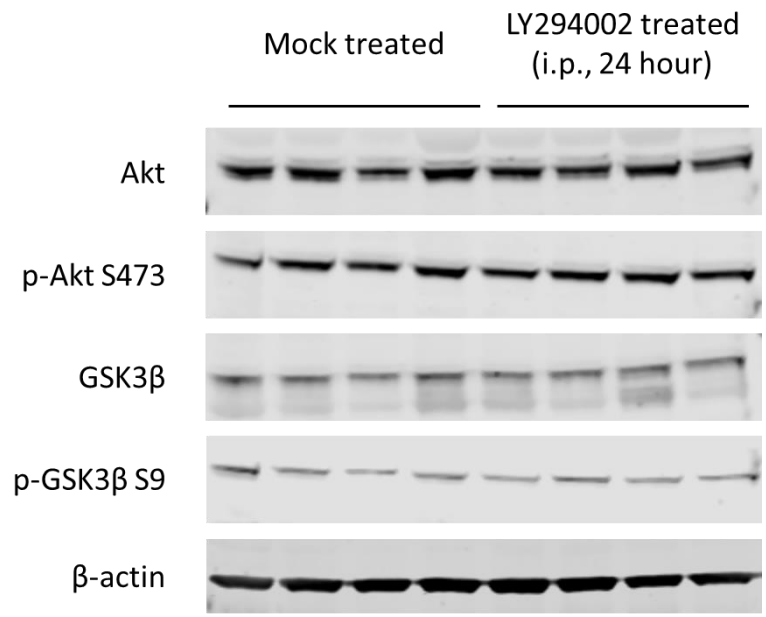

Figure 4. Western blotting revealed no significant differences in AKT signaling. No significant differences in AKT signaling were identified between tumor-bearing animals treated with LY294002 and tumor-bearing animals treated with vehicle (mock treated control).

Chapter 6

Effect of *Salmonella enterica* serovar Typhimurium VNP20009 and VNP20009 with restored chemotaxis on 4T1 mouse mammary carcinoma progression

This chapter was published in Oncotarget:

Coutermarsh-Ott, S.L.*, Broadway, K.M.*, Scharf, B.E., Allen, I.C. Effect of *Salmonella enterica serovar Typhimurium* VNP20009 and VNP20009 with restored chemotaxis on 4T1 mouse mammary carcinoma progression. *Oncotarget*. 2017 Apr 4;8(20):33601-13. PMID: 28431394

Abstract

A variety of bacteria strains have been evaluated as bio-therapeutic and immunomodulatory agents to treat cancer. One such strain, *Salmonella enterica* serovar Typhimurium VNP20009, which is attenuated by a purine auxotrophy mutation and modified lipid A, is characterized in previous models as a safely administered, tumor colonizing agent. However, earlier work tended to use less aggressive cancer cell lines and immunocompromised animal models. Here, we investigated the safety and efficacy of VNP20009 in a highly malignant murine model of human breast cancer. Additionally, as VNP20009 has recently been found to have a defective chemotaxis system, we tested whether restoring chemotaxis would improve anti-cancer properties in this model system. Exposure to VNP20009 had no significant effect on primary mammary tumor size or pulmonary metastasis, and the tumor colonizing process appeared chemotaxis independent. Moreover, tumor-bearing mice exposed to *Salmonella* exhibited increased morbidity that was associated with significant liver disease. Our results suggest that VNP20009 may not be safe or efficacious when used in aggressive, metastatic breast cancer models utilizing immunocompetent animals.

Introduction

The use of bacteria as bio-therapeutic agents for cancer treatment has a long and interesting history. Some of the earliest documented, large scale observations supporting the use of bacteria as bio-therapy came from William B. Coley over 150 years ago, who reported that a significant fraction of cancer patients went into remission or were completely cured of their cancer following the development of post-operative bacterial infections [1]. Indeed, early studies between 1868 and 1944 evaluated the direct injection of bacterial toxins and bacterial broth cultures to treat malignant tumors, with ample cases reported of both successes and failures [2-4]. Over the last few decades, numerous studies have emerged that re-invigorated the field of bacteria-based bio-therapeutics for the treatment of cancer. Indeed, several bacterial genera have been evaluated in pre-clinical cancer models, including *Bifidobacterium*, *Clostridium* and *Salmonella enterica* serovar Typhimurium [5-7]. However, as evidenced by the volume of studies in the current literature, *Salmonella* is by far the most extensively evaluated and characterized bacterial genus currently being explored as a cancer bio-therapeutic agent [8].

Salmonella is an attractive model for studying tumor targeting due to its facultative anaerobic nature, allowing for the oxygenated circumference of the tumor as well as the hypoxic core region to be colonized by bacteria (reviewed in [9]). In addition, *Salmonella* can be manipulated genetically with relative ease and possesses a facultative intracellular lifestyle [10]. Importantly, attenuated *S*. Typhimurium has resulted in decreased tumor growth in mice bearing B16F10 melanoma and has been suggested to be able to colonize solid tumors up to a reported 9,000 times greater than the liver [11]. This is significant, as it reflects the specificity of the bacteria to colonizing cancerous tissue as opposed to clearance from the host.

Several strains of *S.* Typhimurium have been investigated for the purpose of tumor targeting and chemotherapy delivery, including VNP20009, A1-R, and CRC2631 ([12-14], reviewed in[15]). VNP20009 was constructed by Low et al. from strain 14028 through selection of hyperinvasion by chemical and UV mutagenesis, targeted deletions resulting in purine auxotrophy, and attenuation by modification of lipid A [16]. Success of the strain, due to its anticancer effects and high safety profile in pre-clinical animal models, resulted in a Phase 1 Clinical Trial in 2001. In this study, VNP20009 was introduced as a treatment to patients with nonresponsive metastatic melanoma or renal cell carcinoma. Although colonization was observed for some patients, treatment with VNP20009 did not result in tumor regression [17]. However, attempts to maximize bacterial tumor colonization and anticancer effects continue to be investigated.

Many virulent properties of *S.* Typhimurium have been evaluated for optimization of bacterial localization and retardation of tumors. These include components of virulence such as pathogenicity islands SPI-1 and SPI-2, motility, chemotaxis, biofilm formation and metabolism ([18, 19], reviewed in [20]). Utilization of chemotaxis is a particularly interesting concept, because the machinery can be manipulated to facilitate bacterial colonization of specified regions of tumors based on the nutrient content. Generally, it has been found that bacterial chemotaxis is favorable for tumor spheroid colonization *in vitro*, with specific receptors facilitating tumor microenvironment localization [21, 22]. In contrast, the role of chemotaxis *in vivo* is controversial, reasons for which may include the use of different bacterial strains, cancer cell lines, and experimental conditions. In a CT26 colon carcinoma model, intravenously injected *S.* Typhimurium SL7207 with a functional chemotaxis system yielded an advantage to tumor colonization over chemotaxis deficient strains 12 hours after injection, but no differences were

observed after 24 hours [18]. A few studies have assessed bacterial chemotaxis in an *in vivo* 4T1 mammary carcinoma model. Using high-throughput screening of single-gene deletion mutants of *S.* Typhimurium 14028, chemotaxis was found to be beneficial for tumor colonization 2 days after infection [8]. However, chemotaxis had no significant influence after 2 days for strain SL1344 [23]. VNP20009 was recently discovered to be deficient in chemotaxis, due to a non-synonymous SNP in the gene encoding the chemotaxis two component response regulator, *cheY* [24]. Upon replacing the deficient copy of *cheY* with the wild-type copy, chemotaxis was recovered to 70% of the parental strain [24].

In the present study, we sought to evaluate the effects of VNP20009 and VNP20009 with restored chemotaxis in the context of 4T1 mammary carcinoma progression. The 4T1 cell line in mice is an attractive model of triple-negative breast cancer due to its high degree of clinical relevance, the ability to use immunocompetent mice, and the fact that metastasis occurs through a highly predictable mechanism that accurately mimics human breast cancer malignancies [25]. Previous studies have evaluated VNP20009 in other models of tumorigenesis, including diverse sub-types of cancer in mouse models, prostate, pancreatic, and breast cancer, as well as sarcoma and glioma [13, 26-30]. However, the majority of these prior reports were focused on xenograft studies using immunocompromised animals inoculated with minimally aggressive tumors and nominal assessments of either metastasis or systemic pathology. Here, we provide a robust evaluation of 4T1 cancer progression in the presence of chemotaxis positive or chemotaxis deficient VNP20009 as indicated by morbidity and mortality evaluations of wild-type BALB/c mice, assessments of primary tumor burden, measurements of metastatic cell potential in the lungs, immune system function, and comprehensive pathological evaluations over the time course of the experiment. Our results reveal that treatment with VNP20009 does not have a

significant effect on primary mammary tumor growth or pulmonary metastasis. While we did observe tumor colonization, this process appeared to be independent of chemotaxis. Furthermore, tumor bearing mice infected with VNP20009 demonstrated increased morbidity that was associated with significant liver disease. Together, these data suggest that VNP20009 may not be safe or efficacious in models of highly aggressive, metastatic cancer.

Materials and Methods

Experimental animals

All experiments were conducted under institutional IACUC approval and in accordance with the NIH Guide for the Care and Use of Laboratory Animals. All experiments were conducted with 6-10 week-old, female BALB/C mice purchased from Jackson Laboratories. Animals were allowed to acclimate in the facilities for one week prior to tumor injections.

Cell culture and injection

4T1 cells were grown under standard cell culture conditions in Roswell Park Memorial Institute (RPMI 1640) supplemented with 10% fetal bovine serum (FBS), 100 units/ml penicillin, and 100 µg/ml streptomycin. Cells used for injection were grown for 4-6 generations, washed, and re-suspended in sterile phosphate-buffered saline (PBS) prior to injection. Mice were anesthetized and maintained on isoflurane anesthesia throughout the tumor injection procedure. 1.2×10^6 cells were injected into the mammary fat pad of each mouse. Control mice received the same volume of sterile PBS. Mice were recovered on room air. Mice were monitored 3 times per week, and weights and tumor measurements were recorded twice weekly. Calipers were used to measure two perpendicular diameters of each tumor. These were used to then determine a calculated tumor diameter [25]. Animals were euthanized when (i) weight loss exceeded 10-

15% of original body weight, (ii) tumor growth reached 1.4-1.6 cm of calculated diameter, or (iii) if considered clinically moribund. In our experience with this model, measurable subcutaneous mammary tumors develop within 2-4 days of injection. These tumors progress reliably with evidence of metastatic disease present in the lungs by week 2 (unpublished data). By the end of 30 days, the tumors are approximately 1.4-1.6 cm in calculated diameter.

Bacterial strains, growth and injection conditions

S. Typhimurium VNP20009 and VNP20009 *cheY*$^{+}$ were grown in MSB media (1% tryptone, 0.5% yeast extract, 2 mM $MgSO_4$, 2 mM $CaCl_2$) at 37 °C to an OD_{600} of 1.0, washed 3 times with PBS and adjusted to the final concentration of 2 x 10^5 CFU/mL. A 100 μL dose of this final concentration was injected i.v. via the tail vein at day 16 post tumor-injection, or directly into the tumor at day 6 post tumor-injection. Control mice were injected with an equal amount of PBS.

Tissue collection and processing

At euthanasia, whole blood was collected via cardiac puncture and a full necropsy was performed. The large lung lobes were partially inflated in formalin and, along with samples of primary tumor and liver, fixed in formalin for at least 24 hours (h). They were then submitted for histopathology. Individual liver and primary tumor specimens were also collected for bacterial enumeration and storage at -80 °C for downstream protein and nucleic acid extraction. For bacterial enumeration, specimens were weighed, homogenized using a hand held pestle system, serially diluted in PBS, plated on MSB plates, and incubated for 14 h at 37 °C. The remaining smaller lung lobes were enzymatically digested using Type IV collagenase

(collagenase from *Clostridium histolyticum*, Sigma-Aldrich) and porcine elastase (elastase from porcine pancreas, MPBiomedicals). After a series of washes in Hank's buffered saline solution (HBSS), cells were resuspended in Dulbecco's modified eagle medium (DMEM) with 10% FBS, 100 units/ml penicillin, and 100 µg/ml streptomycin, 60 µM 6-thioguanine, and plated onto cell culture plates. After 5-10 days of incubation at 37 °C and 5% CO_2, media was removed, cells were briefly fixed in methanol, stained with 0.03% new methylene blue, and tumor colonies were counted (**Figure 1**).

Histopathology

Formalin-fixed tissues were embedded in paraffin and stained with routine hematoxylin and eosin (H&E) staining for histopathologic examination by a board certified veterinary pathologist (S.C.O). For lung sections, numbers of individual pulmonary tumors were counted in a single, 5 µm section. For each animal, the entire right lung lobe was embedded and sectioned at the level of the mainstem bronchus. For liver sections, a single, 5 µm section was evaluated. Amounts of inflammation, EMH, and necrosis were scored individually as follows: 0; no inflammation/EMH/necrosis identified, 1; 1% to 33% of the examined section was composed of inflammation/EMH/necrosis, 2; 34%-66% of the examined section was composed of inflammation/EMH/necrosis, and 3; greater than 67% of the section was composed of inflammation/EMH/necrosis. These individual scores were then summed to give a total composite score for each animal.

Results

_S_. Typhimurium infection in combination with the presence of mammary tumors increased morbidity

It is well known that multiple strains of bacteria can colonize a variety of *in vivo* tumors. *S.* Typhimurium VNP20009 has been previously reported to exhibit preferential tumor colonization and dosage-related safety in a variety of tumor-infected animals including monkeys, pigs, and mice, as well as, humans [12, 17, 31]. The recently constructed VNP20009 derivative with restored bacterial chemotaxis, VNP20009 *cheY*$^{+}$, has yet to be assessed *in vivo* for tumor colonizing ability [24]. We therefore evaluated the effects of intravenously (i.v.) injected *S.* Typhimurium VNP20009 on primary tumor burden and pulmonary metastasis in the 4T1 mammary carcinoma model over the course of 8 days. Mice were injected with 1.2 x 10^6 4T1 mammary carcinoma cells and tumors were allowed to grow for 16 days. Animals were then i.v. injected with 2 x 10^4 CFUs of either *S.* Typhimurium VNP20009, which is non-chemotactic, or a chemotaxis-restored derivative VNP20009 *cheY*$^{+}$. Control animals were injected i.v. with the same volume of PBS. Our results showed that animals with both tumors and either VNP20009 strain had a markedly increased morbidity when compared to all other treatment groups (**Figure 2**). Animals that received both tumors and VNP20009 had an 8-10% decrease in weight compared to either VNP20009 strain or 4T1 groups alone, suggesting a synergistic effect between the tumor and bacterial infection (**Figure 2**). The effect was independent of the chemotactic ability of the VNP20009 strains.

Systemic exposure to _S_. Typhimurium had no effect on primary tumor size

Because multiple studies suggested the importance of *S.* Typhimurium chemotaxis on both the ability of bacteria to colonize tumor tissue and to influence tumor growth, we

investigated the effects of VNP20009 and VNP20009 *cheY*$^{+}$ on primary mammary tumor growth in the 4T1 model. Mice were monitored three times per week and tumor size was recorded twice per week (**Figure 3A**). All animals injected with 4T1 cells developed mammary tumors that progressed as expected [25]. Control animals receiving PBS injections into the mammary fat pad instead of 4T1 cells did not develop spontaneous mammary tumors. Grossly, tumors appeared as spherical, raised, firm masses with an ulcerated surface (**Figure 3A**). Histologically, mammary tumors from all tumor-bearing animals appeared similar. All of the mammary tumors were composed of typical neoplastic epithelial cells with marked atypia and numerous mitotic figures (**Figure 3B**). Large areas of necrosis were also present (**Figure 3B**). There was no statistically significant difference in the size of the primary tumor between animals infected with either VNP20009 strain or those only bearing 4T1 mammary tumors (**Figure 3C**).

Systemic exposure to *S*. Typhimurium had no effect on the presence or amount of pulmonary metastasis

Systemic metastasis is an important cause of death in women with breast cancer. Previous publications proposed that the use of attenuated, tumor-targeting *S*. Typhimurium strains can decrease metastatic tumorigenesis in mice without having systemic effects [32, 33]. The 4T1 model is not only a well-established and commonly used model for primary mammary tumorigenesis, but also for systemic metastasis [25]. In our experience, tumor cells reliably metastasized to the lungs by the end of week 2 following 4T1 cell injection (data not shown). To investigate this phenomenon further, we evaluated pulmonary metastasis using both qualitative and quantitative methodologies. At necropsy, the large lung lobe was removed and prepared for histopathology evaluation by a board certified veterinary pathologist (S.C.O.). Individual tumor

cell aggregates (classified as metastases) were identified and counted. Histopathological analysis of pulmonary metastasis revealed no differences between the number of tumor cell aggregates identified histologically among any of the tumor-bearing groups, regardless of exposure to either *S.* Typhimurium strain (**Figures 4A and 4B**). 4T1 cells are unique in their inherent resistance to 6-thioguanine, a purine agonist that is lethal to most cells. Therefore, 4T1 metastatic cells can be grown in media supplemented with 6-thioguanine until they form small colonies, which enables a quantitative evaluation of lung metastasis. Concurrent with our histopathologic evaluation, our results confirm that no significant differences in numbers of metastatic colonies were identified among any of the tumor-bearing groups (**Figure 4C**). We attempted to discern the presence of *Salmonella* in fixed lung samples by reverse transcription followed by 16S RNA PCR amplification and by immunohistochemistry. However, we were unsuccessful in verifying the presence of VNP20009 in our lung tissue specimens using these approaches. It is possible that we did not detect the *Salmonella* due to technical limitations of our assay (low amounts or poor quality of RNA) or the quantity of *Salmonella* in the lungs were below the level of detection for our methodology.

All animals bearing tumors and infected with *S*. Typhimurium developed significant liver disease

A very important finding in this study was the presence of significant morbidity in tumor-bearing animals exposed to either VNP20009 strain (**Figure 2**). *S.* Typhimurium VNP20009 has not previously been associated with significant morbidity in animal models, but instead is considered a safe strain to evaluate the effects of bacterial colonization on tumor development [34, 35]. Additionally, we found it interesting that the morbidity seen in tumor-bearing animals

exposed to *S.* Typhimurium was not also seen in the non-tumor bearing animals exposed to the same bacteria (**Figure 2**). The increased morbidity cannot be explained by differences in primary tumor size or numbers of pulmonary metastases, because these were not significantly different from 4T1 tumor-bearing animals not exposed to *S.* Typhimurium (**Figures 3 and 4**). To evaluate the potential systemic effects of *S.* Typhimurium, livers of all animals were examined grossly and histologically. At necropsy, tumor-bearing animals infected with *S.* Typhimurium had gross evidence of liver damage. Livers from this animal group had large, sharply demarcated foci that were pale yellow and most often present at the edges of liver lobes (data not shown). No gross abnormalities were identified in the livers of any other treatment or control groups. Liver samples from all animals were processed for histopathology. These were then evaluated and scored by a board certified veterinary pathologist (S.C.O.) for amounts of inflammation, extramedullary hematopoiesis (EMH), and necrosis. Histopathological assessments revealed that liver lesions were significantly different in each of the treatment groups (**Figure 5A**). Livers from control animals were characterized by no or rare, small aggregates of mononuclear cells that made up less than 1% of the section (**Figure 5A**). Livers from animals only infected with either strain of *S.* Typhimurium were characterized by randomly scattered, variably-sized foci of inflammation composed of aggregates of mononuclear cells often admixed with neutrophils (**Figure 5A**). Livers from animals bearing mammary tumors only (with no exposure to *S.* Typhimurium) were characterized by multiple, variably-sized foci of EMH composed of aggregates of both immature myeloid and erythroid progenitors (**Figure 5A**). These aggregates were most commonly isolated to portal tracts; however, aggregates could be also identified randomly scattered throughout the parenchyma. Livers from tumor-bearing animals infected with either *S.* Typhimurium strain had large areas of inflammation similar to the

bacteria-only treated groups and large amounts of EMH similar to 4T1-only animals (**Figure 5A**). However, these mice additionally displayed large coalescing foci of necrosis characterized by dead hepatocytes and replacement by fibrin (**Figure 5A**). To more quantitatively evaluate these histologic changes, scores were generated to reflect levels of inflammation, EMH, and necrosis. These individual scores were then totaled to generate a composite score for each animal (**Figure 5B**). All animals receiving any experimental treatment exhibited composite liver scores $\geq$1 while control animals exhibited composite liver scores equal to 0. Results revealed that the composite liver scores from those tumor-bearing animals exposed to either strain of VNP20009 were significantly higher than any other treatment group (**Figure 5B**). These results suggested that the presence of two types of disease may lead to a more complicated systemic health status than either disease alone.

S. Typhimurium chemotaxis did not contribute to mammary tumor colonization

The efficiency of bacterial tumor-targeting was evaluated by the ratio of tumor to liver colonization. Tissue homogenates were serially diluted and dilutions were plated on nutrient agar to obtain bacterial colony counts. No differences were present upon comparing liver colonization of mice that did not receive 4T1 cells, but were only infected with *S.* Typhimurium (data not shown). Primary tumor and liver colonization by VNP20009 and VNP20009 *cheY*$^{+}$, respectively, were not significantly different (**Figure 6**). We observed a significant increase in numbers for both bacterial strains in tissues, with tumor:liver colonization ratios ranging from 675:1 and 2,800:1 for mice exposed to VNP20009 or VNP20009 *cheY*$^{+}$, respectively.

Route of *S.* Typhimurium injection did not significantly affect disease pathobiology

To investigate whether the delivery route of *S.* Typhimurium to the animal could influence its effects on tumor growth and disease pathobiology, experiments were repeated following direct injection of the bacterial strains into the tumor. Tumors were allowed to develop and progress for 6 days before VNP20009 or VNP20009 *cheY*$^+$ (or PBS for control animals) were injected directly into the tumor at a concentration of approximately 2 x 10^4 CFU/mouse. Similar to the previous experiment, tumor-bearing animals injected with either VNP20009 strain displayed decreased weight gain when compared to the remaining groups (**Figure 7A**). No clinically relevant differences were present in the calculated diameter of the mammary tumors in tumor-bearing animals independent of *S.* Typhimurium presence (**Figure 7B**). Tumor-bearing mice infected with either strain of VNP20009 presented a higher liver composite score than tumor only bearing mice or the PBS-control mice (**Figure 7C**). Primary tumor and liver colonization by VNP20009 and VNP20009 *cheY*$^+$ did not differ significantly (**Figure 7D**). However, both bacterial strains were retained in the tumor, with tumor:liver colonization ratios ranging from 195:1 and 820:1 for mice exposed to VNP20009 or VNP20009 *cheY*$^+$, respectively.

Discussion

We have presented a detailed report on the status of mice bearing 4T1 mammary carcinoma treated with *S.* typhimurium VNP20009. Historically, this strain of *Salmonella* has been attributed as a safe anticancer agent in the context of several murine tumor models [34, 35]. These studies culminated in the 2001 phase 1 human clinical trial using VNP20009 for the treatment of metastatic melanoma which ultimately found that though VNP20009 appeared to be safe for the use in human patients, its anti-tumor effects were equivocal [17]. Based on this, we

formulated an experimental design to test both the safety and efficacy of *S.* Typhimurium as a treatment in the 4T1 mammary carcinoma model, as well as, the potential contribution of bacterial chemotaxis to primary tumor localization and metastatic potential to the lungs. Gaining a better understanding of how the bacteria react in different tumor microenvironments will be essential to future uses of VNP20009 as a cancer bio-therapeutic agent.

The majority of research analyzing the use of *Salmonella* as an anti-cancer agent has focused on its primary tumor burden effects. Fewer studies have been undertaken evaluating its ability to attenuate metastatic tumor burden. The 4T1 mammary carcinoma model represents a more natural study of metastatic tumors, as it accounts for the heterogeneity of cells in a primary tumor and allows for the biological selective pressures encountered by tumor cells to drive metastatic potential. This is opposed to artificial metastasis models that are based on the direct intravenous injection, where all tumor cells are placed into circulation to settle and grow into new tumors [36]. Perhaps the most relevant data pertinent to the present study evaluated *S.* Typhimurium A1-R in the 4T1 model using nude mice [36]. Here, the authors orthotopically-injected mice and surgically resected the primary tumor once it was established to maximize evaluation of brain metastasis [36]. In this particular model, *S.* Typhimurium A1-R was able to arrest the growth of breast-cancer associated brain metastasis and increased the survival of the orthotopically-transplanted, primary tumor resected mice [36]. In our present study, we chose to focus on lung metastasis, as the lung is the most common metastasis site of breast cancer found at autopsy and lung metastasis is also a prominent feature of the 4T1 model [25, 37]. While we observed a trending decrease in lung metastases in one of the quantitative assessments for the VNP20009 *cheY*$^{+}$ strain (**Figure 3C**), the consensus data revealed only a minor reduction in metastatic burden (**Figure 3**). There are a variety of suggested reasons for the discrepancies

found between the A1-R and VNP20009 studies, including the *Salmonella* strains utilized, the site of metastasis evaluated, the aggressiveness of the tumor model (surgically resected primary tumor versus non-resected), and the immune status of the animals. Together, these data emphasize the need to not only better define the genetic and phenotypical differences of *S.* Typhimurium strains in the context of different cancer sub-types, but also in the context of metastasis.

Beyond the ability of attenuated *Salmonella* strains to combat various types of cancer, assessments associated with the safety of the bacterial strain for use as a bio-therapeutic agent is also paramount. Many prior studies have been conducted evaluating the safety of VNP20009 and this particular strain likely has the best characterized safety profile of any of the therapeutic *Salmonella* strains. However, even though this strain of *Salmonella* is considered attenuated, there are significant clinical side effects related to its use [17, 38]. Indeed, one of the most striking aspects of our study is the observation that all tumor bearing animals exposed to VNP20009 exhibited significant morbidity associated with severe liver disease, which was not observed in any other experimental group of animals (**Figure 4**). One possible explanation for the increased morbidity and liver disease in tumor-bearing mice exposed to bacteria is that the mammary tumor could be acting as a reservoir for bacterial infection. We were unable to identify evidence of significant differences in bacterial burdens in tumor tissues taken at necropsy via immunohistochemistry. Moreover, no significant differences were identified in bacterial CFU identified in the livers from tumor-bearing versus non tumor-bearing mice (data not shown) suggesting that the systemic bacterial burdens were similar between the two groups. A second explanation for the observed morbidity and liver disease is that 4T1 mammary carcinoma cells have been previously reported to secrete soluble factors inducing

immunosuppression[39]. Thus, it is possible that tumor-bearing animals exposed to bacteria were unable to control their systemic bacterial infections as well as those animals that did not have tumors and exposed to bacteria.

While some prior studies have reported increased morbidity and liver pathology accompanied by VNP20009 treatment, this particular side effect has not been extensively characterized and the significance of these liver outcomes has typically been underestimated [40, 41]. A previous study evaluating the administration of VNP20009 using the B16F10 tumor model, found that bacteria treatment mildly attenuated tumor growth and reported the presence of small foci of neutrophilic inflammation throughout the liver that increased over time and occurrence of hepatocyte necrosis [40]. However, this pathology was presented as mild and the liver appeared to recover over the course of the model [40]. Similarly, in another study evaluating the toxicity of VNP20009 and A1-R strains of *Salmonella* in a Lewis lung carcinoma model in nude mice, non-tumor bearing animals were intravenously administered two different doses of each bacterial strain [41]. By day 3, hemorrhagic foci were identified in the livers of all mice injected with bacteria, but no evaluation of liver histopathology was performed in tumor-bearing mice exposed to *Salmonella* [41]. Consistent with these prior studies, we also observed relatively mild liver lesions following VNP20009 treatment when administered alone (**Figure 4**). However, in the 4T1 mammary carcinoma model, we detected large areas of EMH in the liver, which was not reported in the other cancer models (**Figure 4**). Likewise, the combination of 4T1 mammary carcinoma and VNP20009 treatment appeared to act synergistically, causing significantly increased inflammation, EMH, and liver necrosis that ultimately resulted in increased morbidity (**Figure 4**). Thus, despite the clinical potential of VNP20009, more data associated with the safety of this bacterial strain is clearly necessary.

Despite the absence of anticancer effects by the *S.* Typhimurium strains tested, bacteria were retained in the tumor after 8 days, with an average tumor to liver colonization of 580:1 and 2,800:1 by VNP20009 and VNP20009 *cheY*$^{+}$, respectively (**Figure 5**). For a variety of *in vivo* tumor models and timelines, including murine melanoma after 3 days and human melanoma and human colon carcinoma after 5 days, VNP20009 has been reported to have a tumor to liver colonization ratio at ≥1,000:1 which is in line with our data [12]. The targeting of *Salmonella* to tumor tissue remains a significant barrier in therapeutic applications (reviewed in [20]). Any and all improvements in this regard are critical. Our data reveals that chemotaxis does not significantly contribute to *S.* Typhimurium VNP20009 colonization of the primary 4T1 mammary tumor (**Figure 5**). The nature in which VNP20009 was constructed, by UV and chemical mutagenesis, left the strain with several genetic alterations, including 50 non-synonymous SNPs and the loss of 128 genes in the Suwwan deletion region [42]. Since restoration of one of the genes containing a non-synonymous SNP, *cheY*, did not significantly facilitate the promotion of tumor colonization by VNP20009, this raises the question if the remaining alterations in the genome are assisting or hindering the strain from its full tumor targeting potential.

To evaluate the possibility that the route of administration could have negatively influenced *S.* Typhimurium VNP20009 effectiveness in the 4T1 breast cancer model, we evaluated both intravenous and intratumoral injection. We originally speculated the following: (i) a direct injection into the tumor would be less likely to be associated with negative systemic affects, including liver lesions; and (ii) direct injection of a chemotaxis null strain would increase tumor colonization compared to the same strain systemically administered. However, we observed similar results between the two injection models. In both cases, tumor-bearing animals

exposed to either VNP20009 strain had increased morbidity due to a high frequency of severe liver lesions not identified in the other treatment groups and no significant differences in tumor colonization regardless of the route of administration. In sum, we were unable to identify any significant differences in disease pathobiology between intravenous and intratumoral injection.

The data presented here expands the growing body of literature that suggests that individual *S.* Typhimurium strains with unique phenotypical characteristics will have differing levels of success as a cancer bio-therapeutic agent, depending on the cancer sub-type being targeted and the specific tumor microenvironmental niches present in the model. Additional studies are both necessary and ongoing to determine the safest and most efficacious utilization of *S.* Typhimurium VNP20009 in future anticancer therapies.

Acknowledgements

We would like to thank Charlene Santos (UNC Chapel Hill) and Lissett Bickford (Virginia Tech) for providing technical assistance with the 4T1 mammary carcinoma model. We would also like to thank Bettina Heid (Virginia Tech) for mouse colony assistance.

References

1. McCarthy EF. The toxins of William B. Coley and the treatment of bone and soft-tissue sarcomas. Iowa Orthop J. 2006; 26: 154-8. doi:

2. Nauts HC, Swift WE, Coley BL. The treatment of malignant tumors by bacterial toxins as developed by the late William B. Coley, M.D., reviewed in the light of modern research. Cancer Res. 1946; 6: 205-16. doi:

3. Wiemann B, Starnes CO. Coley's toxins, tumor necrosis factor and cancer research: a historical perspective. Pharmacol Ther. 1994; 64: 529-64. doi:

4. Rihova B, Stastny M. [History of Immuno-therapy - from Coley Toxins to Check-points of the Immune Reaction]. Klin Onkol. 2015; 28 Suppl 4: 4s8-14. doi:

5. Yazawa K, Fujimori M, Amano J, Kano Y, Taniguchi S. Bifidobacterium longum as a delivery system for cancer gene therapy: selective localization and growth in hypoxic tumors. Cancer Gene Ther. 2000; 7: 269-74. doi: 10.1038/sj.cgt.7700122.

6. Taniguchi S, Fujimori M, Sasaki T, Tsutsui H, Shimatani Y, Seki K, Amano J. Targeting solid tumors with non-pathogenic obligate anaerobic bacteria. Cancer Sci. 2010; 101: 1925-32. doi: 10.1111/j.1349-7006.2010.01628.x.

7. Theys J, Pennington O, Dubois L, Anlezark G, Vaughan T, Mengesha A, Landuyt W, Anne J, Burke PJ, Durre P, Wouters BG, Minton NP, Lambin P. Repeated cycles of Clostridium-directed enzyme prodrug therapy result in sustained antitumour effects in vivo. Br J Cancer. 2006; 95: 1212-9. doi: 10.1038/sj.bjc.6603367.

8. Silva-Valenzuela CA, Desai PT, Molina-Quiroz RC, Pezoa D, Zhang Y, Porwollik S, Zhao M, Hoffman RM, Contreras I, Santiviago CA, McClelland M. Solid tumors provide niche-

specific conditions that lead to preferential growth of Salmonella. Oncotarget. 2016; 7: 35169-80. doi: 10.18632/oncotarget.9071.

9. Leschner S, Weiss S. Salmonella-allies in the fight against cancer. J Mol Med (Berl). 2010; 88: 763-73. doi: 10.1007/s00109-010-0636-z.

10. Nallar SC, Xu DQ, Kalvakolanu DV. Bacteria and genetically modified bacteria as cancer therapeutics: Current advances and challenges. Cytokine. 2016. doi: 10.1016/j.cyto.2016.01.002.

11. Pawelek JM, Low KB, Bermudes D. Tumor-targeted Salmonella as a novel anticancer vector. Cancer Res. 1997; 57: 4537-44. doi:

12. Clairmont C, Lee KC, Pike J, Ittensohn M, Low KB, Pawelek J, Bermudes D, Brecher SM, Margitich D, Turnier J, Li Z, Luo X, King I, et al. Biodistribution and genetic stability of the novel antitumor agent VNP20009, a genetically modified strain of Salmonella typhimurium. J Infect Dis. 2000; 181: 1996-2002. doi: 10.1086/315497.

13. Zhao M, Yang M, Ma H, Li X, Tan X, Li S, Yang Z, Hoffman RM. Targeted therapy with a Salmonella typhimurium leucine-arginine auxotroph cures orthotopic human breast tumors in nude mice. Cancer Res. 2006; 66: 7647-52. doi: 10.1158/0008-5472.can-06-0716.

14. Eisenstark A, Kazmierczak RA, Dino A, Khreis R, Newman D, Schatten H. Development of Salmonella strains as cancer therapy agents and testing in tumor cell lines. Methods Mol Biol. 2007; 394: 323-54. doi: 10.1007/978-1-59745-512-1_16.

15. Wang CZ, Kazmierczak RA, Eisenstark A. Strains, Mechanism, and Perspective: Salmonella-Based Cancer Therapy. Int J Microbiol. 2016; 2016: 5678702. doi: 10.1155/2016/5678702.

16. Low KB, Ittensohn M, Luo X, Zheng LM, King I, Pawelek JM, Bermudes D. Construction of VNP20009: a novel, genetically stable antibiotic-sensitive strain of tumor-targeting Salmonella for parenteral administration in humans. Methods Mol Med. 2004; 90: 47-60. doi:

17. Toso JF, Gill VJ, Hwu P, Marincola FM, Restifo NP, Schwartzentruber DJ, Sherry RM, Topalian SL, Yang JC, Stock F, Freezer LJ, Morton KE, Seipp C, et al. Phase I study of the intravenous administration of attenuated Salmonella typhimurium to patients with metastatic melanoma. J Clin Oncol. 2002; 20: 142-52. doi:

18. Crull K, Bumann D, Weiss S. Influence of infection route and virulence factors on colonization of solid tumors by Salmonella enterica serovar Typhimurium. FEMS Immunol Med Microbiol. 2011; 62: 75-83. doi: 10.1111/j.1574-695X.2011.00790.x.

19. Crull K, Rohde M, Westphal K, Loessner H, Wolf K, Felipe-Lopez A, Hensel M, Weiss S. Biofilm formation by Salmonella enterica serovar Typhimurium colonizing solid tumours. Cell Microbiol. 2011; 13: 1223-33. doi: 10.1111/j.1462-5822.2011.01612.x.

20. Chorobik P, Czaplicki D, Ossysek K, Bereta J. Salmonella and cancer: from pathogens to therapeutics. Acta Biochim Pol. 2013; 60: 285-97. doi:

21. Kasinskas RW, Forbes NS. Salmonella typhimurium specifically chemotax and proliferate in heterogeneous tumor tissue in vitro. Biotechnol Bioeng. 2006; 94: 710-21. doi: 10.1002/bit.20883.

22. Kasinskas RW, Forbes NS. Salmonella typhimurium lacking ribose chemoreceptors localize in tumor quiescence and induce apoptosis. Cancer Res. 2007; 67: 3201-9. doi: 10.1158/0008-5472.can-06-2618.

23. Stritzker J, Weibel S, Seubert C, Gotz A, Tresch A, van Rooijen N, Oelschlaeger TA, Hill PJ, Gentschev I, Szalay AA. Enterobacterial tumor colonization in mice depends on bacterial metabolism and macrophages but is independent of chemotaxis and motility. Int J Med Microbiol. 2010; 300: 449-56. doi: 10.1016/j.ijmm.2010.02.004.

24. Broadway KM, Denson EA, Jensen RV, Scharf BE. Rescuing chemotaxis of the anticancer agent Salmonella enterica serovar Typhimurium VNP20009. J Biotechnol. 2015; 211: 117-20. doi: 10.1016/j.jbiotec.2015.07.010.

25. Pulaski BA, Ostrand-Rosenberg S. Mouse 4T1 breast tumor model. Curr Protoc Immunol. 2001; Chapter 20: Unit 20.2. doi: 10.1002/0471142735.im2002s39.

26. Zhao M, Yang M, Li XM, Jiang P, Baranov E, Li S, Xu M, Penman S, Hoffman RM. Tumor-targeting bacterial therapy with amino acid auxotrophs of GFP-expressing Salmonella typhimurium. Proc Natl Acad Sci U S A. 2005; 102: 755-60. doi: 10.1073/pnas.0408422102.

27. Zhao M, Geller J, Ma H, Yang M, Penman S, Hoffman RM. Monotherapy with a tumor-targeting mutant of Salmonella typhimurium cures orthotopic metastatic mouse models of human prostate cancer. Proc Natl Acad Sci U S A. 2007; 104: 10170-4. doi: 10.1073/pnas.0703867104.

28. Nagakura C, Hayashi K, Zhao M, Yamauchi K, Yamamoto N, Tsuchiya H, Tomita K, Bouvet M, Hoffman RM. Efficacy of a genetically-modified Salmonella typhimurium in an orthotopic human pancreatic cancer in nude mice. Anticancer Res. 2009; 29: 1873-8. doi:

29. Hayashi K, Zhao M, Yamauchi K, Yamamoto N, Tsuchiya H, Tomita K, Hoffman RM. Cancer metastasis directly eradicated by targeted therapy with a modified Salmonella typhimurium. J Cell Biochem. 2009; 106: 992-8. doi: 10.1002/jcb.22078.

30. Kimura H, Zhang L, Zhao M, Hayashi K, Tsuchiya H, Tomita K, Bouvet M, Wessels J, Hoffman RM. Targeted therapy of spinal cord glioma with a genetically modified Salmonella typhimurium. Cell Prolif. 2010; 43: 41-8. doi: 10.1111/j.1365-2184.2009.00652.x.

31. Lee KC, Zheng, L., Luo, X., King, I. Comparative Evaluation of the Acute Toxic Effects in Monkeys, Pigs and Mice of a Genetically Engineered Salmonella Strain (VNP20009) Being Developed as an Antitumor Agent. International Journal of Toxicology. 2000; 19: 19-25. doi: 10.1080/109158100225006.

32. Miwa S, Yano S, Zhang Y, Matsumoto Y, Uehara F, Yamamoto M, Hiroshima Y, Kimura H, Hayashi K, Yamamoto N, Bouvet M, Tsuchiya H, Hoffman RM, et al. Tumor-targeting Salmonella typhimurium A1-R prevents experimental human breast cancer bone metastasis in nude mice. Oncotarget. 2014; 5: 7119-25. doi: 10.18632/oncotarget.2226.

33. Matsumoto Y, Miwa S, Zhang Y, Hiroshima Y, Yano S, Uehara F, Yamamoto M, Toneri M, Bouvet M, Matsubara H, Hoffman RM, Zhao M. Efficacy of tumor-targeting Salmonella typhimurium A1-R on nude mouse models of metastatic and disseminated human ovarian cancer. J Cell Biochem. 2014; 115: 1996-2003. doi: 10.1002/jcb.24871.

34. Sznol M, Lin SL, Bermudes D, Zheng LM, King I. Use of preferentially replicating bacteria for the treatment of cancer. J Clin Invest. 2000; 105: 1027-30. doi: 10.1172/jci9818.

35. Luo X, Li Z, Lin S, Le T, Ittensohn M, Bermudes D, Runyab JD, Shen SY, Chen J, King IC, Zheng LM. Antitumor effect of VNP20009, an attenuated Salmonella, in murine tumor models. Oncol Res. 2001; 12: 501-8. doi:

36. Zhang Y, Miwa S, Zhang N, Hoffman RM, Zhao M. Tumor-targeting Salmonella typhimurium A1-R arrests growth of breast-cancer brain metastasis. Oncotarget. 2015; 6: 2615-22. doi: 10.18632/oncotarget.2811.

37. Weigelt B, Peterse JL, van 't Veer LJ. Breast cancer metastasis: markers and models. Nat Rev Cancer. 2005; 5: 591-602. doi: 10.1038/nrc1670.

38. Thamm DH, Kurzman ID, King I, Li Z, Sznol M, Dubielzig RR, Vail DM, MacEwen EG. Systemic administration of an attenuated, tumor-targeting Salmonella typhimurium to dogs with spontaneous neoplasia: phase I evaluation. Clin Cancer Res. 2005; 11: 4827-34. doi: 10.1158/1078-0432.ccr-04-2510.

39. Kano A. Tumor cell secretion of soluble factor(s) for specific immunosuppression. Sci Rep. 2015; 5: 8913. doi: 10.1038/srep08913.

40. Rosenberg SA, Spiess PJ, Kleiner DE. Antitumor effects in mice of the intravenous injection of attenuated Salmonella typhimurium. J Immunother. 2002; 25: 218-25. doi:

41. Zhang Y, Zhang N, Zhao M, Hoffman RM. Comparison of the selective targeting efficacy of Salmonella typhimurium A1-R and VNP20009 on the Lewis lung carcinoma in nude mice. Oncotarget. 2015; 6: 14625-31. doi: 10.18632/oncotarget.3342.

42. Broadway KM, Modise T, Jensen RV, Scharf BE. Complete genome sequence of Salmonella enterica serovar Typhimurium VNP20009, a strain engineered for tumor targeting. J Biotechnol. 2014; 192 Pt A: 177-8. doi: 10.1016/j.jbiotec.2014.07.006.

Figures

Figure 1

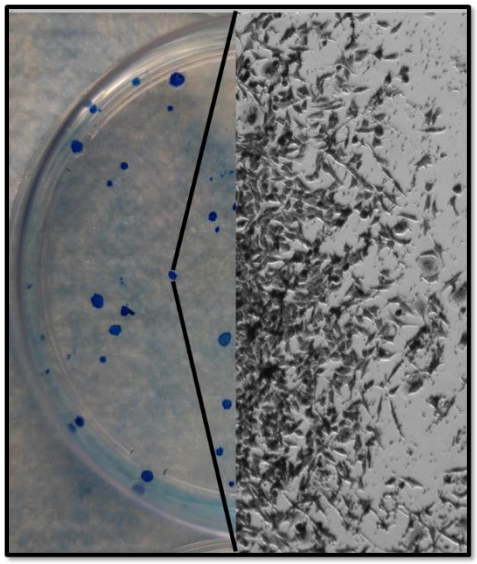

Figure 1. Metastatic 4T1 cells can be isolated from organs of interest and grown in supplemented media to yield quantitative evaluations of metastatic tumor burden. Following necropsy, the small lung lobes were enzymatically digested, filtered, and grown on cell culture plates in media supplemented with 6-thioguanine. 4T1 cells are inherently resistant to 6-thioguanine and, thus, individual metastatic cells are able to grow into tumor cell colonies and manually counted.

Figure 2

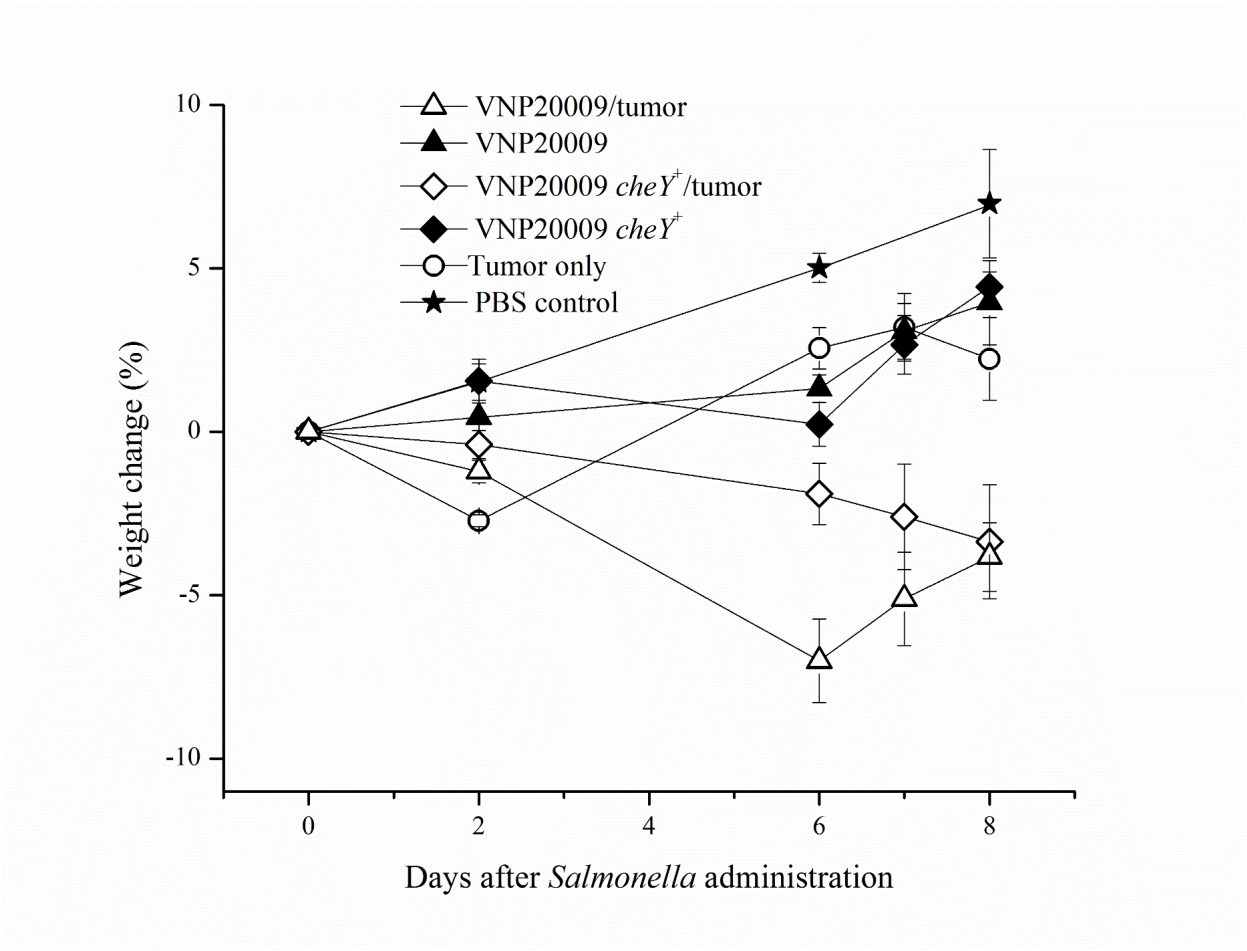

Figure 2: Weight change following exposure to *Salmonella*. 4T1-tumor bearing animals or non-tumor bearing control animals were injected intravenously with *S.* Typhimurium VNP20009, *S.* Typhimurium VNP20009 *cheY*$^+$, or PBS. Animals were monitored three times per week and weights were measured twice weekly. PBS control, n=3; *S.* Typhimurium only, n=4; Tumor only, n=3; VNP20009 and tumor, n=8; VNP20009 *cheY*$^+$ and tumor, n=8. Data points and error bars denote mean ± SEM. Statistical significance was determined in relation to the tumor only sample by a two-tailed Student's T-test (* $p<0.05$, ** $p<0.01$).

Figure 3

A.

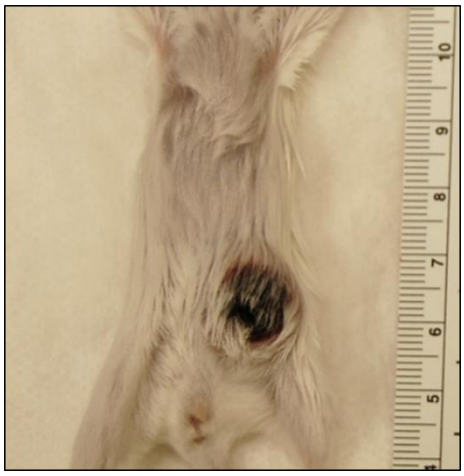

B.

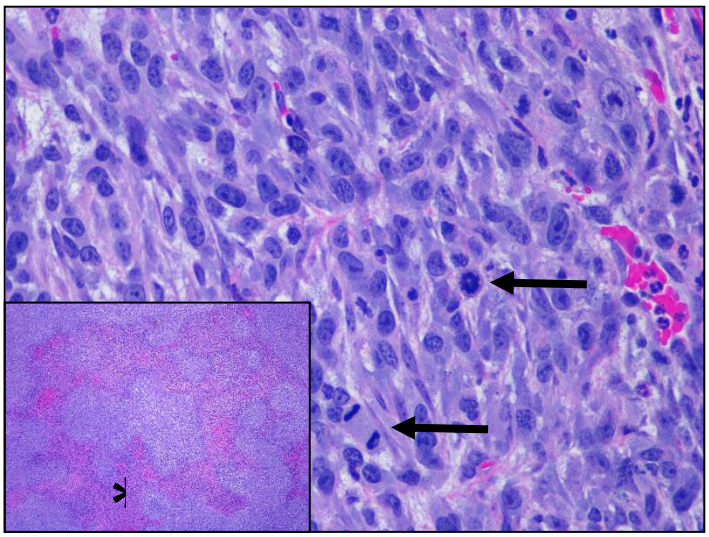

C.

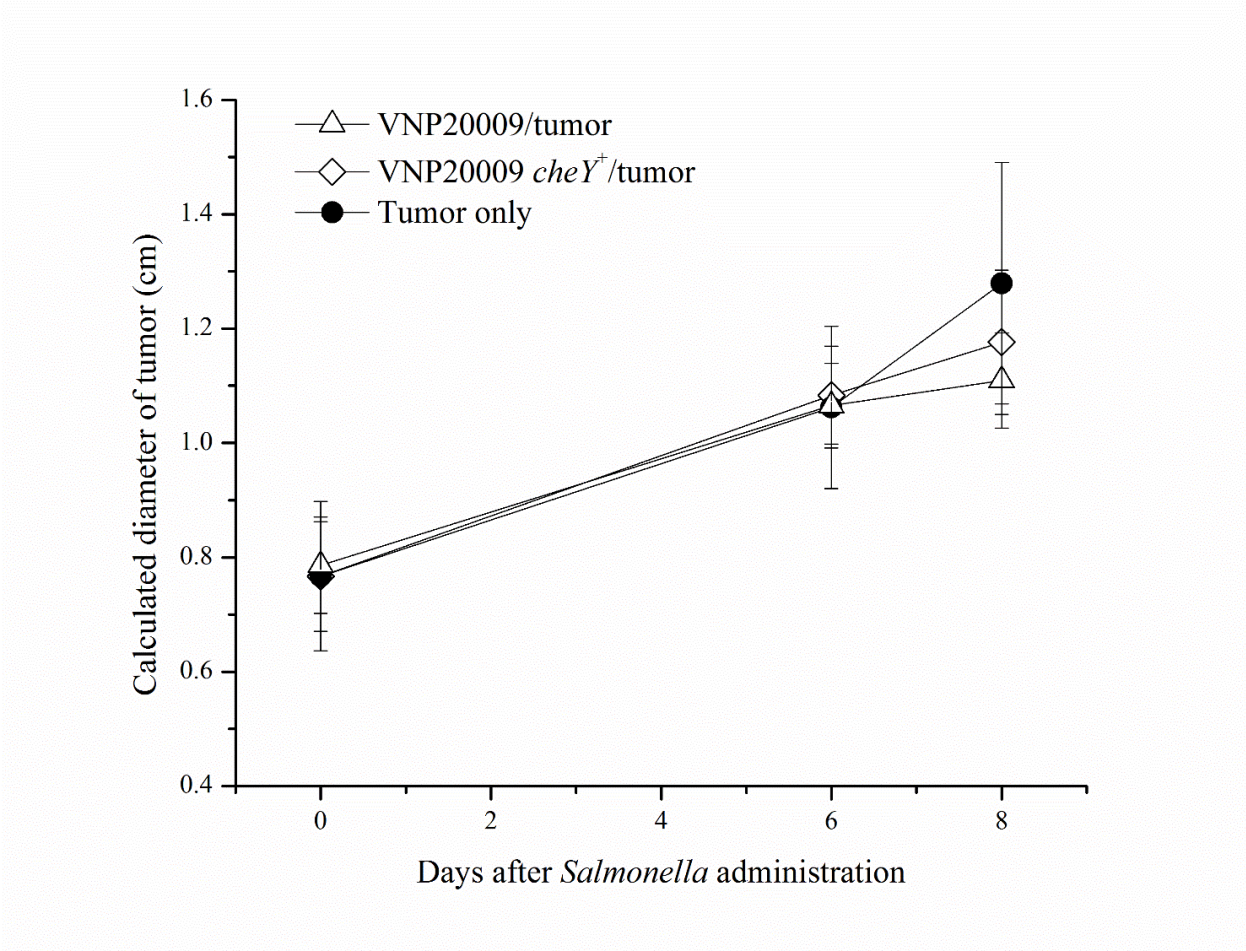
VNP20009/tumor
VNP20009 cheY+/tumor
Tumor only
Calculated diameter of tumor (cm)
1.6
1.4
1.2
1.0
0.8
0.6
0.4
0
2
4
6
8
Days after Salmonella administration

Figure 3. Mammary tumors developed in all 4T1-injected animals. **A**. Grossly, tumors appeared as spherical, raised, firm masses with an ulcerated surface. **B**. Histologically, tumors were composed of a pleomorphic population of neoplastic epithelial cells with numerous mitotic figures (arrows) and large areas of necrosis (inset, asterisk). **C**. All animals injected with 4T1 cells developed mammary tumors. Tumors were monitored three times per week and measurements were recorded twice per week. Measurements were taken using calipers and measuring two perpendicular diameters. The square root of the product of these two measurements was taken to give a calculated diameter for each tumor. PBS control, n=3; *S.* Typhimurium only, n=4; Tumor only, n=3; VNP20009 and tumor, n=8*;* VNP20009 *cheY*$^{+}$ and tumor, n=8. Data points and error bars denote mean ± SEM.

Figure 4

A.

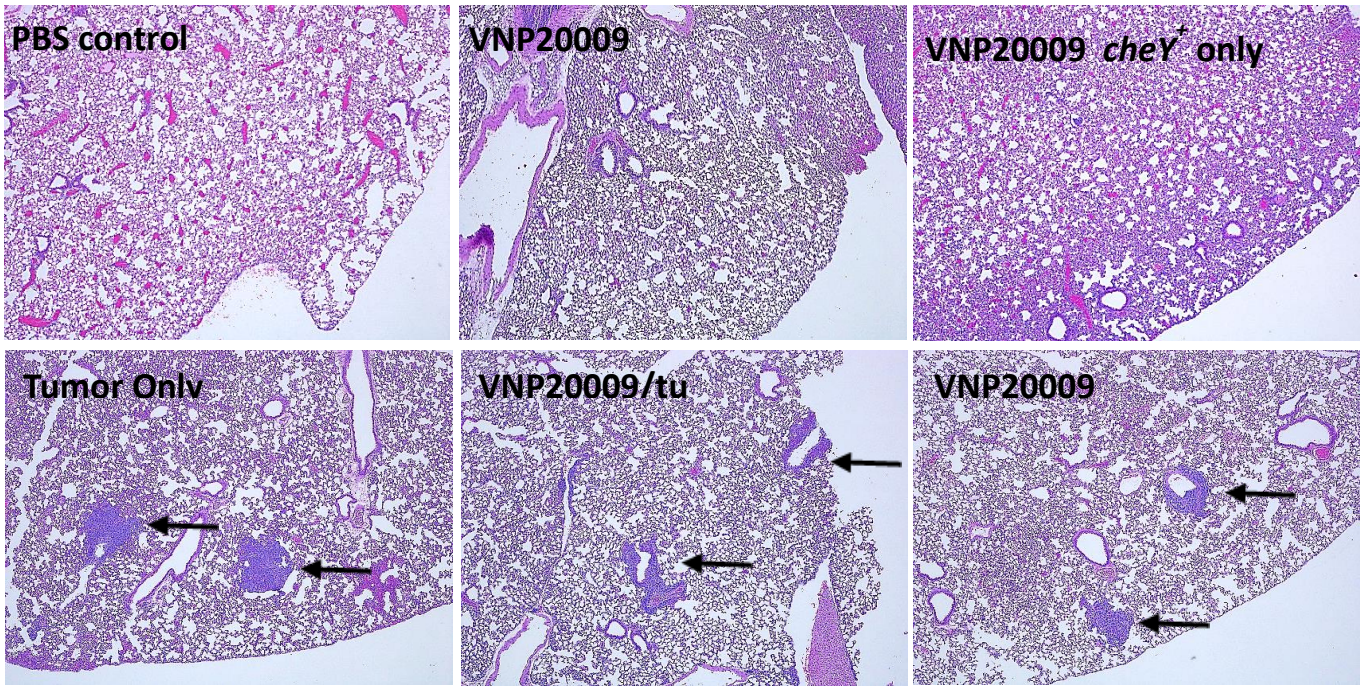
PBS control
VNP20009
VNP20009 cheY+ only
Tumor Only
VNP20009/tu
VNP20009

B.

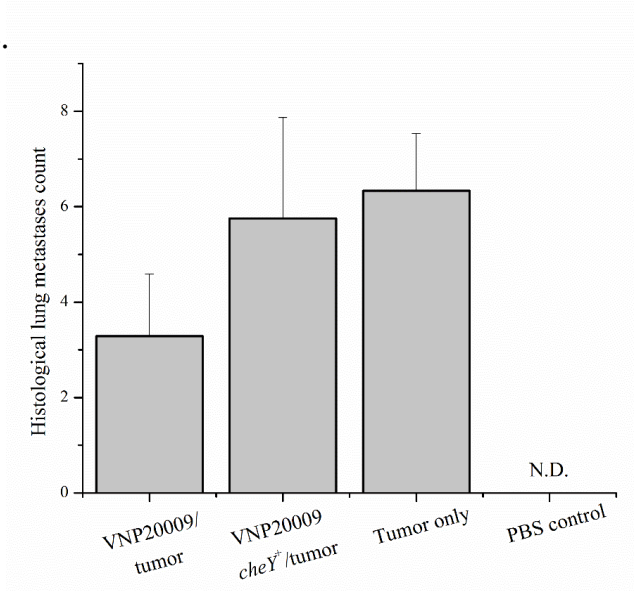
Histological lung metastases count
0
2
4
6
8
N.D.
VNP20009/ tumor
VNP20009 cheY+ /tumor
Tumor only
PBS control

C.

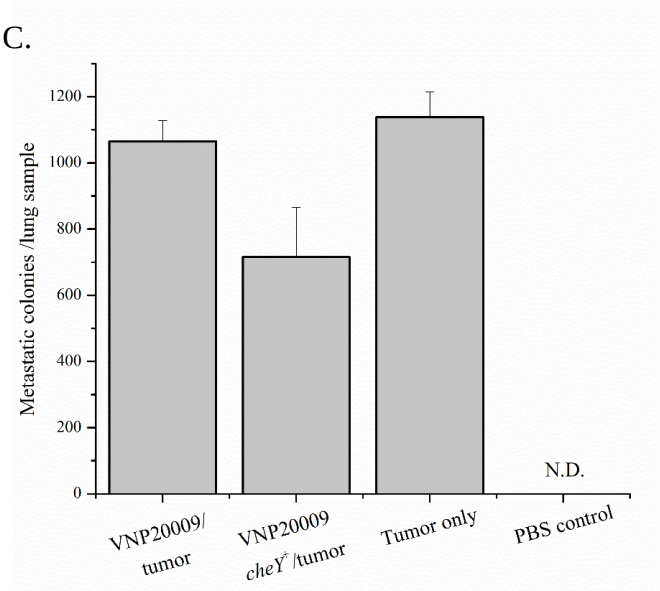
Metastatic colonies /lung sample
0
200
400
600
800
1000
1200
N.D.
VNP20009/ tumor
VNP20009 cheY+ /tumor
Tumor only
PBS control

Figure 4. All 4T1-tumor bearing animals developed pulmonary metastases. A. Histologically, pulmonary metastases were identified as random accumulations of neoplastic epithelial cells often centered on small airways (arrow). Neither control animals nor animals injected with *S.* Typhimurium alone developed histologic evidence of metastasis. **B.** The large lung lobe from each animal was placed in formalin and processed for H&E staining. The number of individual pulmonary metastases were counted per histologic section. **C.** The small lung lobes from each animal were taken at necropsy and subsequently enzymatically digested. Cell suspensions were plated on cell culture plates and grown in media containing 6-thioguanine. After 8 days, metastatic colonies were fixed in methanol, stained with 0.03% methylene blue, and counted. PBS control, n=3; VNP20009 only, n=4; Tumor only, n=3; VNP20009 and tumor, n=7*;* VNP20009 *cheY*$^{+}$ and tumor, n=8. Error bars denote SEM, N.D, not detected.

Figure 5

A.

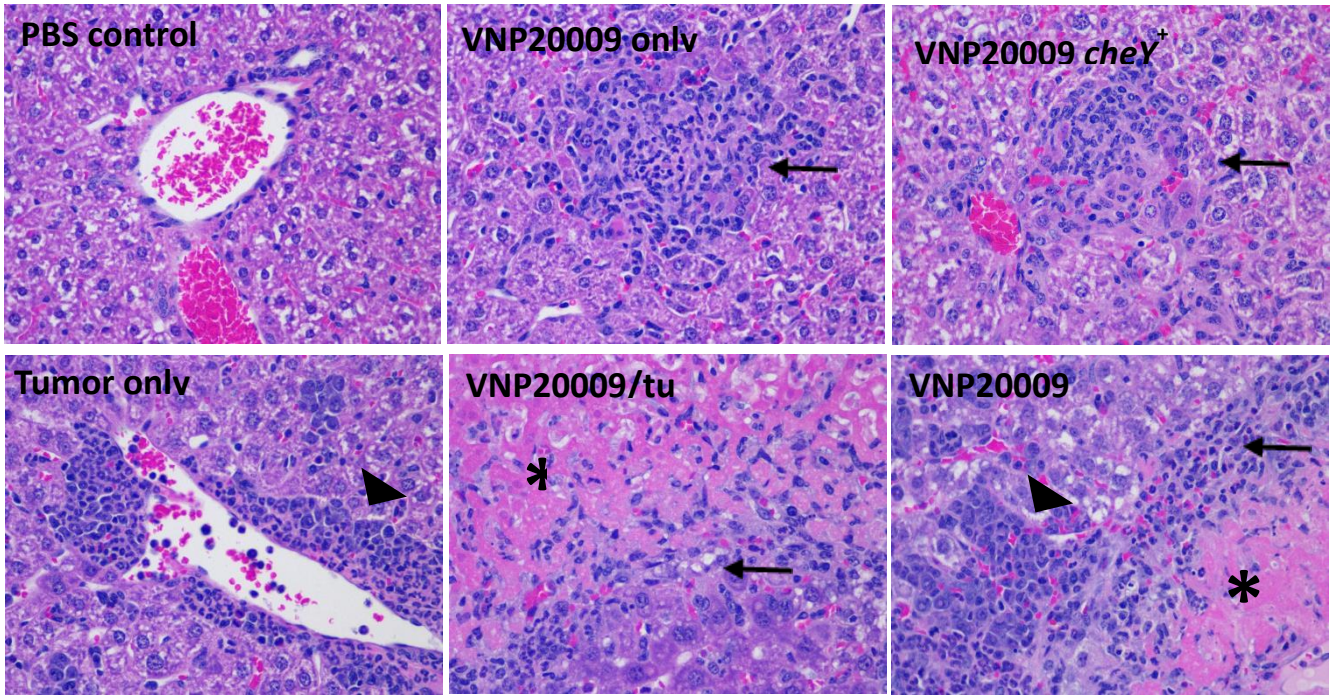
PBS control
VNP20009 onlv
VNP20009 cheY+
Tumor onlv
VNP20009/tu
VNP20009

B.

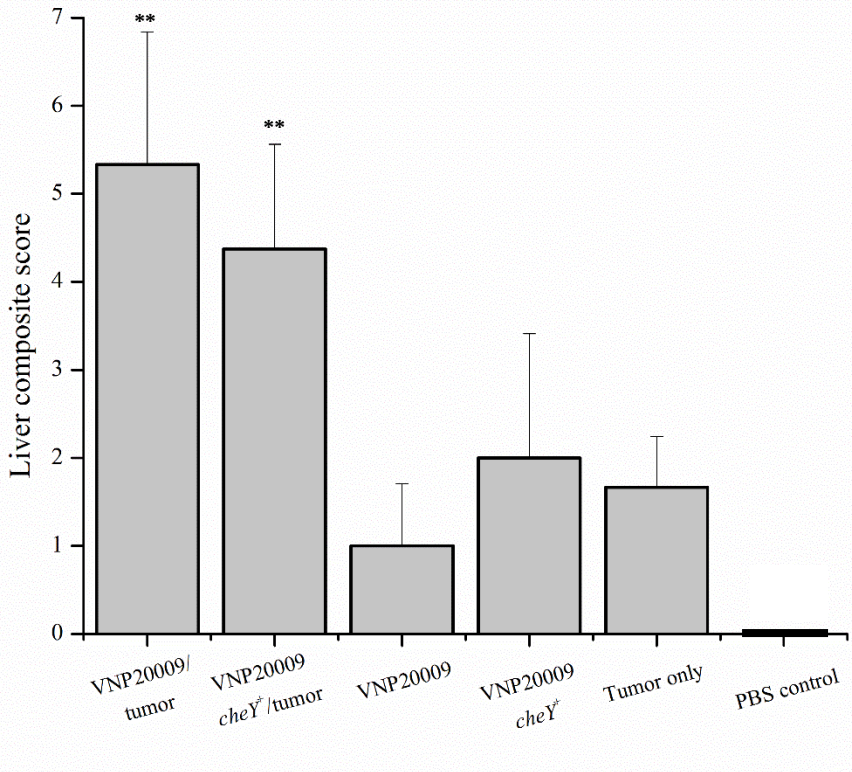
Liver composite score
0
1
2
3
4
5
6
7
**
**
VNP20009/ tumor
VNP20009 cheY+/tumor
VNP20009
VNP20009 cheY+
Tumor only
PBS control

Figure 5. All experimental animals developed liver lesions. A. Animals receiving intravenous *S.* Typhimurium developed mild to moderate, multifocal inflammation characterized by random aggregates of mononuclear cells and neutrophils (arrows). Animals receiving 4T1 mammary carcinoma cells developed large amounts of extramedullary hematopoiesis predominantly in the area of large and small vessels, but also occasionally scattered throughout the parenchyma (large arrowheads). These areas were characterized by a heterogeneous group of erythroid and myeloid precursors as well as megakaryocytes. Those mice receiving both *S.* Typhimurium (regardless of strain) and 4T1 cells had significant amounts of inflammation (arrow) and extramedullary hematopoiesis (large arrowhead), as well as, large foci of liver necrosis (asterisk). **B.** Inflammation, extramedullary hematopoiesis, and necrosis were individually scored for each sample. Individual scores were then summed to create a composite liver histopathology score for each animal. PBS control, n=3; VNP20009 only, n=2; VNP20009 *cheY+* only, n=2; 4T1 only, n=3; VNP20009 and tumor, n=6*;* VNP20009 *cheY*$^{+}$, n=8. Error bars denote SD. Statistical significance was determined in relation to the tumor only sample by a two-tailed Student's T-test (** $p<0.01$).

Figure 6

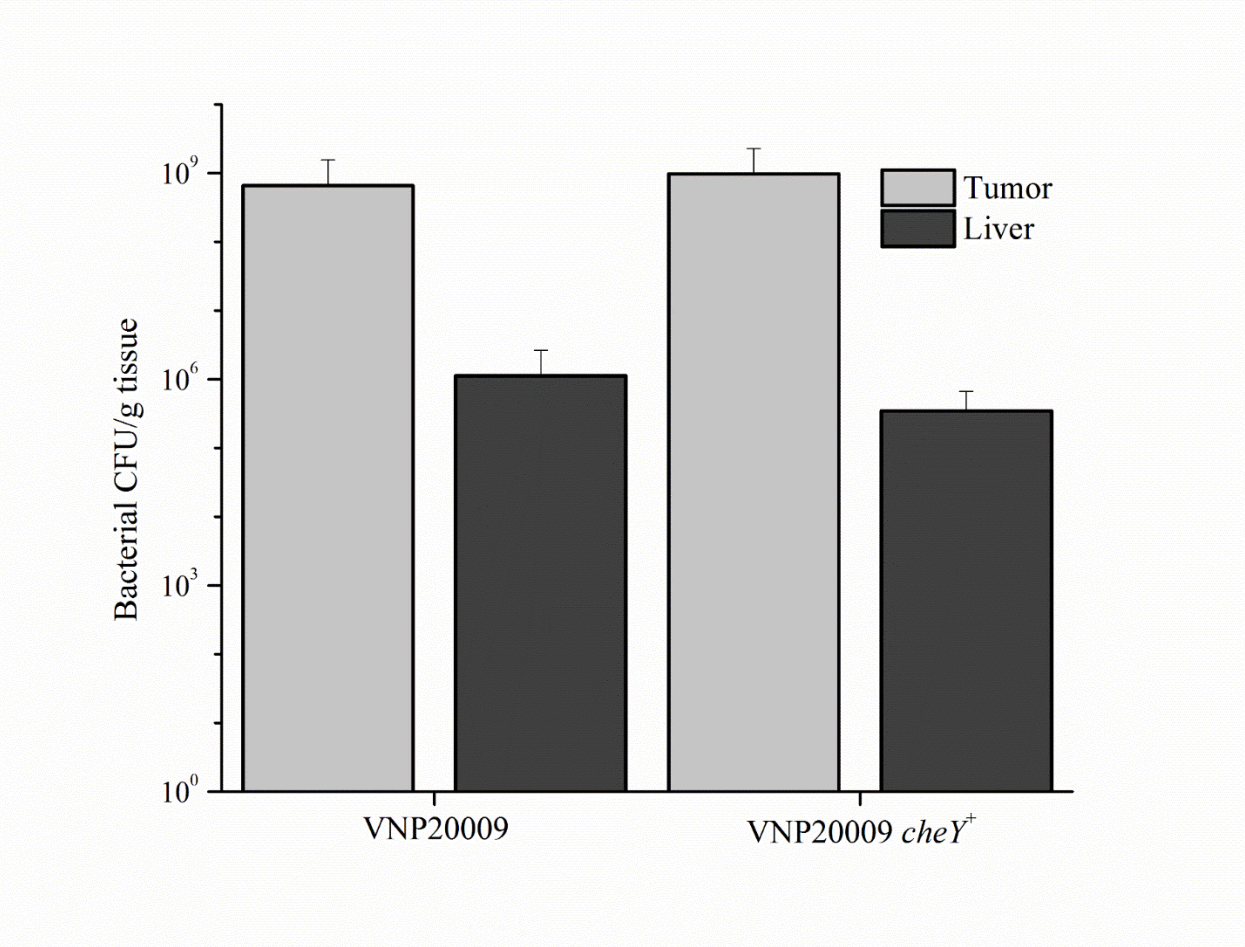

Figure 6: Bacterial colonization of tumor and liver tissue. Intravenous injected VNP20009 or VNP20009 *cheY*$^+$ were respectively recovered from tumor and liver samples and enumerated. No statistical differences were found between any groups. Data represents VNP20009, n=6; VNP20009 *cheY*$^+$, n=8., with error bars denoting SD.

Figure 7

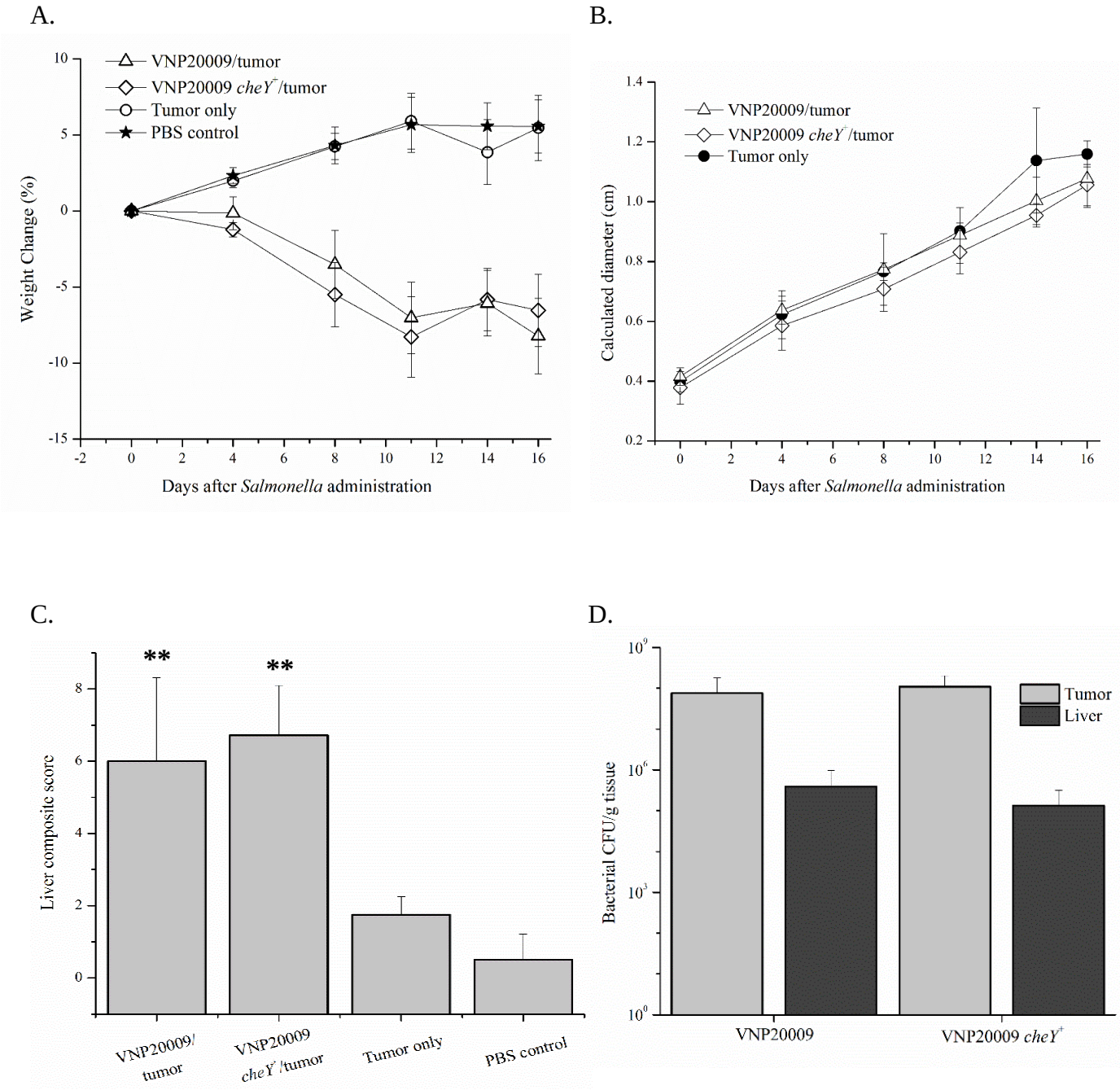
A.
B.
VNP20009/tumor
VNP20009 cheY-/tumor
Tumor only
PBS control
Weight Change (%)
Days after Salmonella administration
Calculated diameter (cm)
Days after Salmonella administration
C.
D.
Liver composite score
**
**
VNP20009/ tumor
VNP20009 cheY-/tumor
Tumor only
PBS control
Bacterial CFU/g tissue
Tumor
Liver
VNP20009
VNP20009 cheY+

Figure 7. Disease pathobiology was evaluated following intratumoral injection of *S.* Typhimurium. Six days following 4T1 tumor cell injections into the mammary fat pad, animals were administered either VNP20009 or VNP20009 *cheY*$^{+}$ directly into mammary tumors. Similar parameters were assessed as in the previous intravenous experiment including (**A**) weight change, (**B**) calculated diameter of the primary mammary tumor, (**C**) histopathologic scoring of liver sections, and (**D**) number of bacterial cells recovered from the liver or primary tumor of infected animals. PBS control, n=2; Tumor only, n=4; VNP20009 and tumor, n=6; VNP20009 *cheY*$^{+}$ and tumor, n=7. Error bars denote SEM for **A** and **B**, SD for **C** and **D**. Statistical significance was determined in relation to the tumor only sample by a two-tailed Student's T-test (* $p<0.05$, ** $p<0.01$).

Chapter 7

Conclusion

Collectively, these works will make clinically relevant contributions to the diagnosis and treatment of neoplastic diseases. The majority of the work focused on histiocytic sarcoma (HS). Both from the review in Chapter 2, as well as, the studies described in Chapters 3-5, it is obvious that therapeutic options are limited for both canine and human patients diagnosed with HS. Currently, options include surgical excision, radiation, and chemothetherapy. Surgical excision aims to reduce the overall presence of gross disease while radiation and chemotherapy facilitate the reduction of gross and microscopic disease through non-specific cell killing. Unfortunately, these treatments have variable efficacy and impacts on overall survival rates illustrating the need for more targeted therapies. However, targeted therapies are not possible without a better understanding of disease pathogenesis. Recent studies evaluating new or re-purposed drugs like YM155 and dasatinib (discussed in Chapter 2), as well as, LY294002 (discussed in Chapter 5) have begun to address this need [1, 2]. The results of our studies in both Chapter 3 and Chapter 4 have suggested that NF-κB and AKT signaling are important in the development and progression of HS in mice and dogs [3]. This suggests that there may be specific proteins within these pathways that could be targeted by drugs. A great example of this is our pilot study investigating LY294002 in Chapter 5. LY294002 is a PI3 kinase inhibitor which is one target that we found increased in expression in patient samples. Our studies were unable to show any changes in AKT signaling with this drug. However, we had some difficulties with drug delivery. Future studies are planned to evaluate the possibility of packaging the drug in nanoparticles thus enhancing the ability to reach the tumor to exert its affects [4]. Another potential therapeutic target revealed by exploring mechanisms of HS could be IL-1β, a second gene shown to be

increased in expression in patient samples. The drug Kineret (Anakinra) is an Il-1R antagonist currently approved for treatment of rheumatoid arthritis and cryopyrin-associated periodic syndromes in humans. Theoretically, the hypothesis could be made that if IL-1β is increased in HS than reducing its effects by blocking the receptor could reduce tumorigenesis. This is somewhat of a broad, oversimplified claim. However, it illustrates the relevance of mechanistic insight on therapeutic possibilities. Our studies in HS have begun to reveal these mechanisms and targeted studies using qRT-PCR analysis on clinical samples are planned to refine important targets in the NF-κB and AKT signaling pathways.

The investigations into *Salmonella* in our breast cancer model described in Chapter 6 also have significant therapeutic implications. Like in HS, surgical excision with chemotherapy or radiation are often a mainstay for treatment of certain sub-types of breast cancer. However, unlike HS, a great deal of research has been done investigating more successful, targeted therapies. One of the more well-known of these is the anti-Her2 antibody, Herceptin. This drug has been shown to be useful in those breast cancers with overexpression of the growth-factor receptor Her2. Unfortunately, Her2 positive tumors only represent a percentage of all breast cancer patients. Our study investigated the use of a therapy targeted at overwhelming the tumor's immunosuppressive abilities, a mechanism shared by most breast cancer sub-types. Though there was no significant reduction in tumor burden or metastases, our results reveal the need for thorough evaluation of bacterial strains in a variety of different models and tumor types [5].

Another way in which the results here contribute to the overall clinical relevance of the described works, is the potential implications for the diagnosis and differentiation of HS versus hemophagocytic HS. As described in Chapters 2 and 4, the diagnosis of HS in general can be

somewhat laborious. In both canines and humans, morphology alone is not often sufficient to diagnose these tumor. Pathologists rely on a host of immunohistochemical methods to support their diagnosis. Unfortunately, IHC is not always straight forward. It requires specialized training and equipment not commercially available in clinical settings. Additionally, the antibody required for diagnosing HHS, CD11d, performs best on frozen tissue which is often not available. Since these often have to be sent to diagnostic labs, performed by specialized personnel, and interpreted by experienced pathologists, many IHC tests take at least a few days if not longer. The results of our canine gene expression studies (detailed in Chapter 4) found differences in the expression of genes in HHS versus HS which could serve as candidate markers for a PCR assay. PCR assays are a relatively inexpensive, rapid alternative to IHC that could be done on frozen or formalin-fixed patient samples.

The preceding chapters add to the growing body of knowledge investigating the complicated roles of inflammation in tumorigenesis. The transformation from a normal cell to a neoplastic cell involves a host of genetic and environmental changes. These are eloquently reviewed in Hanahan and Weinberg's "Hallmarks of Cancer". The authors describe tumor-promoting inflammation as an enabling characteristic facilitating this transformation and evasion of the immune system as an emerging hallmark of transformed cells. The studies described here support these roles and further our knowledge of both of these disease mechanisms. Chapters 2 and 3 both reveal that the central pro-inflammatory cell signaling pathway NF-κB exhibits increases in gene expression in both murine and canine HS [3]. This is a novel role pathway and mechanism of disease for this tumor. Future studies will focus on refining these findings to determine specific causative mechanisms. We have suggested that there are increases in overall expression of genes from this pathway but have not identified the specific mechanisms upstream

of this. Moreover, we would also like to perform protein analyses to support our gene expression data. The current studies were limited by the fact that only FFPE tissues were available. Future studies will utilize frozen samples received from the Canine Comparative Oncology and Genomics Consortium (CCOGC) for protein analysis. Additionally, in Chapter 5 we discuss the development of our xenograft model. This will be useful in future studies investigating both therapeutic possibilities and further mechanistic data. For example, additional studies looking into NLRX1 and its role in HS (described in Chapter 3) using knockdown methods are possible in this model. DH82 cells are an easily managed cell line making knockdown and overexpression of NLRX1 possible. By injecting these modified cell lines into mice and following tumor growth and analyzing downstream signaling patterns, we could better develop mechanistic insight regarding NLRX1 and its contribution to HS tumorigenesis.

Though tumor-promoting inflammation and immune system evasion have been well-studied, our results discussed in Chapter 6 also suggest that the balance between the two is an important consideration. In our studies, we attempted to reduce tumorigenesis by creating inflammation by way of bacterial infection. Though we succeeded, the inflammation ultimately overwhelmed the animal leading to systemic disease and hepatic failure [5]. We also were unable to see any significant changes in tumor growth or metastasis. Did we choose the wrong bacteria? Were the immunosuppressive capabilities of the tumor cells so strong that a bacteria with reduced virulence could lead to overwhelming systemic infection? These are interesting questions that future studies will attempt to investigate.

Finally, our investigations into multiple models of HS provide translational relevance to a rare and understudied human disease. Transgenic mouse models are important models for investigating basic mechanisms of disease. However, the overall goal is to be able to produce

data that is translatable to other species. In Chapters 3 and 4, we do just this. Our initial studies in mouse models revealed important signaling pathways relevant to HS in mice. However, we were also able to show that these pathways translate into a naturally-occurring disease model of HS in the dog. By using these disease models, we can refine our hypotheses and make predictions of what pathways are likely to contribute to the disease in humans. The goal of research whether basic or clinical is almost always to have broad implications on human and animal health and well-being. This is especially true for biomedical research. In the previously described works, we have made clinically impactful conclusions and provided further support to the claims that inflammation plays a dichotomous role in tumorigenesis.

References

1. Yamazaki H, Takagi S, Hosoya K, Okumura M. Survivin suppressor (YM155) enhances chemotherapeutic efficacy against canine histiocytic sarcoma in murine transplantation models. Res Vet Sci. 2015; 99: 137-44. doi: 10.1016/j.rvsc.2015.02.003.

2. Ito K, Kuroki S, Kobayashi M, Ono K, Washizu T, Bonkobara M. Identification of dasatinib as an in vitro potent growth inhibitor of canine histiocytic sarcoma cells. Vet J. 2013; 196: 536-40. doi: 10.1016/j.tvjl.2012.12.016.

3. Coutermarsh-Ott S, Simmons A, Capria V, LeRoith T, Wilson JE, Heid B, Philipson CW, Qin Q, Hontecillas-Magarzo R, Bassaganya-Riera J, Ting JP, Dervisis N, Allen IC. NLRX1 suppresses tumorigenesis and attenuates histiocytic sarcoma through the negative regulation of NF-kappaB signaling. Oncotarget. 2016; 7: 33096-110. doi: 10.18632/oncotarget.8861.

4. McDaniel DK, Jo A, Ringel-Scaia VM, Coutermarsh-Ott S, Rothschild DE, Powell MD, Zhang R, Long TE, Oestreich KJ, Riffle JS, Davis RM, Allen IC. TIPS pentacene loaded PEO-PDLLA core-shell nanoparticles have similar cellular uptake dynamics in M1 and M2 macrophages and in corresponding in vivo microenvironments. Nanomedicine. 2017; 13: 1255-66. doi: 10.1016/j.nano.2016.12.015.

5. Coutermarsh-Ott SL, Broadway KM, Scharf BE, Allen IC. Effect of Salmonella enterica serovar Typhimurium VNP20009 and VNP20009 with restored chemotaxis on 4T1 mouse mammary carcinoma progression. Oncotarget. 2017; 8: 33601-13. doi: 10.18632/oncotarget.16830.

Appendix A

Complete List of Published Works

1. Coutermarsh-Ott S*, Eden K*, Allen IC.. Beyond the Inflammasome: Regulatory NLR Modulation of the Host Immune Response Following Virus Exposure. J Gen Virol. 2016 Apr;97(4):825-38. Epub 2016 Jan 13. Review. PMID: 26763980.
2. Coutermarsh-Ott S, Simmons A, Capria V, LeRoith T, Wilson JE, Heid B, Philipson CW, Qin Q, Hontecillas-Magarzo R, Bassaganya-Riera J, Ting JP, Dervisis N, Allen IC. NLRX1 suppresses tumorigenesis and attenuates histiocytic sarcoma through the negative regulation of NF-κB signaling. Oncotarget. 2016 May 31;7(22):33096-110. doi: 10.18632/oncotarget.8861. PMID: 27105514.
3. Coutermarsh-Ott SL*, Doran JT*, Campbell C, Williams TM, Lindsay DS, Allen IC. (2016). Caspase-11 Modulates Inflammation and Attenuates Toxoplasma gondii Pathogenesis. Mediators Inflamm. 2016;2016:9848263. Epub 2016 Jun 9. PMID: 27378827.
4. Coutermarsh-Ott, S.L.*, Broadway, K.M.*, Scharf, B.E., Allen, I.C. (2017.) Effect of Salmonella enterica serovar Typhimurium VNP20009 and VNP20009 with restored chemotaxis on 4T1 mouse mammary carcinoma progression. Oncotarget 2017 May 16;8(20):33601-33613. PMID: 28431394.
5. Williams, Tere M., Rachel A. Leeth, Daniel E. Rothschild, Dylan K. McDaniel, Sheryl L. Coutermarsh-Ott, Alysha E. Simmons, Kye H. Kable, Bettina Heid, and Irving C. Allen. "Caspase-11 attenuates gastrointestinal inflammation and experimental colitis pathogenesis." American Journal of Physiology-Gastrointestinal and Liver Physiology 308, no. 2 (2015): G139-G150. PMID: 25414099.

6. Williams, Tere M., Rachel A. Leeth, Daniel E. Rothschild, Sheryl L. Coutermarsh-Ott, Dylan K. McDaniel, Alysha E. Simmons, Bettina Heid, Thomas E. Cecere, and Irving C. Allen. "The NLRP1 Inflammasome Attenuates Colitis and Colitis-Associated Tumorigenesis." The Journal of Immunology 194, no. 7 (2015): 3369-3380. PMID: 25725098.
7. Brickler T, Gresham K, Meza A, Coutermarsh-Ott S, Williams TM, Rothschild DE, Allen IC, Theus MH. Nonessential Role for the NLRP1 Inflammasome Complex in a Murine Model of Traumatic Brain Injury. Mediators Inflamm. 2016;2016:6373506. Epub 2016 Apr 20. PMID: 27199506.
8. Goswami, I., Coutermarsh-Ott, S., Morrison, R.G., Allen, I.C., Davalos, R.V., Verbridge, S.S., Bickford, L.R. (2016). Irreversible electroporation inhibits pro-cancer inflammatory signaling in triple negative breast cancer cells. Bioelectrochemistry. 2016 Sep 25;113:42-50. 2016.09.003. PMID: 27693939.
9. McDaniel, D. K., Jo, A., Ringel, V., Coutermarsh-Ott, S., Rothschild, D.E., Powell, M., Long, T.E., Oestreich, K., Riffle, J.S., Davis, R.M., Allen, I.C. TIPS Pentacene Loaded PEO-PDLLA Core-Shell Nanoparticles have Similar Cellular Uptake Dynamics in M1 and M2 Macrophages and In Corresponding In Vivo Microenvironments. Nanomedicine: Nanotechnology, Biology, and Medicine. 2016 Dec 29. PMID: 28040495
10. Brickler, T., Meza, A., Coutermarsh-Ott, S., Hazy, A., Gris, D., Theus, M., Allen, I. (2017.) “Loss of NLRX1 exacerbates neural tissue damage and NF-κB Signaling following brain injury.” Journal of Immunology. 2017 Oct 9. PMID: 28993512.